THE *IN VITRO* EFFECTS OF HAART ON THE EXPRESSION OF MUC1 AND NFkB1 IN A CERVICAL CANCER CELL LINE, HCS-2

KUTLWANO REKGOPETSWE THABETHE

A dissertation submitted to the Faculty of Health Sciences, University of the Witwatersrand, in fulfilment of the requirements for the degree of Master of Science in Medicine

Johannesburg

2014

Supervisor: Associate Professor Margot Hosie

DECLARATION

I Kutlwano Rekgopetswe Thabethe, declare that this dissertation is my own unaided work. It is being submitted for the Master of Science in Medicine degree at the University of the Witwatersrand, Johannesburg. It has not been submitted before for any degree or examination in any other university.

_____
(Signature of candidate)

_____ day of _____ 2014.

DEDICATION

In memory of my late grandparents;

Thomas Thabethe

1932-1992

Christina Malekane

1951-2008

Jacobeth Thabethe

1938-2012

ABSTRACT

Cervical cancer is the third most commonly diagnosed cancer globally and it has also been identified as one of three AIDS defining malignancies. Highly active antiretroviral therapy (HAART) is a combination of three or more antiretroviral drugs which are classified as nucleoside/nucleotide reverse transcriptase inhibitors (NRTIs), non-nucleoside reverse transcriptase inhibitors (NNRTIs) and protease inhibitors (PIs). HAART has been shown to play a significant role in reducing the incidence of some AIDS defining malignancies, although its effect on cervical cancer is still unclear. It is hypothesized that HAART might reduce cancer risk by interacting with different signalling molecules and pathways that are involved in cancer in order to induce cell death and thus inhibit cell proliferation. The broader aim of this study was to understand the relationship between cervical cancer and HAART. This was achieved by studying the expression of key signalling molecules in cancer; MUC1 and NFkB (P65) and morphological features using scanning electron microscopy following 24 hour treatment of a cervical cancer cell line, HCS-2 with drugs which are commonly used as part of HAART; Emtricitabine (FTC), Tenofovir disoproxil fumarate (TDF), Efavirenz (EFV), Atripla combination (ATP) and Kaletra combination (LPV/r) at their clinical plasma concentrations. Quantitative real time polymerase chain reaction (qPCR) was used in order to study the gene expression of *MUC1* and *P65* and the data was analysed using the $2^{-\Delta\Delta CT}$ method to calculate fold change. The statistical analysis was conducted using JMP 11 software. *MUC1* and *P65 g*ene expression was reduced following drug treatment. Protein expression was studied by means of Immunofluorescence and MUC1 and P65 protein expression was reduced following drug treatment. Scanning electron microscopy revealed characteristic features of apoptotic cell death such as loss of cell contacts, reduced density and size of microvilli, increase in surface blebbing and budding and degradation of apoptotic bodies following treatment with all the drugs. In conclusion, the drugs used in this study

showed some anticancer effects. The drugs facilitated cell death by decreasing the gene and protein expression of MUC1 and P65. In addition, distinct morphological features characteristic of apoptosis and/or secondary necrosis were induced following treatment with all the drugs used in this study.

ACKNOWLEDGEMENTS

With thanks to;

- My heavenly Father for the continued strength to persevere and conquer every challenge that comes my way, it is by your grace alone that I have made it this far. I honour you.
- My family; mom, dad and sisters, thank you for always supporting me throughout my studies and for continuing to believe in me even when I have stopped believing in myself, you see greatness in me which I sometimes don't see but I draw strength from those moments. I love you all very much.
- My partner Sphamandla Xulu for the love and support. I struggle to find the words to describe just how grateful I am for all that you are and how much I appreciate you. You are such a blessing.
- My supervisor Professor Margot Hosie thank you for always being encouraging. I appreciate your depth knowledge and passion for microscopy and your contribution in shaping this project was invaluable in making it successful. Thank you also for believing in me enough to give me the responsibility of running my own project allowing me space to learn on my own and enjoy the joys and disappointments that come with it. I have learned to be independent as a result.
- Mr Gbenga Adefolaju for your willingness to help and constant encouragement throughout this project, Thank you.
- Mrs Pamela Sharp for training and assisting me with using the confocal microscope
- All the technicians at the School of Anatomical Sciences for the excellent technical support offered.

- The Department of Internal Medicine for allowing me to use their facilities to conduct the PCR work, especially Ms Therese Dix-Peek for kindly providing her expertise in qPRC
- The Microscopy and Microanalysis Unit at the University of Pretoria for granting me permission to use their facilities to conduct the scanning electron microscopy work.
- The financial aid and scholarships office at the University of the Witwatersrand for granting me the Postgraduate Merit Award and NRF-DAAD scholarship for funding my studies.
- The Medical Research Council for funding the project
- My fellow colleagues and friends; Nikiwe, Stacey, Jacqui and Anthony for the support and encouragement, I appreciate you all.

TABLE OF CONTENTS **PAGE**

LIST OF FIGURES

LIST OF TABLES

LIST OF ABBREVIATIONS

HPV: Human Papilloma Virus

CIN: Cervical Intraepithelial neoplasia

HIV: Human Immunodeficiency Virus

DNA: Deoxyribonucleic acid

NFkβ: Nuclear Factor kappa beta

AIDS: Acquired Immunodeficiency Syndrome

HAART: Highly Active Antiretroviral Therapy

ARV: Antiretroviral

NRTI: Nucleoside/Nucleotide Reverse Transcriptase Inhibitors

NNRTI: Non Nucleoside/Nucleotide Reverse Transcriptase Inhibitors

PI: Protease Inhibitor

RT: Reverse Transcriptase

FTC: Emtricitabine

TDF: Tenofovir Disoproxil Fumarate

EFV: Efavirenz

LPV: Lopinavir

RTV: Ritonavir

cDNA: Complementary deoxyribonucleic acid

HCS-2: Human squamous cell carcinoma from Uterine Cervix

qPCR: Quantitative real time Polymerase Chain Reaction

SEM: Scanning Electron Microscope

CHAPTER ONE: INTRODUCTION

1.1 GENERAL INTRODUCTION

1.1.1 Cervical cancer; a public health issue

Cervical cancer is the third most commonly diagnosed cancer globally among women and it is second in developing countries following breast cancer (Jemal *et al.,* 2011; Baiocchi *et al.,* 2012). More than 80% of women globally who are diagnosed with cervical cancer are from developing countries (Yang *et al.,* 2004; Uleberg *et al.,* 2011). Cervical cancer is the fourth leading cause of cancer death in women globally and over 85% of the deaths occur in developing countries (Jemal *et al.,* 2011).

High risk Human Papilloma Virus (HPV), for example HPV 16 – HPV 18, infection acquired by cervical epithelial cells is the most important risk factor for cervical cancer development (Uleberg *et al.,* 2011). Once infected with HPV, the cervical epithelium undergoes transformation and develops a non-invasive neoplastic lesion called cervical intraepithelial neoplasia (CIN) (Uleberg *et al.,* 2011). Three CIN grades have been identified by the World Health Organisation (WHO) namely CIN 1- 3, and they are distinguished by the degree of epithelial transformation caused (Uleberg *et al.,* 2011).

Diagnoses with CIN 2-3 following a histological punch biopsy is usually treated by cone excision therapy because often when patients are diagnosed with CIN 2-3, 5-30% of them eventually develop invasive cervical cancer when they are left untreated, so this aggressive invasive therapy employed is often mandatory (Uleberg *et al.,* 2011). This does not apply for all cases as CIN 2-3 regression occurs in 10-40% of the cases (Uleberg *et al.,* 2011). The tumour itself takes ~10-25 years to develop (Uleberg *et al.,* 2011).

Women diagnosed with cervical cancer often die at a younger age than those diagnosed with any other cancer (Goldie, 2006). It is noteworthy that despite its high mortality rate amongst

women globally, cervical cancer can be prevented by vaccination and screening (Xu *et al.*, 2009; Uleberg *et al.*, 2011). Moreover it is treated effectively by various interventions such as cone excision therapy, radiotherapy, chemotherapy and hormone therapy, when identified at a sufficiently early stage (Xu *et al.*, 2009; Uleberg *et al.*, 2011).

In developed countries, higher levels of screening for the early detection of cervical cancer has kept its mortality rate low (Anorlu, 2008; Sibiya, 2012). Unfortunately, the opposite is true in many developing countries because a majority of them have resource poor settings so cytologic screening and vaccination are challenging to implement and sustain; consequently mortality from cervical cancer continues to increase (Goldie, 2006; Anorlu, 2008; Sibiya, 2012).

Africa has the highest prevalence of and mortality from cervical cancer in the world (Anorlu, 2008). In South Africa, cervical cancer accounted for 18.10% of new cancer cases in women of all races by 2007, making it the second most commonly diagnosed cancer in women following breast cancer which accounted for 21.02% of new cases (South African National Cancer Registry Report, 2007).

The high prevalence of cervical cancer in these regions can be attributed to factors including lack of vaccination, poor access to medical facilities, poor nutrition and co-morbid conditions, for example malaria and human immunodeficiency virus (HIV) infection, diagnoses at a later stage of disease, insufficient quality care provided by many health services, loss of follow-up and women unable to finish treatment for other sexually transmitted infections (STIs) namely Herpes simplex 2, *Chlamydia trachomatis* and *Neisseria gonorrhoea* which have been linked to increased risk for CIN and invasive cervical cancer (Anorlu, 2008). After infecting the cells, these STIs induce a chronic inflammatory response

which results in the generation of free radicals which are suggested to play a vital role in carcinogenesis (Anorlu, 2008).

1.1.2 The progression from HPV infection to cervical cancer

Papillomaviruses are small viruses with a double-stranded deoxyribonucleic acid (DNA); they commonly infect and undergo a full infectious cycle exclusively in fully differentiated squamous epithelium and its precursors (Villa, 2006; Gomez and Santos, 2007; Stanley, 2010).

Papillomaviruses are specific to species like Human Papillomavirus (HPV) and they are classified according to genotype (Villa, 2006). Approximately 200 HPV types have been identified; a common feature among them is a circular double-stranded DNA genome of ~8000 base pairs; however, of the 30-40 HPV types that are commonly found in the genital tract, only 12 are considered to be carcinogens (Villa, 2006; Gomez and Santos, 2007; Stanley, 2010; Baiocchi *et al.*, 2012).

The small HPV genomes are arranged into an early, late and a long control region (Villa, 2006). The early control region produces two genes that are essential to the cellular transformation and cell immortalization induced by HPV genes E6 and E7 (Villa, 2006). In contrast the late control region produces two genes that are critical for encoding the viral capsid proteins, genes L1 and L2 (Villa, 2009; Ferenczi *et al.*, 2013). The late control region governs the transcription of viral oncogenes of Papillomaviruses (Ferenczi *et al.*, 2013).

There are various clinical conditions that result from HPV infection, including innocuous lesions to cancer; however, the majority of the HPV infections lead to benign tumours (Gomez and Santos, 2007). Certain types of HPV are more recurrent in malignant than in benign lesions (Villa, 2006). Infection with high-risk HPV types has been identified as the

main risk factor for the development of uterine and/or cervix cancer because they promote malignant transformation (Villa, 2006; Baiocchi *et al.,* 2012).

All high-risk HPV types encode two oncoproteins, E6 and E7, which are responsible for the transformation and immortalisation of human epithelial cells (Baiocchi *et al.,* 2012). E6 and E7 genes produce oncoproteins E6 and E7 respectively which bind to and inactivate tumor suppressor proteins P53 and retinoblastoma (pRb) within the cell (Villa, 2006). The prolonged expression of the early proteins, E6 and E7, results in the gradual accumulation of defects in the cellular DNA, which promotes malignant transformation (Villa, 2006). Both E6 and E7 contribute equally to activate epithelial cell transformation (Villa, 2006).

The alpha genus of HPV has a subset of mucosotrophic HPV types that infect mucosal surfaces, for example, high-risk HPV16 and 18 (Villa, 2006). It is these types that account for over 99% of cervical carcinomas (Villa, 2006). The viral genome of HPV integrates with the host cells chromosomes (Villa, 2006). The expression of viral genes E6 and E7 is higher in cells when HPV16 is integrated into the genome; and so they multiply faster *in vitro* than cervical epithelial cells with extra chromosomal HPV16 (Villa, 2006). In invasive cervical cancer, HPV16 is detected in 55% of the cases and HPV 18 is detected in 12.8%, making these two types the most common HPV types found in invasive cervical cancer (Stanley, 2010).

HPV oncoproteins have been shown to activate the nuclear factor kappa beta (NFkβ) pathway (Baiocchi *et al.,* 2012). HPV16 E5 facilitates cervical cancer in part by increasing COX-2 expression through NFkβ and AP-1, whereas HPV16 E6 and E7 increase the expression of genes controlled by NFkβ and AP-1 and induces the secretion of precise pro-inflammatory and immuno regulatory cytokines (Baiocchi *et al.,* 2012). In addition, HPV16 E6 activates NFkβ DNA binding sites (Baiocchi *et al.,* 2012). The significance of NFkβ as a prognostic

biomarker has only been identified recently; however, NFkβ expression has long been correlated with poor clinical outcomes in many cancers (Baiocchi *et al.,* 2012).

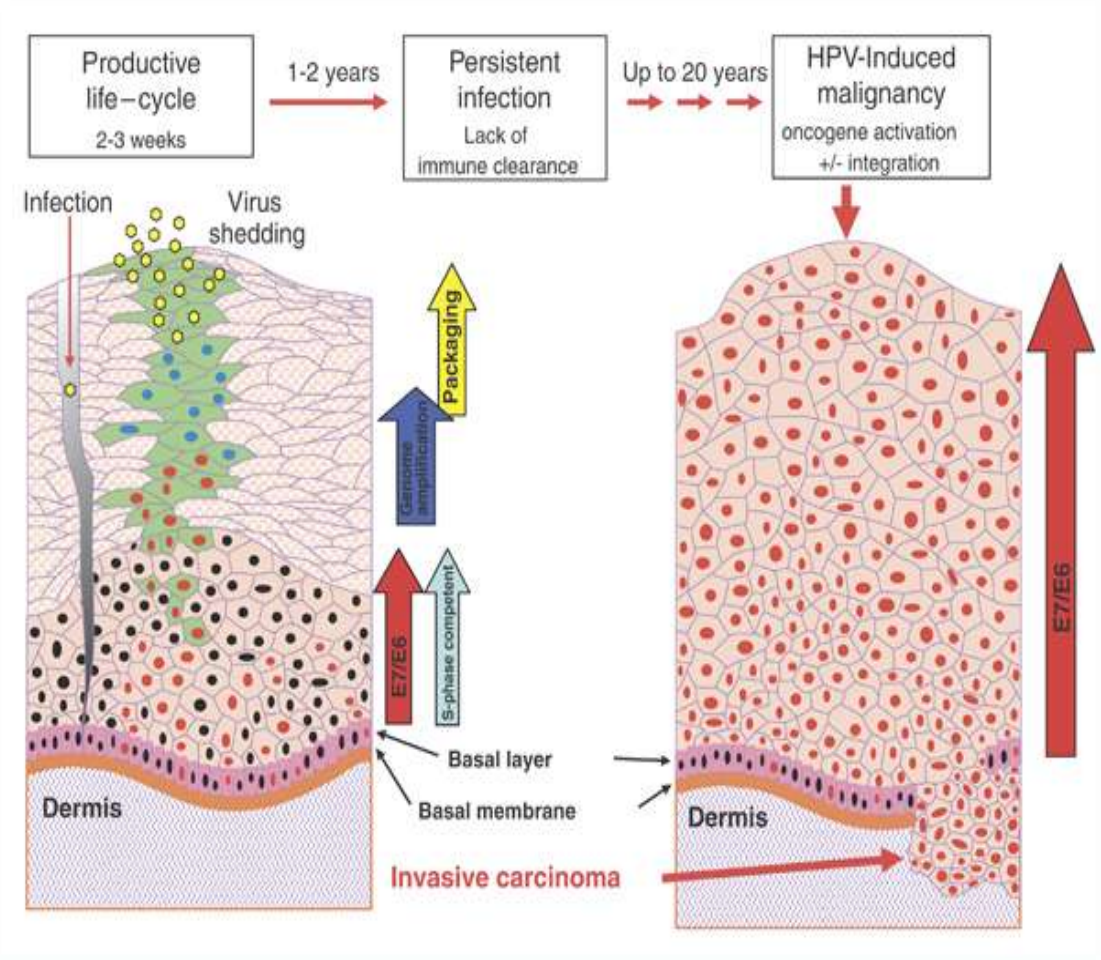

Figure 1.1: An illustration of the progression of HPV infection to cancer. The route of HPV infection (yellow dots) on the epithelial mucosa basal cell layer through micro traumas is shown in the left-hand panel. Different viral gene products are expressed and E6/E7 proteins increase s-phase competent cells thus promoting the amplification of viral genome which will result in the synthesis and shedding of new viral particles within 2-3 weeks. In cases where persistent infections occur, pre-cancerous lesions are not treated and high levels of viral DNA are detected gradually. Finally the host is pre-disposed to the development of cancer. This stage is characterised by loss of differentiation, inhibition of viral replication and increased levels of E6 and E7 oncoproteins as shown in the right-hand panel (Thomas *et al.,* 2008).

1.1.3 The risk and prevalence of cervical cancer in South Africa

In South Africa (SA), there are approximately 6800 new HPV infections per annum and approximately 3700 deaths resulting from cervical cancer annually (Bomela and Stevens, 2009). This means that cervical cancer is the leading cause of cancer death among women in SA (Bomela and Stevens, 2009). The national cervical cancer screening policy in SA is aimed at screening a minimum of 70% of women who use public sector services during a 10 year period by means of the Papanicolaou cytology technique (Pap smear) (Bomela and Stevens, 2009).

Despite its existence, implementing effective screening programmes has proven to be a difficult task, although women are encouraged to undergo Pap smears (Bomela and Stevens, 2009). The development of the HPV vaccine has provided hope in fighting cervical cancer; however, due to its high cost it is not currently available to women who rely on public sector services, which is the majority of affected women (Bomela and Stevens, 2009). Therefore preventative measures and early detection are often relied upon as strategies to manage this disease and prevent its high prevalence (Sibiya, 2012).

The severity of cervical cancer in South Africa is heightened by the HIV epidemic (Batra *et al.,* 2010). HIV positive women have a five times greater chance of developing CIN than HIV negative women (Batra *et al.,* 2010). The progression of CIN to cancer occurs rapidly in the presence of HIV (Batra *et al.,* 2010).

1.1.4 Cervical cancer is an AIDS defining malignancy

Acquired immunodeficiency syndrome (AIDS) has been previously associated with the development of certain cancers (Rabkin, 2001; Mbulaiteye *et al.,* 2003). Kaposi's sarcoma, Non-Hodgkin's lymphoma and cervical cancer are known to be AIDS defining malignancies

because they have been observed to occur more frequently in HIV infected people (Rabkin, 2001; Mbulaiteye *et al.,* 2003). The development of AIDS defining malignancies is mainly due to immuno-suppression; however, the risk for cervical cancer is further increased because both HIV and HPV are sexually transmitted viruses, therefore they have common sexual behavioural risk factors (Rabkin, 2001; Mbulaiteye *et al.,* 2003).

A study conducted in Sub-Saharan Africa revealed that cervical squamous intra-epithelial lesions and invasive cervical cancer are highly prevalent in HIV-positive women (Firnhaber *et al.,* 2012). High-risk HPV infection was found to be dominant among women in Sub-Saharan Africa and it persisted for a longer duration in HIV positive women (Firnhaber *et al.,* 2012). In another study it was observed that ~20% to 35% of HIV positive women without a history of cervical disease were likely to develop squamous intraepithelial lesions within 3 years (Sirera *et al.,* 2008).

HIV positive women in developing countries have had increasing access to highly active antiretroviral therapy (HAART) since 1995 and this has substantially improved life expectancy and reduced the risk and prevalence of opportunistic malignancies (Julg and Bogner, 2008; Sirera *et al.,* 2008; Firnhaber *et al.,* 2012). Studies have shown that HAART has significantly decreased morbidity and mortality in HIV patients; however, there is no consensus regarding the use of HAART and the development of cervical lesions, because some studies have observed no significant increase in cervical pre-cancerous lesions with the use of HAART whereas others have observed a significant increase (Sirera *et al.,* 2008; Firnhaber *et al.,* 2012).

1.1.5 The role of apoptosis in cancer and involvement of MUC1 and NFkβ

Cancer involves the disturbance of tissue growth (Bafna *et al.,* 2010). Normal tissue growth is regulated by the balance between cell proliferation and cell death (Bafna *et al.,* 2010).

Alteration of the genes that control cell growth and cell death is required for the transformation from normal to cancer cells (Bafna *et al.,* 2010).

Apoptosis is a tightly programmed cell suicide which occurs in multiple physiologic and pathological conditions where it plays an important role in tissue development and homeostasis by eliminating unwanted and damaged cells (Debatin, 2004; Plati *et al.,* 2008). During apoptosis harmful cells, especially those that have been genetically altered, are removed, therefore this process maintains the integrity of the organism (Plati *et al.,* 2008).

The underlying mechanism for the activation of apoptosis is not well understood; however, there are common features that have been observed to occur following apoptosis induction, such as damage to DNA and/or sub cellular structures (Debatin, 2004). This damage is spread by cellular stress which acts upon various molecules such as INK, MAPK/ERK, NFkβ, or ceramide and can have a significant impact on apoptosis pathways (Debatin, 2004; Mojakgomo, 2012).

Evasion of apoptosis is the most important hallmark of cancer because appropriate apoptosis signalling is crucial in maintaining the fine balance between cell death and cell survival (Plati *et al.,* 2008). Tumour development requires defects in the cell cycle which will promote uncontrolled proliferation (Plati *et al.,* 2008). On the other hand, cell proliferation is tightly controlled and has mechanisms that serve to detect abnormal proliferation by activating signalling pathways that induce senescence or apoptosis (Plati *et al.,* 2008).

In order to overcome the protective apoptotic signalling response, cancer cells have both proliferation-stimulating mutations and defects in the apoptotic pathway which work together to deregulate apoptosis (Plati *et al.,* 2008). Alternatively cancer cells cause the signalling of aberrantly activated survival pathways as a means to evade apoptosis (Plati *et al.,* 2008). Overall, the inhibition of apoptotic signalling provides enhanced survival capacity to cancer

cells and is responsible for their characteristic uncontrolled proliferation; consequently it has resulted in the development of many anti-neoplastic agents which exhibit their cytotoxic effects by inducing apoptosis (Plati *et al.,* 2008).

Apoptosis is controlled at different levels by various signalling pathways which will ultimately integrate into a complex network (Plati *et al.,* 2008). The defects occurring along the different apoptotic pathways are targets for new therapeutic strategies for cancer treatment (Plati *et al.,* 2008). One of the targets for inhibition of apoptosis in cancer is through survival factors (Plati *et al.,* 2008). Survival signalling pathways promote cellular proliferation; therefore, they are tightly regulated because they maintain homeostasis of healthy tissue (Plati *et al.,* 2008).

Survival pathways are integrated to apoptotic pathways through intricate signalling pathways; however, it has been hypothesised that the activation of survival through signalling pathways such as; phosphatidylinositol-3-kinase (PI3K)-AKT, NFkβ, and Ras-RaF-MEK-ERK pathways can suppress apoptotic signalling (Plati *et al.,* 2008). This linkage between cell survival and cell death pathways is manipulated by cancer cells; they activate survival signalling in order to evade an apoptotic response that would normally be activated by stimuli such as the removal of growth factors and/or genomic defects (Plati *et al.,* 2008).

Mucins have been shown to harbour complex relationships with many cellular pathways associated with cell growth, proliferation and apoptosis (Bafna *et al.,* 2010). It has been established that transformation in cancer refers to either initiation events, which are responsible for the early stages of neoplastic transition, or progression events, which refer to subsequent transformative processes (Bafna *et al.,* 2010). In addition, over expression and down regulation of mucins is often used in order to alter the tumorigenicity and metastasis of

various cancer cells *in vitro*, thus demonstrating their function in cancer pathogenesis (Bafna *et al.,* 2010).

In an attempt to understand the role of HAART in cervical cancer, the relationship between key proteins that act as important biomarkers for most cancers and are involved in various cellular signalling pathways, MUC1 and NFkβ1 (RelA or P65) (Caiscio *et al.*, 2011), was investigated under different antiretroviral drug treatments. The drugs belong to various classes which together comprise the HAART cocktail. The information gathered will assist in predicting the possible role of HAART in cervical cancer; with respect to cancer risk or prognosis with the use of HAART. The following paragraphs will further explain the role of MUC1 and NFkβ1 in cancer signalling.

1.2 LITERATURE REVIEW

1.2.1 Introduction to the mucin family

Various mucosal epithelium and hematopoietic cells express transmembrane glycoproteins known as mucins on their surface (Banerjee *et al.*, 2012). The mucin family is made up of proteins containing tandem repeat structures with a content of prolines, threonines and serines (Zaretsky *et al.*, 2006; Kufe, 2009). Furthermore, they characteristically have long glycosylations of the proline, threonine and serine domain through GalNAc O-linkages at the threonine and serine residues (Gendler, 2001; Zaretsky *et al.*, 2006; Kufe, 2009). The Human Mucin family (MUC) consists of secreted and transmembrane forms (Zaretsky *et al.*, 2006; Kufe, 2009).

The first line of defence for most epithelial surfaces is secreted mucins, including MUC2, MUC5AC, MUC5B, and MUC6 (Gendler, 2001). Mucins form a selective physical barrier between the mucosal surface and extracellular milieu, which becomes a mucous gel and is

responsible for protecting epithelial cells lining the respiratory and gastrointestinal tracts (Gendler, 2001; Zaretsky *et al.,* 2006; Kufe, 2009). Additionally, it forms part of the ductal surfaces of organs such as the liver, breast, pancreas and kidney (Gendler, 2001; Zaretsky *et al.,* 2006; Kufe, 2009). Secreted mucins were first identified in metazoans where they formed part of the epithelial barrier and regulated inflammatory response at the interface between the epithelium and its environment (Kufe, 2009). Mucins have since evolved as more complex transmembrane structures that play a role in the protection, repair and survival of epithelia in vertebrates (Zaretsky *et al.,* 2006; Kufe, 2009).

The transmembrane mucins, including MUC1, MUC4, MUC13 and MUC16, play a role in the second line of defence by detecting any disturbance to the environment and transmitting this information to the cells interior (Gendler, 2001). They are made up of a single membrane spanning region and they have ectodomains of o-glycosylated tandem repeats forming rod-like structures longer than 100nm from the cell surface, where their function is to form a protective mucous gel (Zaretsky *et al.,* 2006; Kufe, 2009). Cancer cells of epithelial origin often over express transmembrane mucins and this distorts their function of promoting growth and survival (Zaretsky *et al.,* 2006; Kufe, 2009; Banerjee *et al.,* 2012).

Mucins are well located in order to facilitate interactions between epithelial cells and their milieu (Dekker *et al.,* 2002). They function like a potent double-edged sword by preventing unwanted substances and organisms from entering the epithelium and simultaneously facilitate interactions through their highly complex structures (Dekker *et al.,* 2002).

Due to their position in cells, mucins are prone to be central in many disease processes, where interactions between epithelial cells and their surroundings have been disturbed, often including inflammatory and infectious diseases, cancer and metastasis, (Dekker *et al.,* 2002). Furthermore, mucins have the ability to initiate transformation and carcinogenesis in animal

models, making them highly attractive targets for anticancer treatment (Zaretsky *et al.*, 2006; Kufe, 2009).

1.2.2 The structure and function of MUC1

MUC1 is translated as a single polypeptide; however, during its auto proteolytic cleavage the MUC1 single peptide forms a stable non-covalent heterodimer which consists of an extracellular domain (MUC1-N) derived from the alpha subunit and a cytoplasmic tail (MUC1-C) derived from the beta subunit (Zaretsky *et al.*, 2006; Kufe, 2009; Banerjee *et al.*, 2012; Kumar *et al.*, 2012).

The MUC1-N is made up of 1000-2000 amino acids which are ordered as variable number of tandem repeats reaching approximately 200-500nm above the plasma membrane (Gendler, 2001; Banerjee *et al.*, 2012; Kumar *et al.*, 2012). The extracellular alpha subunit is glycosylated and it is mainly responsible for lubrication and the anti-adhesive properties of MUC1 on the mucosal surfaces (Meseguer *et al.*, 1998; Zaretsky *et al.*, 2006; Kufe, 2009; Kumar *et al.*, 2012). It is also known to block cell-cell and cell-extracellular matrix interactions (Meseguer *et al.*, 1998; Zaretsky *et al.*, 2006; Kufe, 2009; Kumar *et al.*, 2012). Proteolytic cleavage results in the release of MUC1-N from the cell surface; therefore, MUC1-C then acts as a receptor that interacts with various signalling pathways associated with transformation and tumour progression (Zaretsky *et al.*, 2006; Kufe, 2009; Kumar *et al.*, 2012).

The MUC1-C subunit is made up of a short extracellular domain excluding terminal repeats, a transmembrane domain and the cytoplasmic domain (Kumar *et al.*, 2012). Its cytoplasmic domain is composed of 72 amino acids including various tyrosine, serine, and threonine phosphorylation sites with the ability to bind to several proteins involved in regulating cancer by affecting cell proliferation, apoptosis and transcription of various genes (Bafna *et al.*,

2010; Kumar *et al.*, 2012). MUC1 cytoplasmic tail (MUC1-C) has been identified as a role player in cell signalling and interacts with important signalling molecules that are involved in cell cycle regulation and apoptosis including; EGFR, Wnt-β-catenin, P53, and NFkβ, thus adding another degree of functional complexity to MUC1 (Gendler, 2001; Hiscott *et al.*, 2001; Kumar *et al.*, 2012).

MUC1-C associates with the main effector of the canonical Wnt signalling pathway, β-catenin, and causes anchorage independent growth and tumorigenicity (Banerjee *et al.*, 2012). When MUC1-C interacts with β-catenin it localises to the nucleus where it interacts with many transcription factors and initiates various growth and survival pathways and by so doing suppresses various cell death pathways (Banerjee *et al.*, 2012).

MUC1-C also interacts with the IkB kinase complex resulting in the increase of phosphorylation and degradation of IkBα, and consequently assists in the activation of NFkβ; blocking apoptosis and inducing transformation (Zaretsky *et al.*, 2006; Kufe, 2009; Bafna *et al.*, 2010).

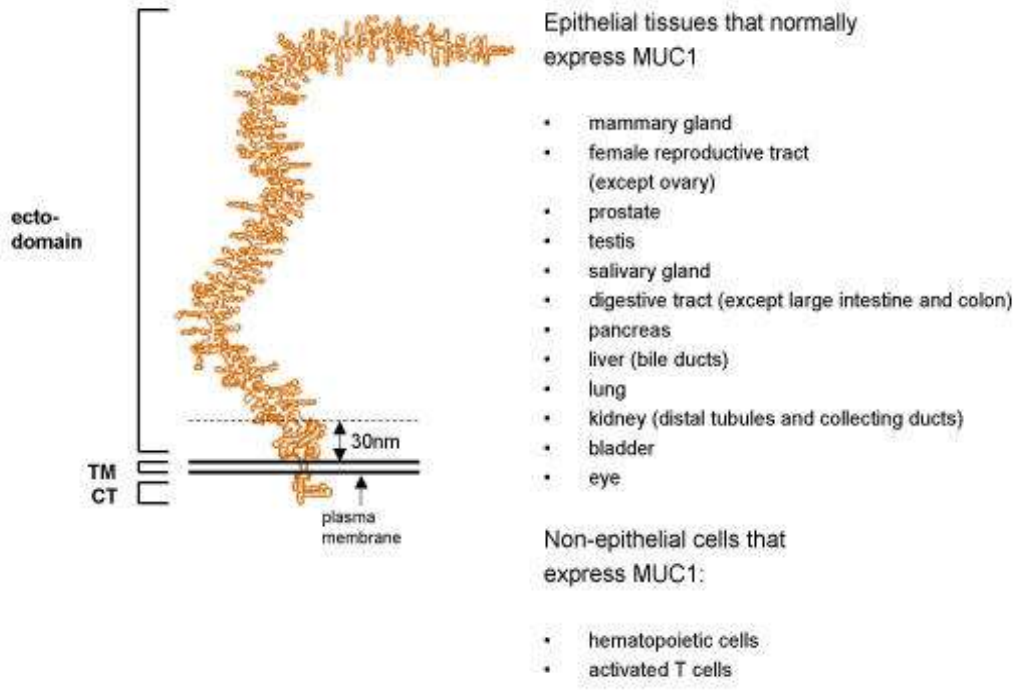

Figure 1.2: An illustration of the protein structure of the full length MUC1 protein in relation to the plasma membrane and normal expression pattern of MUC1 protein. The left-hand panel represents the three domains of MUC1; a long N-terminal extracellular (ecto) domain, the length of this domain above the plasma membrane represents the approximate distance that most cell surface MUC1 proteins extend into the peri-cellular space; a single membrane bound domain (TM); and a C-terminal cytoplasmic domain (CT). The right-hand panel shows the list of epithelial and non-epithelial human tissues that normally express MUC1 (Brayman *et al.*, 2004).

1.2.3 The expression of MUC1

MUC1 is expressed at low levels at the apical membrane of normal secretory epithelial cells; however, following transformation and loss of polarity in various cancer cells it becomes highly expressed over the entire surface (Gendler, 2001; Zaretsky *et al.,* 2006; Kufe, 2009; Kumar *et al.,* 2012). This event is associated with high metastatic potential and poor prognosis (Gendler, 2001; Zaretsky *et al.,* 2006; Kufe, 2009; Kumar *et al.,* 2012).

Statistics show that ~72% of tissue from new breast cancer patients, and ~66% of tissue from deceased breast cancer patients showed expression of MUC1 (Gendler, 2001). For a long time MUC1 was thought to be exclusive to epithelial tissues; however, it has recently been identified in other tissues, for example, haematopoietic cells (Gendler, 2001). Expression of MUC1 is controlled at the transcription level and the MUC1 gene promoter has many potential binding sites for regulators of transcription, including NFkβ (Gendler, 2001).

Although MUC1-C is generally found within the cytoplasm, it can translocate to the nucleus where it plays a role in regulating transcription (Kumar *et al.,* 2012). MUC1-C has attracted much attention in research due to its participation in intracellular signalling and transcriptional regulation and also the observation that it can translocate to the nucleus, unlike MUC1-N (Kumar *et al.,* 2012). The interaction of MUC1-C with various signalling molecules is thought to be responsible for the oncogenic effects of MUC1 (Bafna *et al.,* 2010).

1.2.4 Introduction to the nuclear factor kappa beta family

Nuclear factor kappa Beta (NFkβ) is a family of transcription factors (Hiscott *et al.,* 2001; Huxford *et al.,* 2009; Baiocchi *et al.,* 2012). The human genome encodes five polypeptides

which belong to the family of NFkβ subunits; NFkβ 1 (P50/P105), NFkβ 2 (P52/P100), RelA (P65), RelB and c-Rel (Hiscott *et al.,* 2001; Huxford *et al.,* 2009; Baiocchi *et al.,* 2012).

The Rel family polypeptides are structurally related; they all have a conserved 300aa region within the Rel homology domain and this domain also contains sequences that are essential for forming dimers, DNA binding, nuclear translocation and interaction with heterologous transcription factors (Hiscott *et al.,* 2001; Bharti and Aggarwal, 2002). P65, c-Rel and Rel B are the only members of the Rel family containing a transcription domain, although all members bind to DNA (Bharti and Aggarwal, 2002).

NFkβ subunits are able to form homo- and or heterodimers occurring mostly *in vitro* where the P50/P65 heterodimer predominantly exists (Hertlein *et al.,* 2005). In contrast to many transcription factors, NFkβ is primarily found in the cytoplasm where it is bound to IkB inhibitory proteins and is rendered inactive in that state (Hertlein *et al.,* 2005). Phosphorylation of IkB by the IkB kinase complex activates the common NFkβ pathway and by so doing results in its ubiquitination and proteosome mediated degradation (Baiocchi *et al.,* 2012).

After NFkβ is released and translocates to the nucleus it connects to its targeted genes (Baiocchi *et al.,* 2012). NFkβ activation has been observed in many human cancers, as shown by high nuclear localisation of NFkβ subunits such as P65 and P50 (Baiocchi *et al.,* 2012). NFkβ is suggested to promote cancer development and progression (Baiocchi *et al.,* 2012). High NFkβ signalling has the potential to inhibit apoptosis, increase proliferation and activate epithelial-mesenchymal transition by activating its target genes (Baiocchi *et al.,* 2012).

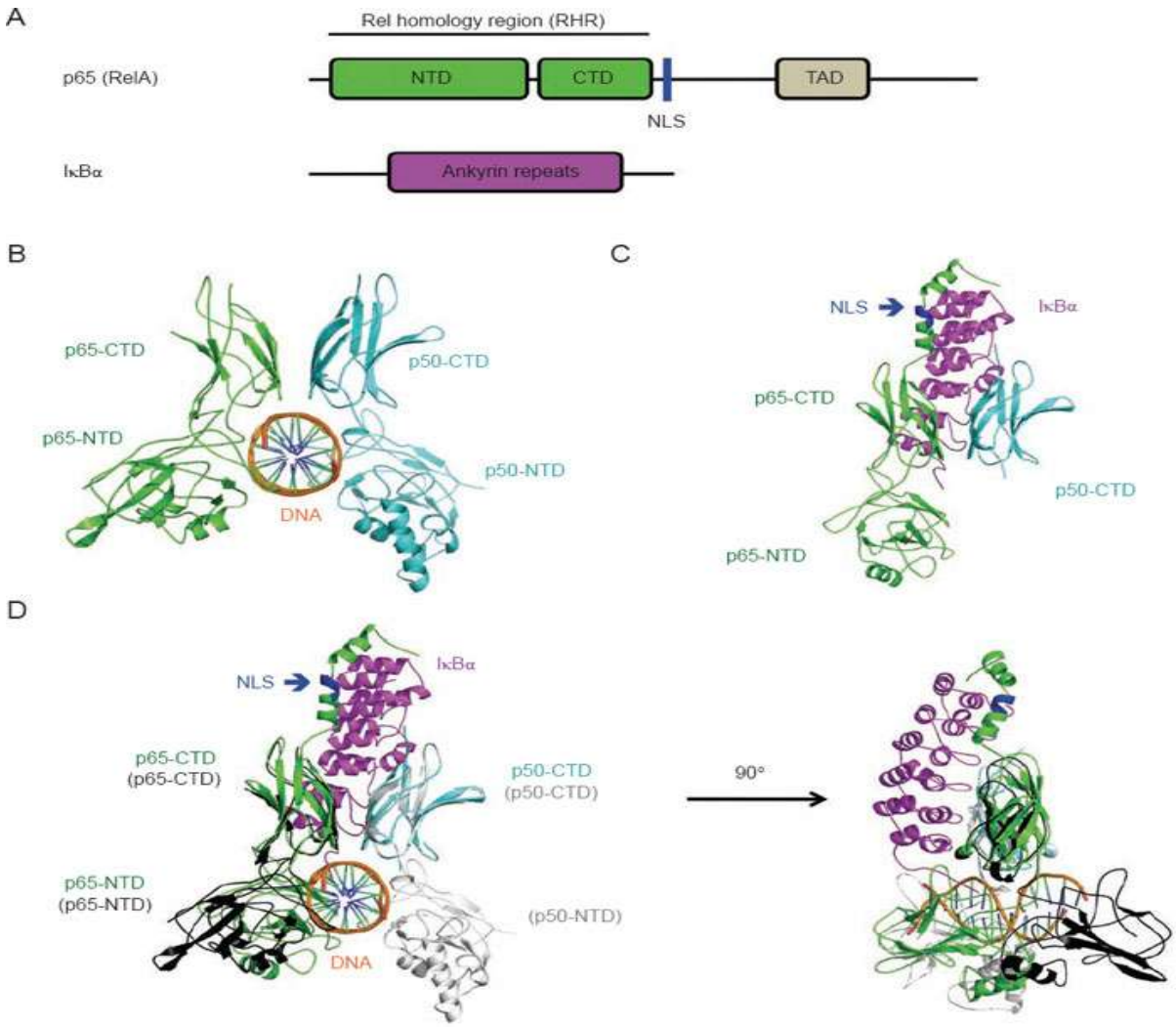

Figure 1.3: An illustration of the structure of NFkB and as complexes with DNA and IkB. **(a)** The upper row shows domain organisation of P65 (green) and IkBα (purple). NTD=N-terminal domain, CTD=C-terminal domain, TAD=trans-activation domain. **(b)** The middle row shows the structure the P65/P50 heterodimer and DNA complex. The location of the nuclear localisation signal (NLS) is also depicted here. **(c)** The bottom row depicts the structure of P65/P50 heterodimer and IkBα complex. Interaction of the P65/P50 heterodimer and IkBα complex results in a helical conformation of the NLS of P65. The P50 subunit (Cyan) is used to crystallise the complex and only contains CTD. The right-hand panel shows the P65/P50 heterodimer superimposed with DNA or IkBα. The P65 and P50 subunits in complex with DNA are shown in black and gray, respectively and when they interact with IkBα, the NTD of P65 changes conformation and thereby prevents DNA interaction (Zheng *et al.,* 2011).

1.2.5 The functions of NFkβ

NFkβ /IKB family includes transcriptional regulators which mediate the expression of more than 100 target genes, many of those genes function in the host immune response (Hiscott *et al.,* 2001; Shukla *et al.,* 2004). Proteins which are encoded by these genes are cytokines and chemokine receptors needed for immune recognition, antigen presenting proteins, and adhesion receptors which play a role in transmigration across blood vessel walls (Hiscott *et al.,* 2001; Shukla *et al.,* 2004). NFkβ has been named the central mediator of the immune response because it has such a broad role in immunity (Hiscott *et al.,* 2001; Shukla *et al.,* 2004).

Besides its extensive role in immunity, NFkβ has been shown to play a role in oncogenesis and in regulating apoptosis (Hiscott *et al.,* 2001; Bharti and Aggarwal, 2002). Tumour promoters activate the NFkβ pathway and therefore enhance cell survival; however, when it is down regulated cells are susceptible to apoptosis resulting from cytokines and chemotherapeutic agents (Bharti and Aggarwal, 2002).

NFkβ pathway presents a potential target against viral pathogens for many reasons; following exposure to a relevant inducer NFkβ is activated rapidly and thus leads to the quick transcription of many early viral, as well as cellular, genes (Hiscott *et al.,* 2001). Viral and bacterial pathogens, cytokines, and stress-inducing agents are but a few stimuli that activate the NFkβ/IkB complex and result in its phosphorylation (Hiscott *et al.,* 2001).

In contrast, NFkβ also regulates promoter activation of selected proapoptotic factors such as CD95L, CD95, TRAIL-R1, and TRAIL-R2 and it has been observed that under certain conditions NFkβ can promote apoptosis (Debatin, 2004). The cytotoxic effect of chemotherapy has been greatly improved by some anticancer treatments that induce the transcriptional activity of the NFkβ signalling pathway together with chemotherapy (Debatin,

2004). As, NFkβ potentially induces chemo resistance, therefore the inhibition of NFkβ needs to be further investigated, as a novel target against cancer (Debatin, 2004).

Tumour metastasis is usually the endpoint of carcinogenesis and makes cancer fatal (Bharti and Aggarwal, 2002). There is evidence to suggest that the activation of NFkβ promotes tumour cell proliferation, invasion, angiogenesis and metastasis (Bharti and Aggarwal, 2002). Therefore, inhibition of NFkβ in cancer cells may be targeted for cancer prevention (Bharti and Aggarwal, 2002). A combination of chemotherapeutic agents or gamma irradiation with NFkβ blockers could potentially be effective cancer therapy and should be further investigated (Bharti and Aggarwal, 2002).

1.2.6 The expression of NFkβ

The inactive form of NFkβ is found in the cytoplasm composed of three subunits; DNA binding P50 and P65 subunits and an inhibitory subunit (IkB) which is attached to P65 (Bharti and Aggarwal, 2002; Shukla *et al.,* 2004). The inhibitory subunit (IkB) is made up of IKK-α, IKK-β, IKK-γ and other unidentified proteins and when it is attached to NFkβ, it prevents it from entering the nucleus by concealing nuclear localisation sequence of NFkβ (Bharti and Aggarwal, 2002; Shukla *et al.,* 2004). When the inhibitory subunit (IkB) is released; NFkβ is activated and it translocates to the nucleus where it binds to target genes in the DNA (Bharti and Aggarwal, 2002; Shukla *et al.,* 2004).

1.2.7 The relationship between MUC1 and NFKβ

MUC1 over expression allows anchorage independent growth for cancer cells partly by activating the NFkβ pathways (Shukla *et al.,* 2004). The MUC1-CT is made up of many phosphorylation sites, consisting of seven tyrosine residues, and interacts with various

kinases such as glycogen synthase kinase 3β, protein kinase Cδ, c-Src and all members of the ErbB family (Thompson *et al.,* 2006).

Tyrosine phosphorylation plays a vital role in regulating the interaction of MUC1 with other proteins (Thompson *et al.,* 2006). Interestingly, in certain cancers it was found that MUC1 was located in the nucleus where it interacted with and regulated transcription factors, a role for MUC1 which was previously regarded unlikely (Thompson *et al.,* 2006).

These studied have highlighted the significance of investigating MUC1 in a new light i.e. probing for new signalling pathways that could be affected by MUC1 and trying to clarify the function of MUC1 in those pathways (Thompson *et al.,* 2006). One such pathway is the NFkβ pathway (Thompson *et al.,* 2006).

Silencing MUC1 in human cancers has been shown to reduce the activation of NFkβ P65 thus suggesting that MUC1-C plays as role in regulating the NFkβ P65 pathway (Shukla *et al.,* 2004; Cascio *et al.,* 2011). MUC1 also blocks the inhibitory proteins of NFkβ P65 by binding to NFkβ P65 and therefore enhancing its function (Shukla *et al.,* 2004; Cascio *et al.,* 2011).

1.2.8 An Introduction to the components of Highly Active Antiretroviral Therapy (HAART)

Prior to 1996, prophylaxis was the only available drug treatment used against HIV-1 opportunistic pathogens and AIDS associated illnesses (Arts and Hazuda, 2012). HIV-1 treatment has since improved with the development of drugs which inhibit reverse transcriptase and protease, which are important enzymes in the HIV life cycle (Arts and Hazuda, 2012). Although initially the antiretroviral (ARV) drugs were initially administered as monotherapy, they are now administered as a drug cocktail because the efficacy and

durability of the drugs is enhanced by combining them into one drug regimen (Arts and Hazuda, 2012).

The introduction of combination therapy known as highly active antiretroviral therapy (HAART), which consists of 3 or more antiretroviral drugs taken together, has been effective in decreasing morbidity and mortality related to HIV infection and AIDS (Arts and Hazuda, 2012). HAART has improved the prognosis and reduced the incidence of opportunistic infections that are associated with HIV/AIDS, in patients who adhere to the treatment plan (Bean, 2005). HAART significantly reduces viral replication and viral load of HIV-1 in the plasma to an extent that it becomes undetected; this results in clinically significant restoration of the immune system (Arts and Hazuda, 2012).

The compounds that are used as part of HAART belong exclusively to the class of Nucleoside/Nucleotide Reverse Transcriptase Inhibitors (NRTI), Non-Nucleoside Reverse Transcriptase Inhibitors (NNRTI) and Protease Inhibitors (PI) (Bean, 2005). These specific drug classes are used in combination because they all target different intracellular steps in the life cycle of HIV which are facilitated by two viral enzymes, Reverse Transcriptase (RT) and HIV protease (Bean, 2005).

Reverse transcription occurs 10 hours after HIV infection and the reverse transcriptase enzyme was the first to be identified and targeted for novel antiretroviral drug development (Arts and Hazuda, 2012). Reverse transcriptase enzyme performs various functions with RNA-dependant DNA polymerase, RNase-H, and DNA-dependant DNA polymerase activities (Arts and Hazuda, 2012). All these enzymes are integral to the conversion of single-stranded HIV-1 viral RNA into double-stranded DNA (Arts and Hazuda, 2012).

The mechanism of action of two classes of ARV agents; NRTIs and NNRTIs is targeted against reverse transcriptase (Arts and Hazuda, 2012). Overall there are twelve agents that

have been approved which belong to both the classes and they make-up for approximately half of all approved antiretroviral drugs (Arts and Hazuda, 2012). NRTIs and NNRTIs interact with the enzyme reverse transcriptase at different sites; however, they both target its ability to facilitate DNA polymerisation and therefore prevent the production of full-length viral DNA (Arts and Hazuda, 2012).

1.2.8.1 The mechanism of action of Nucleoside/Nucleotide Reverse Transcriptase Inhibitors (NRTIs)

The first class of drugs to be approved by the US food and drug administration (FDA) were NRTIs (Arts and Hazuda, 2012). NRTIs are administered as prodrugs, because prior to exhibiting their antiviral effect they have to enter the host cell and undergo phosphorylation by cellular kinases (Arts and Hazuda, 2012). The sugar (2'-deoxyribosyl) moiety of the NRTIs lacks a 3'-hydroxyl group, therefore inhibiting the formation of a 3'-5'-phosphodiester bond between the NRTIs and arriving 5'-nucleoside triphosphate, as a result the newly formed viral DNA-chain is terminated (Arts and Hazuda, 2012). The eight FDA approved NRTIs which are currently in use are; Abacavir (ABC, Ziagen), Didanosine (ddI, Videx), Emtricitabine (FTC, Emtriva), Lamivudine (3TC, Epivir), Stavudine (d4T, Zerit), Zalcitabine (ddC, Hivid), Zidovudine (AZT, Retrovir), and a nucleotide RT inhibitor Tenofovir Disoproxil Fumarate (TDF, Viread) (Arts and Hazuda, 2012).

The structure of NRTIs resembles that of natural nucleosides (Bean, 2005). Therefore following its phosphorylation by intracellular enzymes, it competes with natural nucleosides for incorporation into the new viral DNA by RT (Bean, 2005). When incorporated, NRTI hinders the elongation of the new DNA chain and stops the viral DNA replication process (Bean, 2005).

Nucleotide reverse transcriptase inhibitors involve two separate chemical steps prior to their cellular activation unlike nucleoside reverse transcriptase inhibitors which require three steps, in addition Tenofovir is negatively charged therefore it lingers in the cells and is activated for a prolonged period (Bean, 2005).

1.2.8.2 The mechanism of action of Non Nucleoside Reverse Transcriptase Inhibitors (NNRTIs)

The inhibition of HIV-1 reverse transcriptase by NNRTIs is facilitated by binding of the drugs close to the active site of reverse transcriptase, therefore causing the formation of a hydrophobic pocket (Arts and Hazuda, 2012). When NNRTIs are bound to reverse transcriptase, they alter the spatial conformation of the enzymes binding sites and decrease its activity (Arts and Hazuda, 2012). The newly formed hydrophobic pocket consists of hydrophobic and hydrophilic residues and only binds NNRTIs therefore it is only present when there are NNRTIs (Arts and Hazuda, 2012). There are four drugs belonging to this class that are currently used for therapy; Etravirine, Delavirdine, Efavirenz (EFV) and Nevirapine (Arts and Hazuda, 2012). Other drugs are currently in developmental stages (Arts and Hazuda, 2012).

NNRTIs bind to the reverse transcriptase enzyme downstream from its active catalytic site (Bean, 2005). HIV replication is thus inhibited by disturbing the transcriptional activity of the reverse transcriptase enzyme (Bean, 2005). The ARVs belonging to this class are more potent when co-administered with other ARV drugs (Bean, 2005).

1.2.8.3 The mechanism of action of Protease Inhibitors (PIs)

Protease inhibitors (PIs) were the final class of ARVs to be approved for HIV therapy (Arts and Hazuda, 2012) and they are active at an advanced stage in the life cycle of HIV, during

virus maturation whereby HIV-1 protease plays an important role by cleaving the precursors for the polyproteins which will produce the core protein and enzymes of mature viruses, a crucial step for the production of infectious viral particles (Bean, 2005; Arts and Hazuda, 2012). By inhibiting HIV protease activity the infected cell is rendered unable to produce infectious viruses (Bean, 2005).

PIs have been identified as the most effective agents developed thus far; however, they are large, peptide like compounds and need to be co-administered with an agent for example ritonavir (RTV), that does not significantly contribute to anti-viral activity but will prevent the metabolism and therefore enhance the concentration of other PIs in the cells (Arts and Hazuda, 2012).

There are currently ten approved PIs; Amprenavir (APV, Agenerase), Atazanavir (ATZ, Reyataz), Darunavir (TMC114, prezista), Fosamprenavir (Lexiva), Indinavir (IDV, crixivan), Lopinavir (LPV), Nelfinavir (NFV, Viracept), Ritonavir (RTV, Norvir), Saquinavir (SQV, Fortovase/Invirase) and Tipranavir (TPV, Aptivus) (Arts and Hazuda, 2012). Ritonavir (RTV) is the only available pharmacokinetic enhancer used currently with PIs however there are other drug agents that are being developed for clinical use (Arts and Hazuda, 2012).

The effects of PIs are enhanced when used alongside reverse transcriptase inhibitors (Bean, 2005; Israr *et al.,* 2011). In addition, two PIs, instead of one, are now being used more frequently because the combination has been shown to increase the potency of the PIs and enhance adherence to therapy (Bean, 2005; Israr *et al.*, 2011). The enhanced adherence to therapy is attributed to reduced pill burden, because the PI drug combination instead of individual pills reduces dose frequency and results in lower treatment costs therefore promoting adherence (Bean, 2005). A drug combining two PIs was developed, Kaletra

(Abbott laboratories), and it is currently the most frequently prescribed PI combination (Bean, 2005; Israr *et al.,* 2011).

LPV is a PI, and it inhibits the protease of human immunodeficiency virus type 1 (HIV-1) (Crommentuyn *et al.,* 2004; Israr *et al.,* 2011; Li *et al.,* 2011). Its structure is derived from ritonavir, and they both belong to the same class of ARV drugs and therefore they have similar mechanism of action (Crommentuyn *et al.,* 2004; Israr *et al.,* 2011). LPV has poor oral uptake and it is extensively and rapidly metabolised by the cytochrome P450 (CYP) 34A isoenzyme found in the liver, therefore its bioavailability is very low (Crommentuyn *et al.,* 2004; Israr *et al.,* 2011; Li *et al.,* 2011). As a result its efficacy is reduced when administered alone in ARV regimens (Crommentuyn *et al.,* 2004; Israr *et al.,* 2011).

Clinically the administration of LPV is coupled with RTV, which potently inhibits the activity of hepatic CYP3A4 in order to increase the plasma concentration and efficacy of LPV (Crommentuyn *et al.,* 2004; Israr *et al.,* 2011; Li *et al.,* 2011). Currently the RTV-boosted LPV (LPV/r) regimen is the only PI cocktail that is approved by the FDA to be used against HIV infection in adults and children (Crommentuyn *et al.,* 2004; Israr *et al.,* 2011; Li *et al.,* 2011). The LPV/r drug cocktail is generally well tolerated and does not result in unbearable toxicity (Crommentuyn *et al.,* 2004; Israr *et al.,* 2011; Li *et al.,* 2011). In addition, it decreases the total pill burden and therefore promotes adherence and patient acceptance (Crommentuyn *et al.,* 2004; Israr *et al.,* 2011; Li *et al.,* 2011).

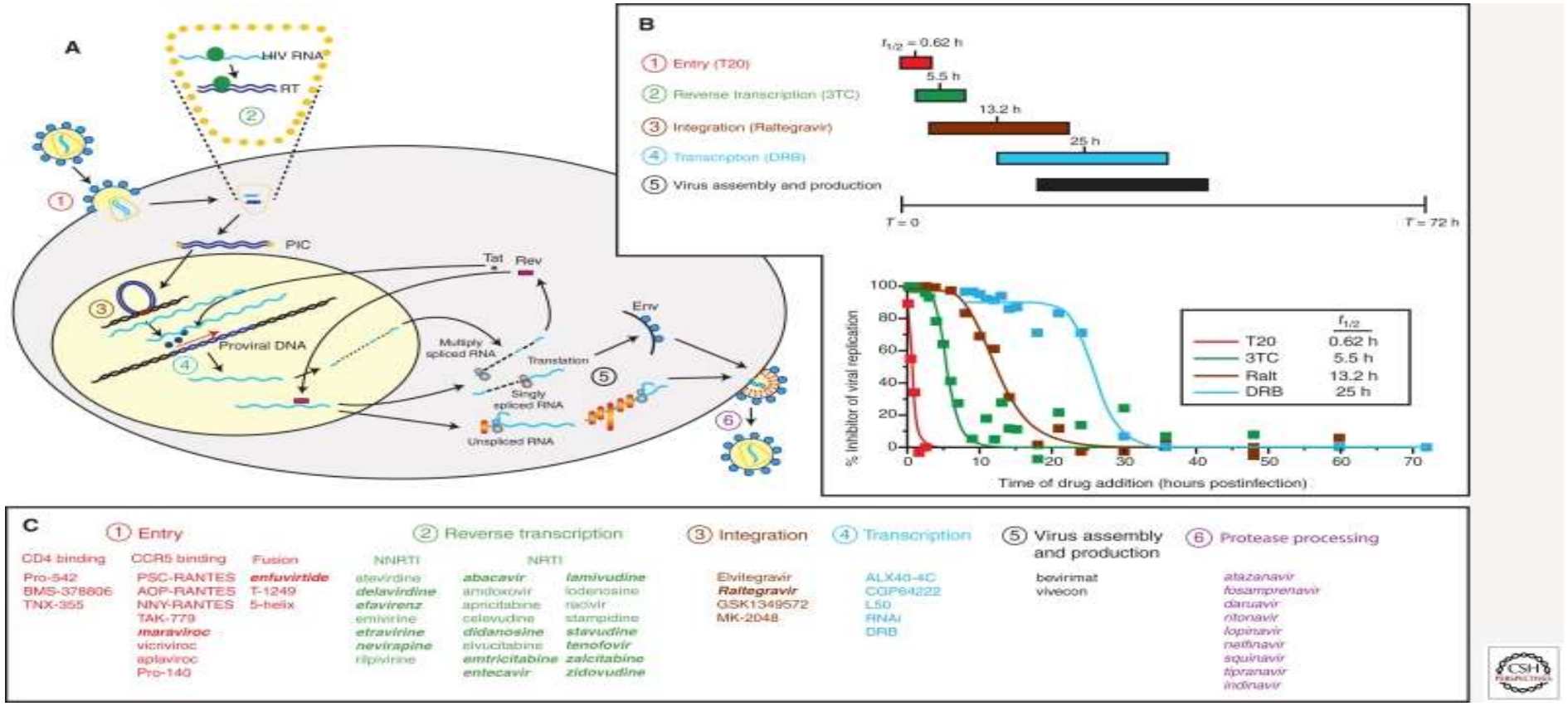

Figure 1.4: An illustration of the important steps in the life cycle of HIV-1 which are potential or current targets for antiretroviral drugs. **(a)** Schematic representation of HIV-1 life cycle in a susceptible CD4+ cell. **(b)** The time outline for the action of antiretroviral drugs during one cycle of HIV-1 replication. **(c)** A list of pre-clinical (represented by normal text) and FDA-approved inhibitors (represented by bold italic text) relative to specificity of action and drug target (Arts and Hazuda, 2012).

1.2.9 HIV/AIDS and associated malignancies

HIV positive women with low CD4+ T-cell counts have been shown to be at higher risk for HPV infection, the virus responsible for cervical cancer (Xi and Kiviat, 2004). In addition infection with HIV markedly increases the risk of cervical cancer and its precursor lesions, high- and low-grade squamous intraepithelial lesions (Xi and Kiviat, 2004). HIV induced immunodeficiency leads to the inability to control HPV infection and therefore this partly contributes to the development of cervical cancer due to HIV (Xi and Kiviat, 2004). Therefore in light of this proposed mechanism, HAART, which restores the immune status of HIV positive patients, is suggested to influence the outcome of HPV associated cervical lesions in HIV positive women (Xi and Kiviat, 2004). Findings from studies conducted on the effect of HAART on cervical lesions are not in agreement (Xi and Kiviat, 2004).

1.2.10 The effect of HAART on AIDS associated malignancies

The onset of HAART has led to major improvements in the clinical outcome and life expectancy of people infected with HIV/AIDS (Bratcher and Sahasrabuddhe, 2010). It was also anticipated that the resultant improved immunological status would lead to enhanced clearance of HPV infection in HIV positive women, unfortunately there has been no clear reduction in the burden and severity of cervical disease with the use of HAART, unlike other AIDS-related malignancies (Bratcher and Sahasrabuddhe, 2010). A better understanding of the interactions between HIV, HPV and HAART is becoming even more important because HIV positive women who are on HAART therapy are living longer and therefore they are at high risk of being infected with invasive cervical cancer (Bratcher and Sahasrabuddhe, 2010).

Antiretroviral regimens including PIs as part of the drug cocktail have been shown to be highly effective in reducing the rate of various opportunistic infections and certain carcinomas (Mistro *et al.,* 2004). Despite this invasive cervical cancer has continued to

increase in the HAART era, thus suggesting that HAART does not decrease its risk and possibly puts women at higher risk due to prolonged life expectancy, where early death would have possibly ensued had it not been available (Mistro *et al.*, 2004).

HIV protease inhibitors have been previously tested against HPV infection and LPV was shown to stabilise P53 and induce apoptosis in cervical carcinoma cells infected with HPV (Batman *et al.,* 2011). It is noteworthy that the dosages used were higher than those accomplished by oral administration however; these results suggest that LPV could act as a topical anti-HPV therapeutic (Batman *et al.*, 2011).

Many viruses including HIV and HPV have been shown to destabilize the function of host proteosomes in an effort to remove proteins that would be harmful to viral persistence (Batman *et al.*, 2011). E6 and E7 oncoproteins in HPV infected cells are mainly responsible for this function (Batman *et al.*, 2011). They assist in destroying certain cellular proteins, e.g. P53 and pRb, so as to initiate the viral life cycle (Batman *et al.*, 2011). In general LPV changes the level of various proteins which facilitate apoptosis and are regulated by proteosomal degradation (Batman *et al.*, 2011). In contrast to these *in vitro* findings HIV patients who are taking oral Lopinavir as part of a drug cocktail, HAART, do not present with better clearance of HPV-related lesions (Batman *et al.*, 2011).

1.3 RESEARCH OUTLINE

1.3.1 HYPOTHESIS

HAART has been shown to play a significant role in reducing the incidence of some AIDS defining malignancies, although its effect on cervical cancer is still unclear (Bratcher and Sahasrabuddhe, 2010). Immune reconstitution resulting from HAART has been attributed this function (Bratcher and Sahasrabuddhe, 2010); however, it is also possible that HAART might reduce cancer risk by interacting with different signalling molecules and pathways that are involved in cancer in order to induce cell death and thus inhibit cell proliferation. The hypothesis states that HAART plays a role in regulating the expression of *MUC1* and *P65*; key signalling molecules in cancer (Caiscio *et al.*, 2011), in order to induce cell death.

1.3.2 RESEARCH QUESTIONS

- Does HAART increase or decrease the gene expression of *MUC1* and *P65*?
- Does HAART change the protein expression pattern of MUC1 and P65?
- Do gene and protein expression of MUC1 and P65 correlate?
- Does HAART induce morphology characteristic of cell death in HCS-2 cells, and if so what type of cell death was induced?

1.3.3 AIMS AND OBJECTIVES

The aim of this study was to examine the expression of MUC1 and NFkβ1/ P65 in cervical cancer cells (HCS2) following treatment with HAART. MUC1 has been widely studied and targeted for therapy in a variety of cancers due to its unique structure which allows it to participate in various cell signalling pathways, Its involvement in the NFkβ pathway has not been widely studied therefore this study will investigate the relationship between MUC1 and a member of NFkβ family, P65 (RelA), when treated with the components of HAART in

order to better elucidate the role of HAART in cervical cancer. The outcome of this study will add new knowledge regarding the role of HAART in cervical cancer. In addition it will provide novel potential targets against cancer.

The objectives of the study were;

i) To quantify and compare the gene expression of *MUC1* and *P65* using quantitative real time Polymerase Chain Reaction (qPCR) following combination treatment with drugs classified as NRTIs, NNRTI and PIs

ii) To study and compare the protein expression of MUC1 and P65 following treatment with the various drugs using Laser Scanning Confocal Microscopy

iii) To study and compare the changes in the cell surface morphology of HCS-2 cells following drug treatment using the Scanning Electron Microscope.

CHAPTER TWO: METHODS AND MATERIALS

2.1 Cell culture

Human Squamous Cell carcinoma from Uterine Cervix, HCS-2 cell line was purchased from the Japanese Collection of Research Bioresources (JCRB) cell bank (National Institute of Health Sciences, Tokyo, Japan). The cells were routinely grown as a monolayer in Nunc tissue culture grade flasks of 25cm^2 or 50cm^2 (Thermo Scientific, Pittsburgh, PA, USA). The cells were maintained in a humidified environment of 5% CO_2 at a temperature of 37°C in Eagle's Minimal Essential Medium (EMEM) (Lonza, Basel, Switzerland) supplemented with 15% foetal calf serum (GIBCO, Darmstadt, Germany). The cells were incubated for approximately 2 days or until they reached ~ 60-80% confluency and were then harvested with 0.1% trypsin and 0.02% EDTA and seeded onto coverslips or they were frozen down in the culture medium supplemented with 5% DMSO (SIGMA, St Louis, MO, USA).

2.2 Cell counting

The cells were counted using a haemocytometer (Masters and Stacey, 2007). Following trypsinisation a cell pellet was collected at the bottom of a 10ml tube by centrifuging at 1250 rpm for 5mins. The cell pellet was re-suspended in 1ml media and 10µl of the cell suspension was diluted with 40µl of Trypan blue in a 1.5ml Eppendorf tube (Greiner Bio-One, Frickenhausen, Germany). The solution was vortexed and 20µl of the cell suspension was pipetted onto the haemocytometer grid. Viable cells excluded the Trypan blue dye whereas dead cells engulfed it, allowing the dead cells to be excluded during counting. An estimate of the cell density was calculated (Appendix I). Following cell counting the volume of cells needed to attain the desired cell density per coverslip was determined (Appendix I).

2.3 Drug preparation

2.3.1 Rationale for the chosen ARV drugs*;* The antiretroviral drugs used in the current study were chosen because they are widely used clinically (Clay *et al*., 2008; Horberg and Klein, 2010) and administered individually or as a drug cocktail in the form of a single pill known as Atripla consisting of Emtricitabine (FTC), Tenofovir disoproxil fumarate (TDF), and Efavirenz (EFV) and/or Kaletra which consists of Lopinavir (LPV) and Ritonavir (RTV) (Atripla®, 2006; Clay *et al*., 2008; Horberg and Klein, 2010; Kaletra®, 2010). Emtricitabine (FTC) (Emtriva, 2003), Tenofovir disoproxil fumarate (TDF) (Viread™, 2001), Efavirenz (EFV) (Atripla, 2006), Lopinavir (LPV) and Ritonavir (RTV) (Kaletra®, 2010) were purchased from Toronto Research Chemicals (North York, Canada).

Drug concentrations; The mean steady-state peak plasma concentration (Cmax) is the most physiologically relevant concentration for the ARVs because it represents naturally occurring concentrations of the drugs following their intake (Viread™, 2001; Emtriva, 2003; Atripla®, 2006; Kaletra®, 2010), hence it was used to treat the cells for 24 hours. Cmax concentrations are as follows for the drugs;

- FTC; Cmax= 1.8 µg/ml (Emtriva, 2003)
- TDF; Cmax= 0.3µg/ml (Viread™, 2001)
- EFV; Cmax= 4.07 µg/ml (Atripla®, 2006)
- RTV; Cmax= 2.45 µg/ml (Kaletra®, 2010)
- LPV; Cmax= 9.8 µg/ml (Kaletra®, 2010)
- Cocktail 1; 1.8 µg/ml FTC + 0.3µg/ml TDF + 4.07 µg/ml EFV
- Cocktail 2; 2.45 µg/ml RTV + 9.8 µg/ml LPV

2.3.2 Drug solutions; The drugs were initially dissolved in 1ml of primary diluent; 3600µg/ml FTC and 600µg/ml TDF were dissolved in distilled water whereas 6000µg/ml RTV, 98000µg/ml LPV and 40700µg/ml EFV were dissolved in methanol (diluents were specified in the certificate of analysis obtained from Toronto Research Chemicals Inc. for each drug). The drugs were further diluted in EMEM in order to obtain the desired Cmax concentrations as indicated above. The final concentration of methanol in working solution was 0.02%.

2.4 *MUC1* and *P65* gene expression

2.4.1 RNA extraction; The Gene-JET RNA Purification Kit purchased from Thermo Scientific was used to isolate RNA from cells and the manufacturer's protocol was followed. RNA was isolated from a minimum of $1X10^6$cells/ml. Following a 24 hour treatment with appropriate drugs (ATP and LPV/r), the growth medium (EMEM) containing the drugs were removed from the cells and the cells were rinsed once in PBS (pH 7.4) in order to remove residual medium. The cells were then harvested in trypsin EDTA and transferred to an RNAse-free microcentrifuge tube (Whitehead Scientific) following which the RNA extraction procedure was followed to isolate RNA from the cells (Appendix II). An aliquot of 5µl was prepared in order to measure the RNA concentration in the samples using a Nanodrop spectrophotometer (Appendix II; table 7.1). Genomic DNA was removed from all RNA samples isolated prior to complimentary DNA (cDNA) synthesis (Appendix II).

2.4.2 cDNA synthesis; The high capacity cDNA reverse transcriptase kit purchased from Applied Bio-systems was used to synthesize cDNA and the manufacturer's protocol was followed (Appendix II).

2.4.3 Primers; Primer sequences for *MUC1* and *P65* were obtained from Primer Bank and those for the reference genes RPLPO and TFRC (Adefolaju *et al*., 2013) were kindly donated by Ms Therese Dix-Peek from the Department of Internal Medicine, University of the Witwatersrand.

Table 2.1: Oligonucleotide sequences used for qPCR.

Gene	**Sequences (5'-3' direction)**	**Gene Bank Accession number**
MUC1	F: TGC CGC CGA AAG TAC G R: TGG GGT ACT CGC TCA TAG GAT	NM_001204294
P65	F: GTG GGG ACT ACG ACC TGA ATG R: GGG GCA CGA TTG TCA AAG ATG	NM_001145138
RPLPO	F: TGC AGC TGA TCA AGA CTG GAG ACA R: TCC AGG AAG CGA GAA TGC AGA GTT	NM_053275.3
TFRC	F: GGC ACC ATC AAG CTG CTG AAT GAA R: GTT GAT CAC GCC AGA CTT TGC TGA	NM_003234.2

MUC1= Mucin 1, cell surface associated; ***P65***= Transcription factor P65 (RELA); ***RPLPO***= Large Ribosomal Protein PO; ***TRFC***= Transferrin receptor.

2.4.4 Real Time PCR; The Power SYBR® Green PCR Master Mix was purchased from Applied Biosystems (Carlsbad, CA, USA) and the RT-PCR master mix was prepared as indicated in table 2.2 below. The final reaction volume was 20µl per tube and the tubes were centrifuged at 3000rpm for 3 minutes in a U-320 BOECO microcenrifuge before starting the PCR reaction.

Table 2.2: The composition of the qPCR reaction tube.

	Volume per reaction tube (µl)
SYBER green master mix	10
Forward primer	0.4
Reverse primer	0.4
cDNA	4
H_2O (nuclease free)	5.2
Total	**20**

The PCR reaction was carried out in the Applied Biosystems (AB) 7500 real time PCR system thermocycler and 40 amplification cycles were run under the following cycling conditions (as indicated in the Power SYBR® Green PCR Master Mix user guide, 2011). There were two technical repeats and the experiments were conducted in triplicates per sample.

Table 2.3: The thermal cycler conditions for the qPCR reaction.

	Hold	**Denature**	**Anneal/ Extension**
Temp °C	95	95	60
Time	10 minutes	15 seconds	1 minute

2.4.5 Data analysis; The $2^{-\Delta\Delta CT}$ method was used in order to calculate the fold change in gene expression relative to the control following treatment with the ARV drugs (Livak and Schmittgen, 2001). The data was first normalised using two reference genes (RPLO and

TRF1) and then the fold change was calculated. JMP11 software was used in order to conduct the statistical analysis on the data; an F-test (Brown-Forsythe test) was conducted in order to check whether the variances were equal. If there was a significant difference observed in the variance the data was transformed using log base10 in order to normalise it (Keen, 1995). A one way ANOVA test was conducted and where there was a significant difference observed, a Tukey Kramer *Post Hoc* test was further conducted in order to determine where the differences occurred.

2.5 Immunocytochemistry for the protein expression of MUC1 and P65

2.5.1 Cell seeding and drug treatment; Approximately $1X10^5$cells/ml were seeded and left overnight in order to attach. They were then supplemented with more EMEM the following day and left in the incubator until they reached ~50% confluency (~1 day). The media was removed and cells were rinsed 3X in PBS (pH 7.4) and treated for 24 hours with the appropriate ARV drugs. Following the drug treatment, the media containing the drugs were removed and cells were rinsed in PBS (pH 7.4). The cells were fixed in 4% Paraformaldehyde (PFA) for 15 minutes at room temperature (RT). The cells were then rinsed 3 times in PBS (pH 7.4) for 5 minutes each (Thabethe *et al.*, 2013). There were three technical repeats per run and the experiments were conducted six times.

2.5.2 Controls; the negative control consisted of untreated cells, whereas a positive control was MCF7 breast carcinoma cells because they are known to express MUC1 as it plays an integral role in breast cancer (Bitler *et al.*, 2009; Gil *et al.*, 2013). Experimental control consisted of samples whereby the primary antibodies were omitted in order to determine the amount of unspecific binding of the secondary antibodies.

2.5.3 Antigen retrieval and permeabilisation; citrate buffer (pH 6), was heated to 95°C and coverslips containing cells were placed in the citrate buffer (pH 6) for 10 minutes. Then they

were rinsed 3 times in PBS (pH 7.4) and permeabilised in 0.25% Triton-X100 in PBS (pH 7.4) at RT for 20 minutes.

2.5.4 Immunostaining; The cells were then rinsed 3 times in PBS (pH 7.4) and blocked in 10% goat serum in PBS (pH 7.4) for 1 hour at RT. Primary antibodies were prepared during the blocking period according to the optimised dilutions (Appendix III) and following which the cells were incubated with the primary antibodies; Anti-MUC1 rabbit monoclonal antibody (Abcam, Cambridge, United Kingdom) at a dilution of 1/150 and Anti-NFkB p65 mouse monoclonal antibody (Abcam, Cambridge, United Kingdom) at a dilution of 1/250 overnight at 4°C. Following the overnight incubation, the primary antibodies were removed and cells were rinsed 3 times in PBS (pH 7.4) and incubated with secondary antibodies; goat polyclonal to rabbit IgG conjugated with TRITC (Abcam, Cambridge, United Kingdom) and goat polyclonal to mouse IgG conjugated with FITC (Abcam, Cambridge, United Kingdom) for 2 hours in the dark at RT. Thereafter the secondary antibodies were removed and cells were rinsed 3 times in PBS (pH 7.4) and the nuclei were stained with 4', 6-diamidino-2-phenylindole, dihydrochloride (Dapi) for 10 minutes at a dilution of 1/10000.

2.5.5 Specimen mounting; The samples were rinsed in distilled water following the final rinse in PBS (pH 7.4), in order to get rid of excess salts. Excess liquid was removed from the specimen with filter paper by capillary action, then a small drop of Fluoromount (SIGMA, St Louis, MO, USA) was placed on the slide, the coverslip was then carefully lowered onto the slide in order to minimise formation of bubbles. Excess mounting media was collected by small filter paper pieces which were placed at the edges of the coverslips. The edges of the coverslips were sealed with nail polish and the slides were wrapped in foil in order to prevent bleaching of the fluorochromes upon exposure to light and they were stored at -20°C (Johnson, 2012).

2.5.6 Imaging and analysis; The cells were then viewed under a Zeiss LSM 780 confocal microscope and cells were visually analysed for the region of localisation of MUC1 and P65 proteins. Protein expression was compared between the treated cells and controls based on the fluorescence intensity of the protein markers and the location of specific fluorescence staining within the cells.

2.6 Surface morphology

2.6.1 Seeding and drug treatment; Approximately $1X10^5$cells/ml were seeded onto 22X22mm glass coverslips (Menzel-Gläser, Braunschweig, Germany) and left overnight in order to attach. They were then supplemented with more EMEM the following day and left in the incubator until they reached ~50% confluency (~1 day). The media was removed and cells were rinsed 3X in PBS (pH 7.4) and treated for 24 hours with the appropriate ARV drugs. Following the drug treatment, the media containing the drugs were removed and cells were rinsed in phosphate buffer (pH 7.4). There were three replicates per samples and the experiment was repeated three times.

2.6.2 Fixation; the cells were fixed for 30 minutes in 2.5% Glutaraldehyde (Agar Scientific, Stansted, United Kingdom), rinsed in phosphate buffer and treated with 1% Osmium tetroxide (Agar Scientific, Stansted, United Kingdom) for 10 minutes. The cells were rinsed in dH_2O and treated for 5 minutes with 1% Thiocarbarhydrizide, acts as a ligand and enhances the binding of Osmium and the conductivity of the sample by increasing the generation of secondary electrons (Murakami *et al.*, 1987; Jongebloed *et al.*, 1999), rinsed in dH_2O, then treated with 1% Osmium tetroxide for 5 minutes and then rinsed in phosphate buffer (pH 7.4).

2.6.3 Dehydration and coating; The cells were then dehydrated through a graded series of alcohols; 50%, 70%, 80%, 95% and 3X 100% for 5 minutes each. Then treated with hexamethyldisilazane (HMDS) (SIGMA, St Louis, MO, USA) for 30 seconds and kept in a desiccator containing silica gel until the samples were coated. The cells were then coated with a double layer of carbon by an EMITECH K950X.

2.6.4 Imaging and analysis*;* HCS-2 cells were viewed under a Zeiss Ultra FEG Scanning Electron Microscope and descriptive and statistical analysis were conducted on the surface morphology of the cells. A scoring system was established and used in order to analyse differences in cell contacts, microvilli density and size, blebbing density and size, and presence of cell secretions. The JMP11 software was used in order to conducts the statistical analysis following the descriptive analysis and a one way ANOVA test and a Tukey Kramer *Post Hoc* test were used.

Table 2.4: Scoring system used in order to analyse surface morphology of the cells

Surface characteristics	**Scoring system**
Microvilli density	**Relative distribution of microvilli on the cell surface;** 1= sparse, 2=medium, 3= dense
Microvilli size	**Relative length of microvilli on the cell surface;** 1= short, 2= mixture of short and long microvilli, 3= long and thin microvilli
Cell contacts	**Relative percentage of long and thin cytoplasmic projections (e.g. Filopodia)per cells and connections between adjacent cells;** 1= ~0-20% of projections from the cell surface and there are less connections to adjacent cells, 2= ~21-50% of projections from the cells surface and many of them are disrupted therefore are not a lot of connections formed between the cells, 3= ~51-100% of projections from the cells and many cell connections between adjacent cells
Blebbing density	**Relative distribution of blebs/surface protrusions on the cell surface;** 1= none, 2= sparse, 3= medium, 4= dense
Bleb size	**Relative size of blebs/ surface protrusions on the cell surface;**1= none, 2=small, 3= medium, 4= large
Cell shape	**Change in cell shape;** 1= round, 2= oval, 3= flattened
Membrane bound secretions	**Relative amount of secretions on the surface of the cell;** 1= none, 2= few, 3= moderate, 4= abundant
Extracellular secretions	**Relative amount of secretions on the extracellular space;** 1= none, 2= few, 3= moderate, 4= abundant

CHAPTER THREE: RESULTS

3.1 *MUC1* and *P65* gene expression in HCS-2 cells using real-time polymerase chain reaction (qPCR)

The expression of *MUC1* and *P65* was examined following treatment with the drug combinations making up HAART namely; Atripla (which consists of one NNRTI and two NRTI's) and Kaletra (which consists of two PI's). MUC1 plays an important role in cell signalling and promotes cell growth in various cancers (Banerjee, *et al*., 2012). P65 is a transcription factor which is responsible for controlling cell growth and differentiation, when its expression is low it promotes apoptosis (Shukla, *et al*., 2004; Bharti and Aggarwal, 2002).

Negative controls whereby the template DNA was substituted for water were included in the experiments in order to determine whether there was contamination or non-specific amplification in the reagents. The results showed that there was no amplification in the wells whereby the template DNA was omitted, therefore the reagents were not contaminated with foreign DNA.

An F-test (Brown-Forsythe test) was conducted in order to check whether the variances were homogenous. P-values obtained; P= 0.07 for *MUC1* and P= 0.02 for *P65* rejected the assumption of homogeneity of variances. In order to normalise the data, it was transformed using log base10 (Keen, 1995). The transformed values were used in order to analyse fold difference in *MUC1* and *P65* expression and a one way ANOVA test was conducted.

Overall there was a decrease in the expression of *MUC1* and *P65* following treatment with the diluent, and the drug treatments (ATP and LPV/r) as indicated in table 3.1 and 3.2. The fold change for *MUC1* expression following treatment with the diluent, ATP and LPV/r was 0.7-fold, 0.8-fold and 0.2-fold respectively. This suggests that there was a 0.3 (30%), 0.2

(20%) and 0.8 (80%) down-regulation in *MUC1* following treatment with diluent, ATP and LPV/r respectively. The fold change for *P65* expression following treatment with the diluent, ATP and LPV/r was 0.5-fold, 0.6-fold and 0.1-fold respectively. This suggests that there was a 0.5 (50%), 0.4 (40%) and 0.9 (90%) down-regulation in *P65* following treatment with diluent, ATP and LPV/r respectively.

The statistical data in table 3.3 show that there was a significant difference in the fold change for *MUC1* expression following drug treatment ($P<0.05$). Although *P65* was down-regulated following treatment with diluent, ATP and LPV/r as shown in table 3.2, the statistical test showed that the fold change for *P65* expression was not significantly different between the different groups ($P>0.05$).

A Tukey-Kramer *Post Hoc* test was conducted for *MUC1* and *P65* expression (Appendix II; table 7.6 and table 7.7), in order to compare the means and the results showed that there was a significant difference observed in fold change between cells treated with the PI combination (i.e. LPV/r) and the other groups (i.e. untreated, 0.02% methanol and Atripla) suggesting that *MUC1* down-regulation was higher in this group (PI) than any other. There was no significant difference observed in *P65* expression.

Table 3.1: The fold change for *MUC1* expression following treatment with various antiretroviral drugs. The values were calculated using the $2^{-\Delta\Delta CT}$ method.

Sample	*MUC1* Ave Ct	HKG Ave Ct	ΔCt *MUC1*-HKG	ΔΔCt= ΔCt (treated) - ΔCt (untreated)	Fold change (RQ) $2^{-\Delta\Delta CT}$	RQ min	RQ max
Negative control	21.27 ± 0.20	18.10 ± 1.67	2.27 ± 0.51	0 ± 0.51	1	0.72	1.46
Diluent control	22.24 ± 0.16	19.40 ± 0.59	2.84 ± 0.63	0.56 ± 0.63	0.7	0.48	1.06
ATP	21.35 ± 0.19	18.68 ± 0.69	2.67 ± 0.80	0.40 ± 0.80	0.8	0.45	1.33
LPV/r	21.00 ± 0.14	16.37 ± 0.84	4.63 ± 0.86	2.36 ± 0.86	0.2	0.11	0.42

Table 3.2: The fold change for *P65* expression following treatment with various antiretroviral drugs. The values were calculated using the $2^{-\Delta\Delta CT}$ method.

Sample	*P65* Ave Ct	HKG Ave Ct	ΔCt *P65*-HKG	ΔΔCt= ΔCt (treated) - ΔCt (untreated)	Fold change (RQ) $2^{-\Delta\Delta CT}$	RQ min	RQ max
Negative control	20.67 ± 0.36	19.00 ± 0.56	1.67 ± 0.69	0 ± 0.69	1	0.63	1.62
Diluent control	21.40 ± 0.23	19.40 ± 0.59	2.00 ± 0.65	0.33 ± 0.65	0.5	0.52	1.27
ATP	24.89 ± 1.36	18.68 ± 0.69	6.21 ± 1.71	4.54 ± 1.71	0.6	0.38	1.05
LPV/r	21.10 ± 0.11	16.37 ± 0.84	4.61 ± 0.85	2.94 ± 0.85	0.1	0.07	0.32

Table 3.3: Analysis of variance on the transformed data, using a one way ANOVA test for *MUC1* and *P65* expression

Source	DF	Sum of Squares		Mean Square		F Ratio		Prob> F	
	MUC1* & *P65	***MUC1***	***P65***	***MUC1***	***P65***	***MUC1***	***P65***	***MUC1***	***P65***
Group	3	0.73222500	4.571100	0.244075	1.52370	23.9289	0.5149	0.0002*	0.6834
Error	8	0.08160000	23.672267	0.010200	2.95903				
C Total	11	0.81382500	28.243367						

*= p value is significantly different

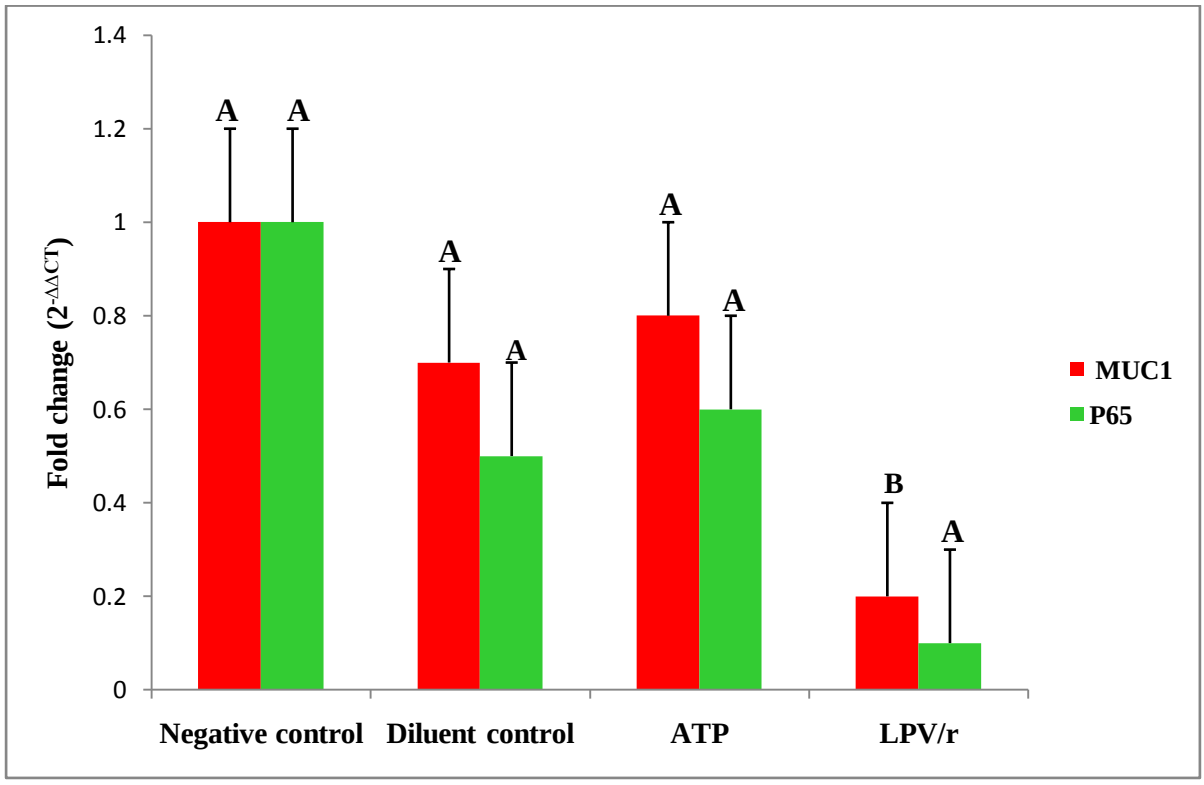

Figure 3.1: The effects of antiretroviral drugs (Atripla and Kaletra combinations) on *MUC1* and *P65* expression following 24 hours treatment. The fold change for *MUC1* expression between the groups show that there was a significant difference observed (P<0.05); the protease inhibitor combination, LPV/r, significantly reduced *MUC1* expression in comparison to the controls and ATP treatment. In contrast there was no significant difference observed (P>0.05) in fold change for *P65* between the different groups, however; treatment with the diluent control and the drugs reduced *P65* expression. Bar graphs not connected by the same letter (per characteristic) are significantly different, Tukey Kramer *Post Hoc* analysis.

3.2 Immunofluorescence for MUC1 and P65 proteins in HCS-2 cells following treatment with antiretroviral drugs

The cytoplasmic tail of MUC1 plays an important role in cell signalling and has been shown to interact with many transcription factors where it initiates various growth and survival pathways and by so doing suppresses various cell death pathways (Banerjee *et al.,* 2012). It has also been linked to metastasis (Banerjee *et al.,* 2012). NFkβ1 (P65) is a transcription factor that is responsible for growth control, differentiation and apoptosis; however, when it is down regulated cells are susceptible to apoptosis resulting from cytokines and chemotherapeutic agents (Shukla *et al.,* 2004; Bharti and Aggarwal, 2002).

MUC1 and P65 were co-localised in the HCS2 cell line following drug treatment with FTC, TDF, EFV, and drug combinations; ATP and LPV/r. The antibody used for MUC1 was specific to the cytoplasmic domain of MUC1 whereas in its inactive form P65 is highly expressed in the cytoplasm and relocates to the nucleus when activated (Banerjee *et al.,* 2012). Therefore MUC1 staining was expected to be detected in the cytoplasm and if P65 was activated then it's staining was expected to be found in the nucleus as well.

Negative controls (untreated cells) showed a positive expression of MUC1 throughout the cytoplasm; it was highly expressed towards the periphery of the cell and expression was seen also along the cell extensions forming contacts with adjacent cells. P65 was highly expressed in the perinuclear region, since it is mainly active in the nucleus. This location is fundamental to its role because its close proximity to the nucleus ensures that it relocates to the nucleus promptly and with ease when activated (Fig3.2).

The diluent control (0.02% Methanol) reduced the expression of MUC1 and P65 (Fig3.3). MCF7 cell line was used as a positive control in order to validate protein expression because the proteins of interest, MUC1 and P65 are known to be expressed in breast cancer (Cascio *et*

al., 2011). Quality control of the secondary antibody was also included by omitting the primary antibodies in order to determine whether the secondary antibodies bind non-specifically to other targets within the cell and as observed in the photomicrograph, Fig3.4-3.5, there was no non-specific binding.

In drug treated cells, (FTC, TDF, EFV, ATP and LPV/r) there was a relatively decreased expression of MUC1 and P65 in comparison to the controls. MUC1 expression was not vastly distributed within the cytoplasm in treated cells, but mainly localised at the perinuclear region and p65 expression was reduced in the cytoplasm and not observed in the nucleus, the expression of both proteins appeared relatively down regulated with drug treatment in comparison to the controls. Although the degree of reduction appeared to be more variable for MUC1 expression because the drugs did not all have a similar effect on its expression. FTC, EFV and LPV/r treatments reduced MUC1 expression more than TDF and ATP (Fig 3.7-3.11). In contrast the degree of reduction for P65 appeared to be similar for most drug treatments, with exception for ATP treatment because it reduced it more than the other drugs (Figs 3.10).

In addition some cells presented with lateral plasma membrane protrusions, blebs, further suggesting that the cells where undergoing cell death, as this feature is characteristic of cells undergoing cell death especially via apoptosis (Majno and Joris, 1995).

Table 3.4: Summary of MUC1 and P65 co-localisation

	MUC1	**P65**	**Blebbing**
Controls; ➢ Negative ➢ Diluent	Uniformly expressed across the cytoplasm, expression slightly reduced in diluent	Uniformly expressed in the peri nuclear region, expression slightly reduced in diluent	Absent
NRTIs; ➢ FTC ➢ TDF	Sparse cytoplasmic expression	Decreased expression in the peri nuclear region	Present
NNRTIs; ➢ EFV	Sparse cytoplasmic expression	Decreased expression in the peri nuclear region	Present
ATP combination; ➢ FTC+TDF+EFV	Sparse cytoplasmic expression	Decreased expression in the peri nuclear region	Present
PI; ➢ LPV/r	Sparse cytoplasmic expression	Decreased expression in the peri nuclear region	Present

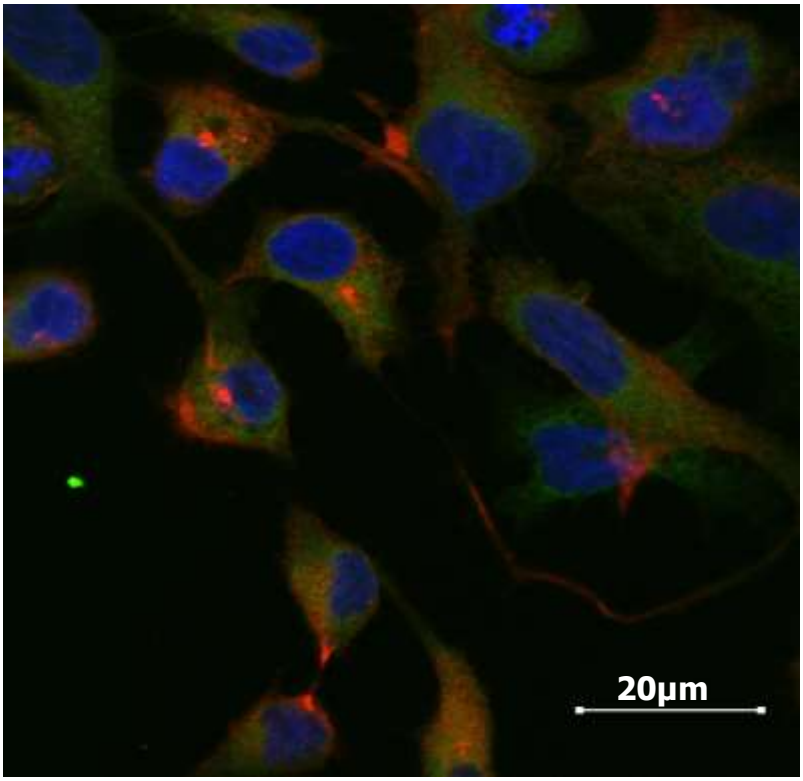

Figure 3.2: Representative micrograph showing untreated HCS-2 cells (negative control). MUC1 was localised with anti-MUC1 rabbit monoclonal antibody and goat polyclonal to rabbit IgG conjugated with TRITC (red fluorochrome). P65 was localised with anti-NFkB P65 mouse monoclonal antibody and goat polyclonal to mouse IgG conjugated with FITC (green fluorochrome). The nuclei were counterstained with Dapi (blue).

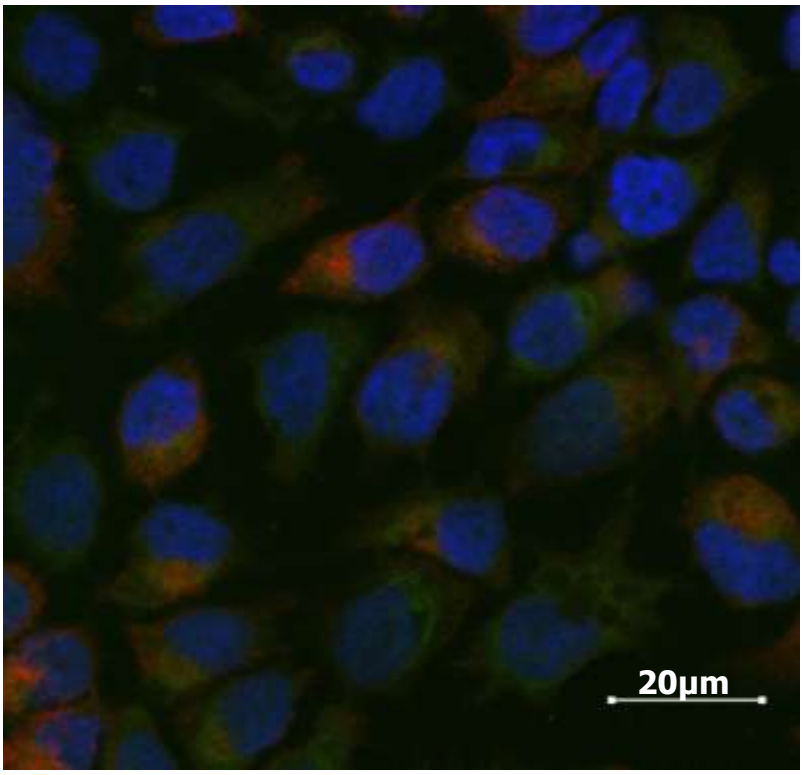

Figure 3.3: Representative micrograph showing HCS-2 cells treated with 0.02% methanol (diluent control). MUC1 was localised with anti-MUC1 rabbit monoclonal antibody and goat polyclonal to rabbit IgG conjugated with TRITC (red fluorochrome). P65 was localised with anti-NFkB P65 mouse monoclonal antibody and goat polyclonal to mouse IgG conjugated with FITC (green fluorochrome). The nuclei were counterstained with Dapi (blue).

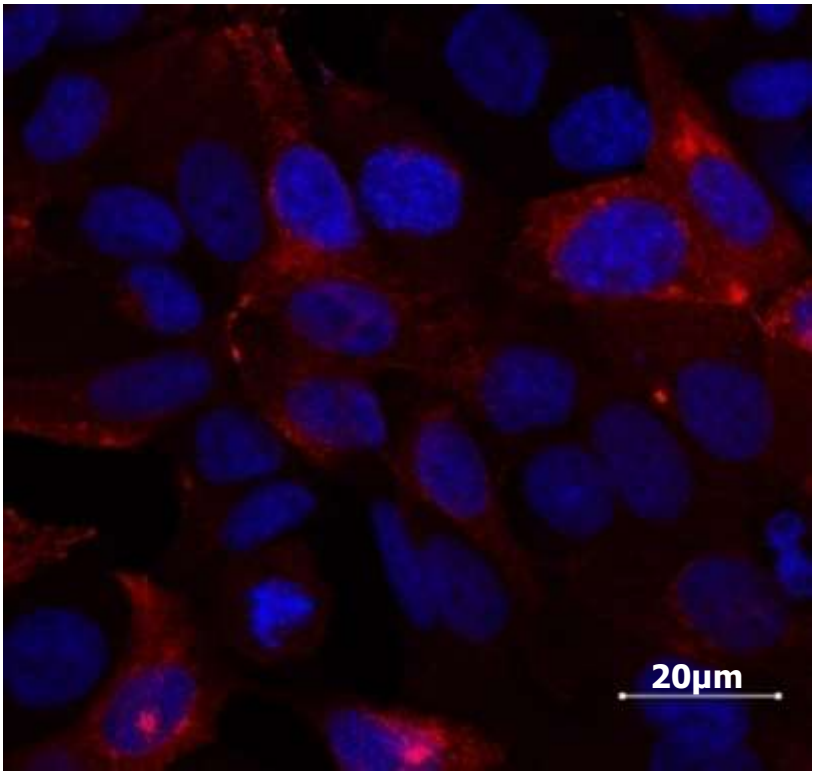

Figure 3.4: Representative micrograph showing MCF-7 cells (positive control). MUC1 was localised with anti-MUC1 rabbit monoclonal antibody and goat polyclonal to rabbit IgG conjugated with TRITC (red fluorochrome). The nuclei were counterstained with Dapi (blue).

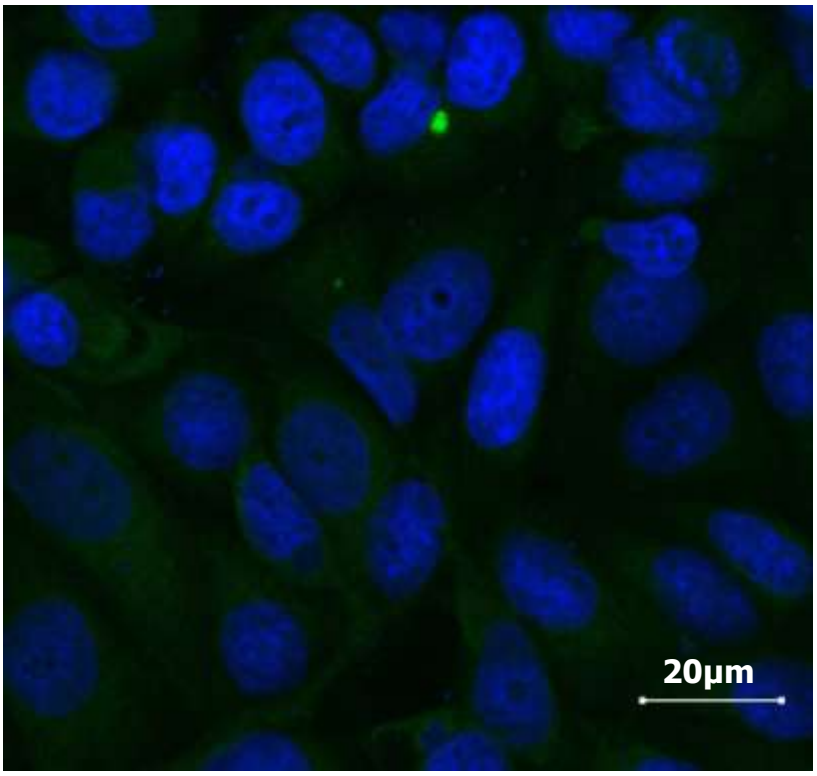

Figure 3.5: Representative micrograph showing MCF-7 cells (positive control). P65 was localised with anti-NFkB P65 mouse monoclonal antibody and goat polyclonal to mouse IgG conjugated with FITC (green fluorochrome). The nuclei were counterstained with Dapi (blue).

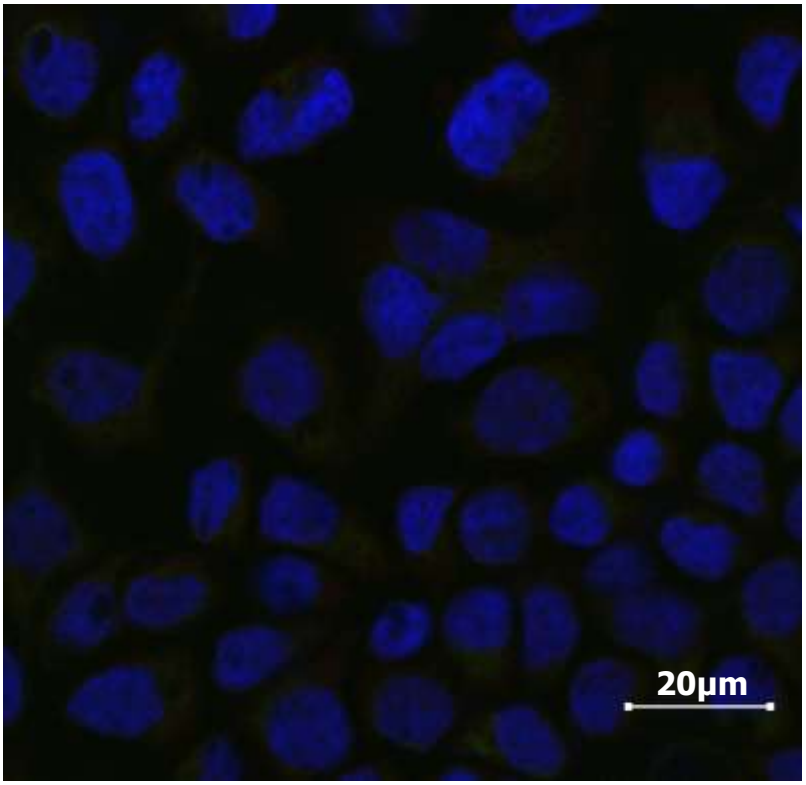

Figure 3.6: Representative micrograph showing untreated HCS-2 cells (without primary antibodies). The primary antibody was omitted in order to determine whether the secondary antibody binds exclusively to their targets. Inconspicuous localisation of the secondary antibodies in the cytoplasm indicates that the primary antibody only binds to the specific target and no other regions within the cells. The nuclei were counterstained with Dapi (blue).

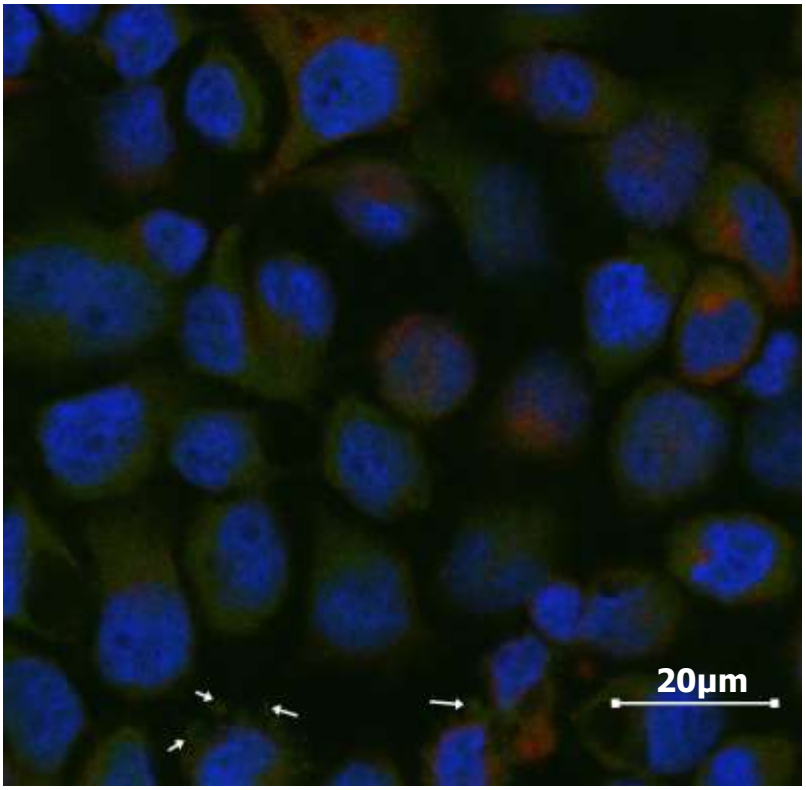

Figure 3.7: Representative micrograph showing HCS-2 cells treated with 1.8 µg/ml of FTC. MUC1 was localised with anti-MUC1 rabbit monoclonal antibody and goat polyclonal to rabbit IgG conjugated with TRITC (red fluorochrome). P65 was localised with anti-NFkB P65 mouse monoclonal antibody and goat polyclonal to mouse IgG conjugated with FITC (green fluorochrome). The nuclei were counterstained with Dapi (blue). The arrows depict plasma membrane blebbing on the surface of the cells.

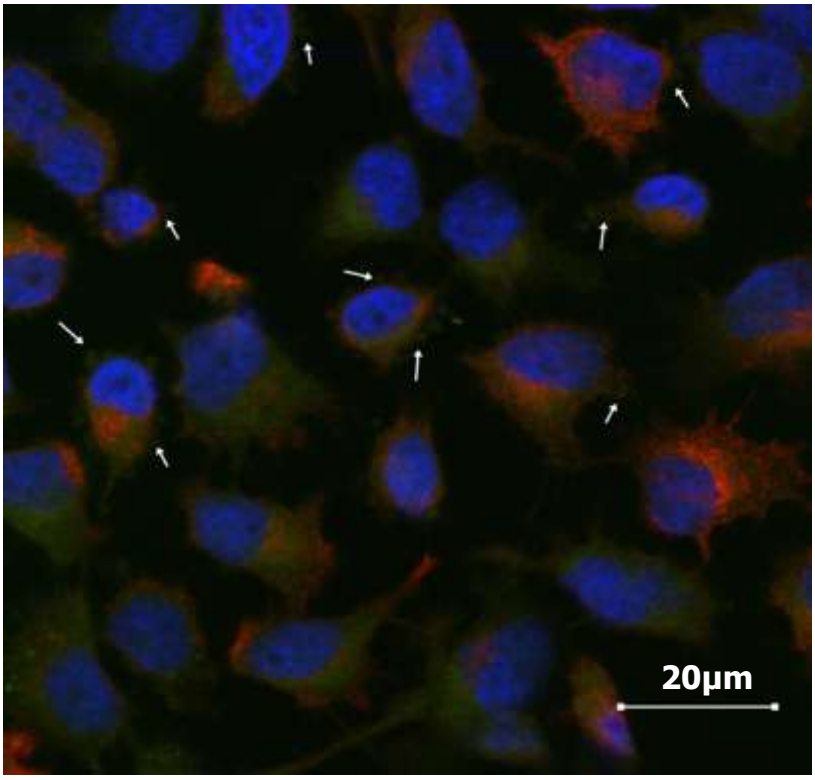

Figure 3.8: Representative micrograph showing HCS-2 cells treated with 0.3 µg/ml of TDF. MUC1 was localised with anti-MUC1 rabbit monoclonal antibody and goat polyclonal to rabbit IgG conjugated with TRITC (red fluorochrome). P65 was localised with anti-NFkB P65 mouse monoclonal antibody and goat polyclonal to mouse IgG conjugated with FITC (green fluorochrome). The nuclei were counterstained with Dapi (blue). The arrows depict plasma membrane blebbing on the surface of the cells.

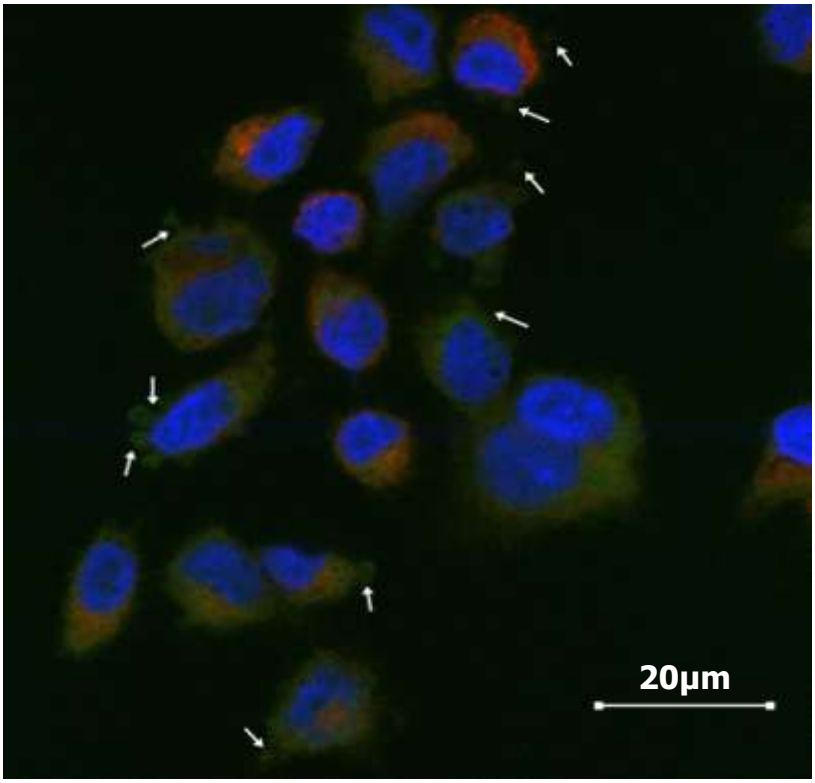

Figure 3.9: Representative micrograph showing HCS-2 cells treated with 4.07µg/ml of EFV. MUC1 was localised with anti-MUC1 rabbit monoclonal antibody and goat polyclonal to rabbit IgG conjugated with TRITC (red fluorochrome). P65 was localised with anti-NFkB P65 mouse monoclonal antibody and goat polyclonal to mouse IgG conjugated with FITC (green fluorochrome). The nuclei were counterstained with Dapi (blue). The arrows depict plasma membrane blebbing on the surface of the cells.

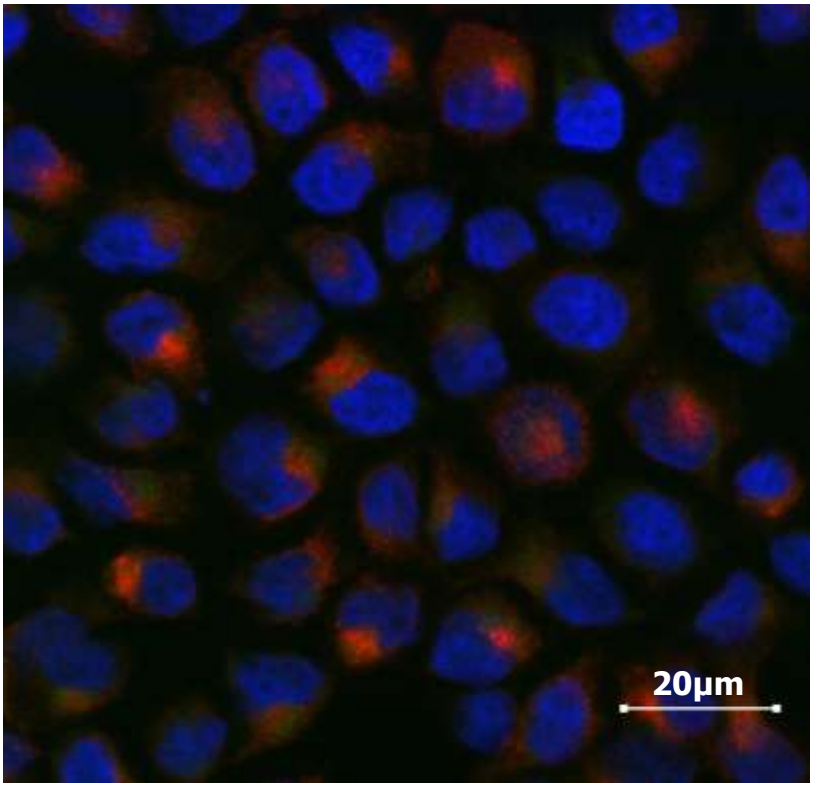

Figure 3.10: Representative micrograph showing HCS-2 cells treated with the drug cocktail, ATP (combination ratio 1FTC:1TDF:1EFV of their Cmax). MUC1 was localised with anti-MUC1 rabbit monoclonal antibody and goat polyclonal to rabbit IgG conjugated with TRITC (red fluorochrome). P65 was localised with anti-NFkB P65 mouse monoclonal antibody and goat polyclonal to mouse IgG conjugated with FITC (green fluorochrome). The nuclei were counterstained with Dapi (blue).

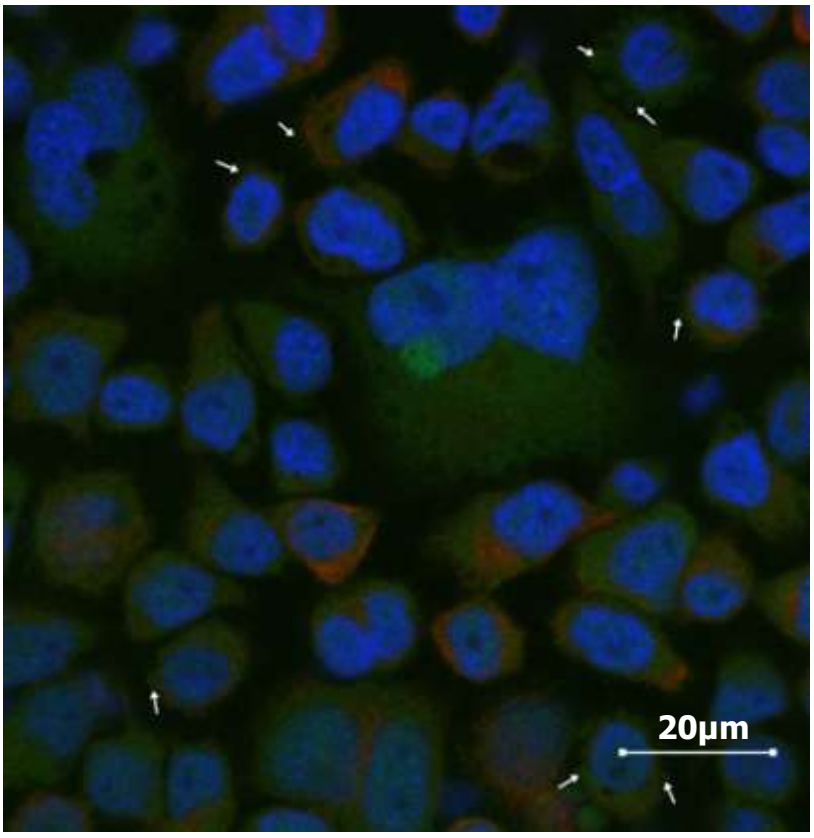

Figure 3.11: Representative micrograph showing HCS-2 cells treated with the PI cocktail LPV/r (combination ratio of 1LPV: 1RTV of their Cmax). MUC1 was localised with anti-MUC1 rabbit monoclonal antibody and goat polyclonal to rabbit IgG conjugated with TRITC (red fluorochrome). P65 was localised with anti-NFkB P65 mouse monoclonal antibody and goat polyclonal to mouse IgG conjugated with FITC (green fluorochrome). The nuclei were counterstained with Dapi (blue). The arrows depict plasma membrane blebbing on the surface of the cells.

3.3 Morphological features observed in HCS-2 cells following treatment with antiretroviral drugs by means of Scanning Electron Microscopy

Drug treatment induced prominent changes in the cell surface morphology and in order to ascertain whether the changes observed in treated cells were significantly different from the negative control (untreated cells) and diluent control (0.02% methanol), statistical analysis was conducted. The micrographs were assessed using a scoring system (table 2.4) prior to the statistical analysis. An F-test (Brown-Forsythe) was conducted in order to check for homogeneity of variances. Following which a one way ANOVA test was conducted in order to determine whether there was a significant difference between the treated cells and controls. A Tukey Kramer *Post Hoc* test was also conducted in order to determine where the significant differences between the means were present. The statistical tests were carried out independently for every morphological criteria tested.

3.3.1 Cell connections

Brown-Forsythe test showed that there was no significant difference between the variances ($p=0.1$). A one way ANOVA test showed that there was a significant difference in cell connections (Fig 3.12 and Fig 3.17) (as indicated by the lateral cytoplasmic protrusions of the cells, filopodia) between the different groups as shown in table 3.5 ($p<0.05$). A Tukey Kramer *Post Hoc* analysis (Appendix IV; table 7.8) showed that a significant difference existed between controls and all treated cells except ATP, thus suggesting that drug treatment, except treatment with ATP, significantly altered cell contacts. The micrographs show that there were relatively fewer and more damaged cell contacts in treated cells in comparison to controls. Further differences were observed between LPV/r and FTC, TDF and ATP in that LPV/r treated cells had relatively lesser and more damaged cell contacts than other treatment groups.

Table 3.5: The analysis of variance using a one way ANOVA test in order to assess changes in cell contacts between the various groups.

Source	DF	Sum of Squares	Mean Square	F Ratio	Prob> F
Group	6	18.166667	3.02778	10.4782	<.0001*
Error	77	22.250000	0.28896		
C. Total	83	40.416667			

*= p value is significantly different

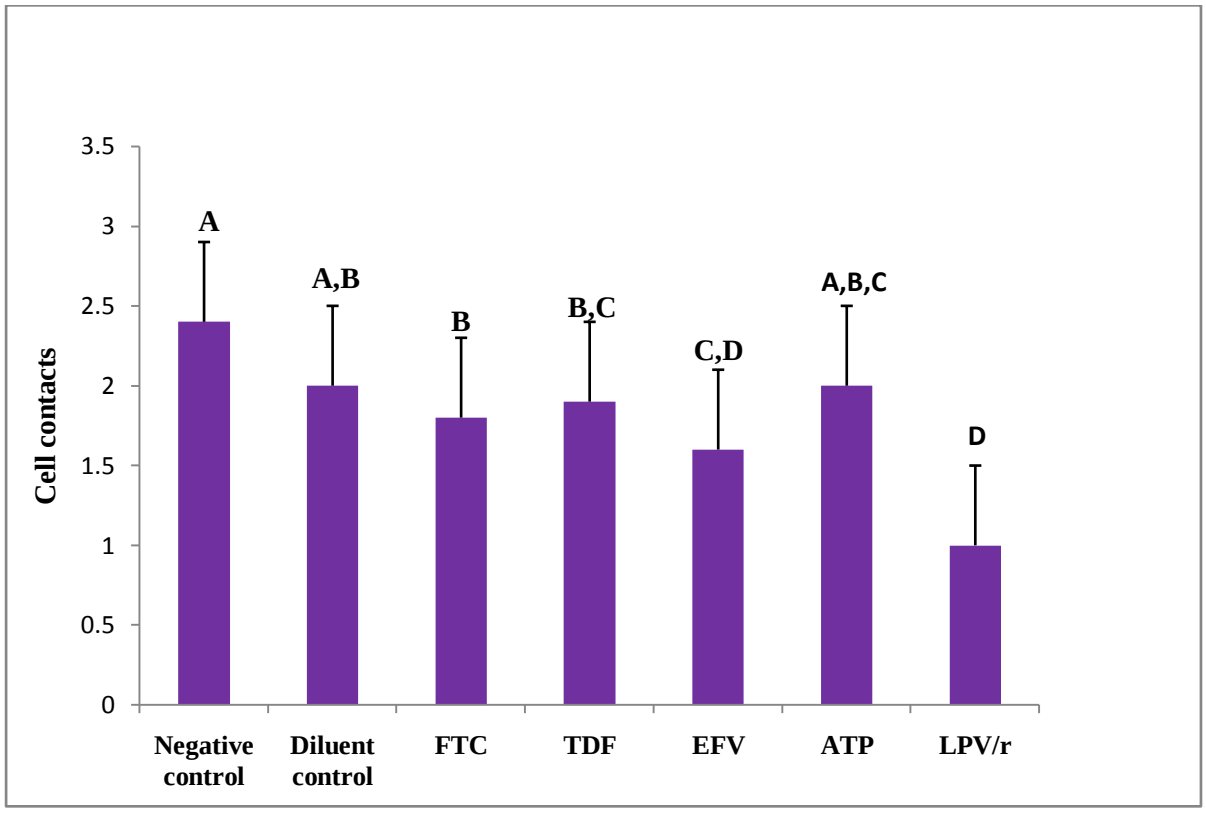

Figure 3.12: Changes observed in cell contacts in HCS-2 cells following treatment with antiretroviral drugs. There was a significant difference observed between the different groups ($p<0.05$). Drug treatment damaged and reduced the amount of contacts present; LPV/r resulted in the most reduction and damage in comparison to controls and other treatment groups. Bar graphs not connected by the same letter are significantly different, Tukey Kramer *Post Hoc* analysis.

3.3.2 Microvilli density and size

Brown-Forsythe test showed that there was no significant difference between the variances ($p=0.4$) for microvilli density (Fig 3.18). In contrast for microvilli size (Fig 3.18) there was a significant difference between the variances ($p<0.05$). In order to normalise the data, it was transformed using log base10 (Keen, 1995).

A one way ANOVA test showed that there was a significant difference in microvilli density and size (Fig 3.13) between the different groups as shown in table 3.6, ($p<0.05$). A Tukey Kramer *Post Hoc* analysis for microvilli density (Appendix IV; table 7.9) showed that a significant difference existed between controls and TDF, ATP and LPV/r treated cells, Furthermore TDF and ATP were significantly different from EFV and 0.02% methanol. The results showed that the different drug treatments did not have a similar effect in altering microvilli density; EFV and FTC treatment showed the least reduction in microvilli density in comparison to the controls whereas ATP, TDF and LPV/r treatment resulted in significant reduction in microvilli density.

For microvilli size, a Tukey Kramer *Post Hoc* analysis (Appendix IV; table 7.10) showed that a significant difference existed between controls and all the treated cells, thus suggesting that treatment with all the ARV drugs significantly reduced microvilli size. Furthermore TDF, ATP and LPV/r treatment resulted in more reduction of microvilli size in comparison to FTC and EFV treatment.

Table 3.6: The analysis of variance using a one way ANOVA test in order to assess changes in microvilli density and size (MD and MS, respectively) between the various groups.

Source	DF	Sum of Squares		Mean Square		F Ratio		Prob> F
	MD & MS	MD	MS	MD	MS	MD	MS	MD & MS
Group	6	14.738095	2.2936452	2.45635	0.382274	5.4823	37.7785	<.0001*
Error	77	34.500000	0.7791495	0.44805	0.010119			
C Total	83	49.238095	3.0727947					

*= p value is significantly different

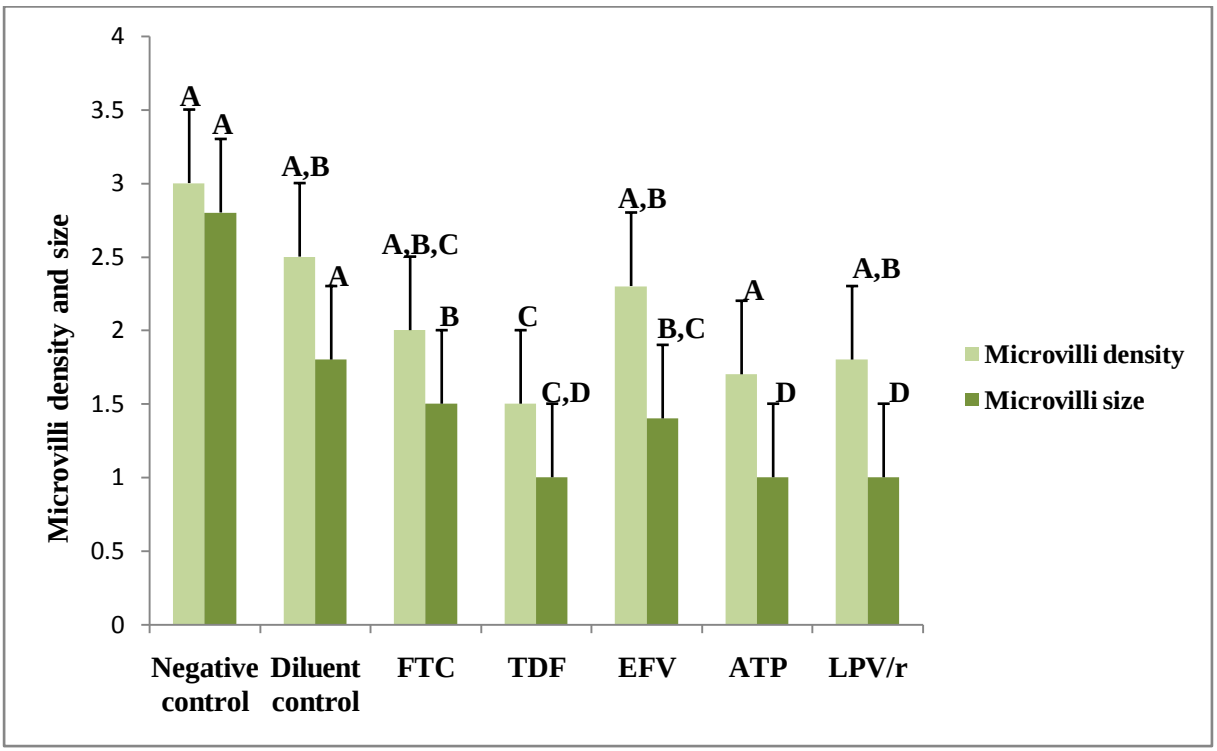

Figure 3.13: Changes observed in microvilli density and size in HCS-2 cells following treatment with antiretroviral drugs. There was a significant difference observed between the different groups ($p<0.05$). Drug treatment reduced the size and density of microvilli although the changes were unique to each drug treatment. TDF, ATP and LPV/r treatment showed the most reduction in microvilli size and density in comparison to controls and other drug treatments. Bar graphs not connected by the same letter (per characteristic) are significantly different, Tukey Kramer *Post Hoc* analysis.

3.3.3 Blebbing density and size

Brown-Forsythe test showed that there was no significant difference between the variances for blebbing density (p= 0.7) and size (p= 0.3) (Fig 3.19). A one way ANOVA test showed that there was a significant difference in blebbing density and size between the different groups as shown in table 3.7 ($p<0.05$) (Fig 3.14).

A Tukey Kramer *Post Hoc* analysis (Appendix IV; table 7.11) for blebbing density showed that a significant difference existed between the controls and ATP and TDF treated cells only, whereas no significant difference was observed between controls and FTC, EFV and LPV/r treated cells. The results suggest that the density of blebs in ATP and TDF were significantly higher than those observed in other groups. Although blebbing density in some treatment groups was not significantly different from the controls, the bleb density was still the least in controls therefore suggesting that high bleb formation was induced by drug treatment.

For bleb size, a Tukey Kramer *Post Hoc* analysis (Appendix IV; table 7.12) showed that a significant difference existed between EFV treated cells and the other groups (i.e. Controls and other drug treatments). The results suggest that the size of the blebs observed following treatment with EFV were significantly larger than blebs observed in other groups which varied between small and medium sized.

Table 3.7: The analysis of variance using a one way ANOVA test in order to assess changes in blebbing density (BD) and size (BS) between the various groups.

Source	DF	Sum of Squares		Mean Square		F Ratio		Prob> F	
	BD & BS	BD	BS	BD	BS	BD	BS	BD	BS
Group	6	18.976190	24.50000	3.16270	4.08333	4.0197	4.1100	0.0015*	0.0012*
Error	77	60.583333	76.50000	0.78680	0.99351				
C Total	83	79.559524	101.00000						

*= p value is significantly different

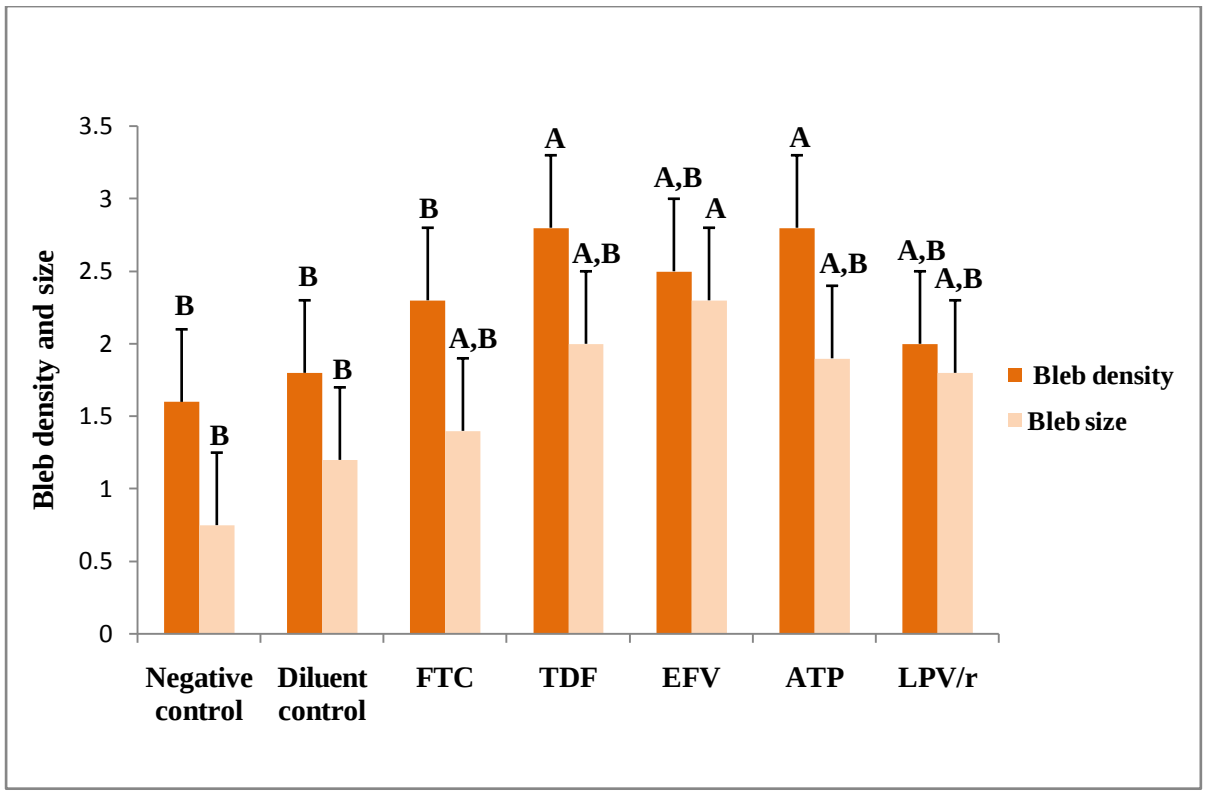

Figure 3.14: Changes observed in blebbing density and size in HCS-2 cells following treatment with antiretroviral drugs. There was a significant difference observed between the different groups ($p<0.05$). The expression of blebs increased with drug treatment, thus controls showed the least expression of small sized blebs. TDF and ATP treatment resulted in high bleb density, whereas EFV treatment resulted in large sized blebs in comparison to controls and other treatment groups. Bar graphs not connected by the same letter (per characteristic) are significantly different, Tukey Kramer *Post Hoc* analysis.

3.3.4 Cell shape

Brown-Forsythe test showed that there was no significant difference between the variances ($p=0.1$). A one way ANOVA test showed that there was a significant difference between the groups in terms of the shape of the cell (Fig 3.15 and Fig 3.30) as shown in table 3.8, ($p<0.05$). A Tukey Kramer *Post Hoc* analysis (Appendix IV; table 7.13) showed that a significant difference existed between both controls and all the treated groups. In general,

drug treatment altered the shape of the cell in varying degrees. FTC, TDF and EFV treated cells acquired mostly a round shape; however, there were a few cells which were ovoid and some flattened, whereas ATP and LPV/r treated cells were mostly round in shape. Overall, cell shape changed from flattened and polyhedral in untreated cells to a transition between ovoid/oval to round in treated cells.

Table 3.8: The analysis of variance using a one way ANOVA test in order to assess differences in cell shape between the various groups.

Source	DF	Sum of Squares	Mean Square	F Ratio	Prob> F
Group	6	15.107143	2.51786	6.5364	<.0001*
Error	49	18.875000	0.38520		
C. Total	55	33.982143			

*= p value is significantly different

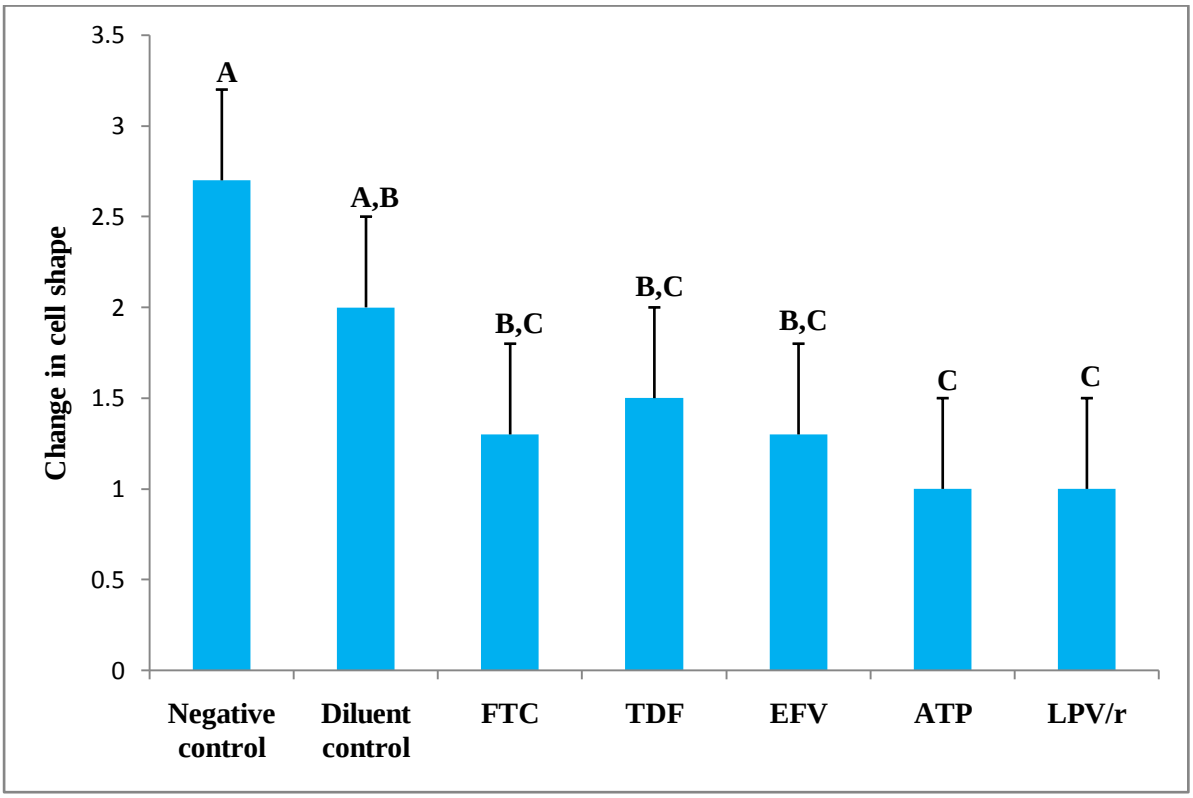

Figure 3.15: Changes observed in cell shape in HCS-2 cells following treatment with antiretroviral drugs. There was a significant difference observed between the different groups ($p<0.05$). Negative controls had a flattened and polyhedral shape; however the shape of the cell acquired a more rounded morphology following drug treatment. Treatment with ATP and LPV/r resulted in the most change in cell shape. Bar graphs not connected by the same letter are significantly different, Tukey Kramer *Post Hoc* analysis.

3.3.5 The presence of membrane bound and extracellular secretions

Brown-Forsythe test showed that there was no significant difference between the variances ($p=0.1$) for extracellular secretions (Fig 3.20). In contrast for membrane bound secretion (Fig 3.20) there was a significant difference between the variances ($p<0.05$) (Fig 3.16). In order to normalise the data, it was transformed using log base10 (Keen, 1995).

A one way ANOVA test showed that there was a significant difference in the presence of membrane bound secretions between the different groups as shown in table 3.9 ($p<0.05$). A Tukey Kramer *Post Hoc* analysis (Appendix IV; table 7.14) for membrane bound secretions showed that a significant difference existed between both controls and treated cells; negative control had no secretions on their surface and 0.02% diluent control had few secretions whereas the drug treated cells had a significant amount of secretions on their surface. Further differences were observed between treated cells in that FTC and TDF had slightly less secretions on their surface than EFV, ATP and LPV/r which had more secretions in comparison.

For extracellular secretions, a Tukey Kramer *Post Hoc* analysis (Appendix IV; table 7.15) showed that both controls and FTC were significantly different to TDF, ATP and LPV/r groups in that the former had none to a few secretions in its extracellular space whereas the latter three groups had significantly more secretions in its extracellular space.

Table 3.9: The analysis of variance using a one way ANOVA test in order to assess the presence of membrane bound and extracellular secretions between the various groups.

Source	DF	Sum of Squares		Mean Square		F Ratio		Prob> F
	MS & ES	MS	ES	MS	ES	MS	ES	MS & ES
Group	6	0.9166667	7.619048	0.152778	1.26984	9.6359	6.2411	<.0001*
Error	77	1.2208333	15.666667	0.015855	0.20346			
C Total	83	2.1375000	23.285714					

*= p value is significantly different

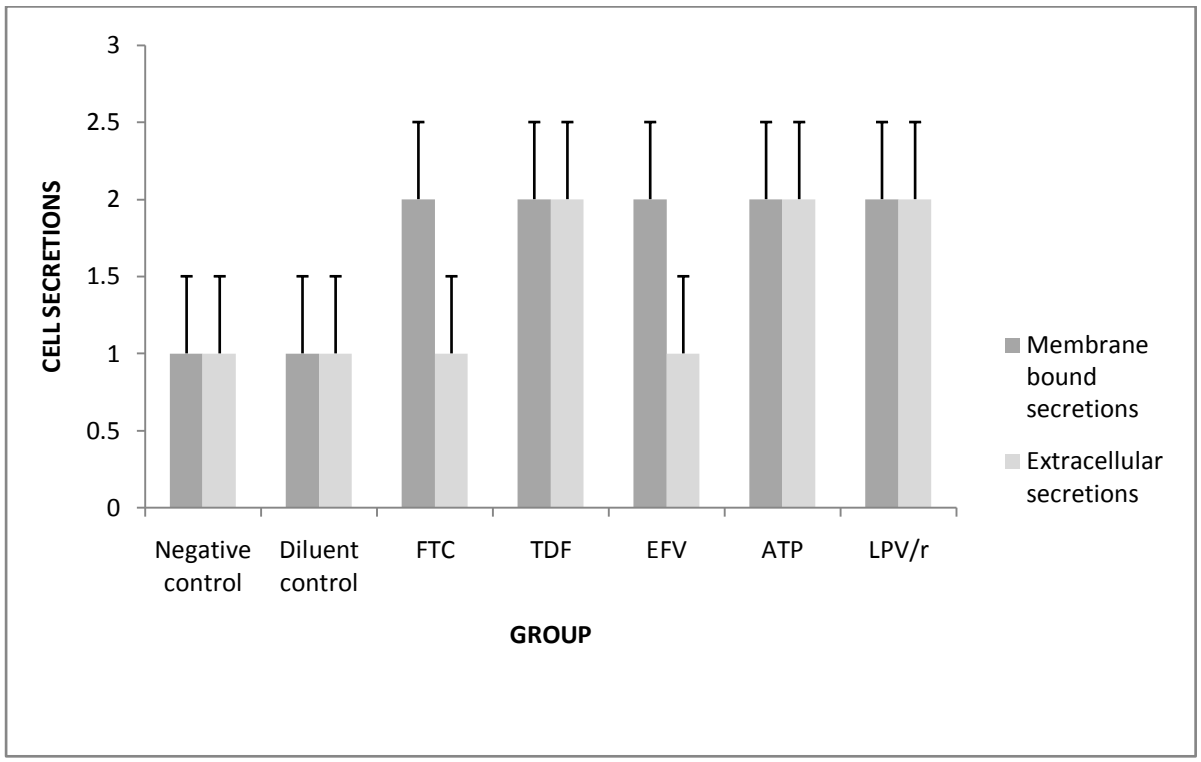

Figure 3.16: The presence of membrane bound secretions in HCS-2 cells following treatment with antiretroviral drugs. There was a significant difference observed between the different groups ($p<0.05$). Untreated cells had very few if any secretions on their surface whereas treated cells had secretions in varying amounts with ATP and LPV/r having the most membrane-bound secretions. In contrast both controls (negative and diluent) and FTC treated cells had very few if any secretions in the extracellular space and were hence significantly different from ATP, LPV/r and TDF treated cells which had more secretions in the ECM.

Table 3.10: Summary table showing the comparison between morphological features observed in the HCS-2 cells following treatment with antiretroviral drugs.

	Controls; negative and diluent	**NRTIs;** FTC and TDF	**NNRTI;** EFV	**Drug cocktails;** ATP and LPV/r
Cell contacts	many	few		
Microvilli density and size	Dense and long in negative control s slightly reduced in density and length in diluent controls	Relatively less dense and short		
Bleb density and size	Sparse and small blebs	Uniformly spread across the PM, medium sized	Large and sparsely distributed across the PM	Uniformly spread across the PM, medium sized
Cell shape	Cells were flattened and polyhedral shaped in negative controls and a mixture of flattened and ovoid, with very few round cells in diluent controls	Mostly round, with a few ovoid cells		All the cells acquired a round shape
Membrane-bound secretions	No distinct secretions observed in negative controls whereas a few cells had small secretions on their surface in diluent controls	A few secretions were observed scattered across the membrane and concentrated towards the cell periphery and along the filopods		
Extracellular matrix secretions	No distinct secretions were observed	Very few if any secretions were present in the ECM with FTC treatment, however a few secretions were present following treatment with TDF	Very few if any secretions were present in the ECM	A few secretions were present in the ECM

Controls;

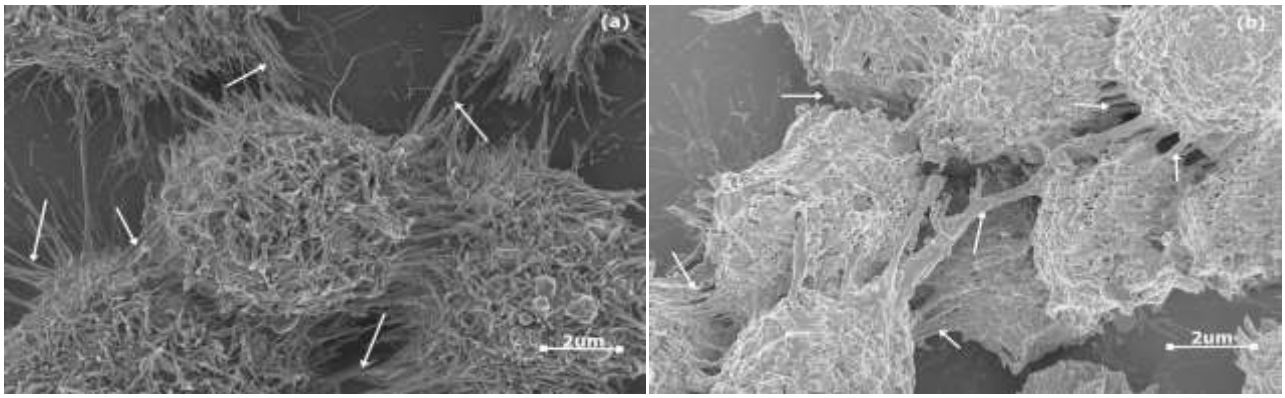

Drug combination;

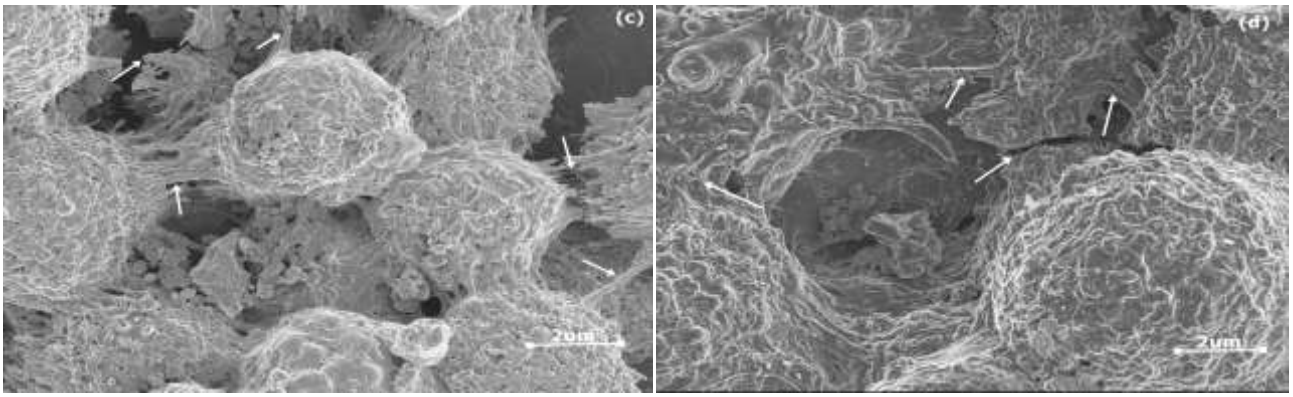

NRTIs;

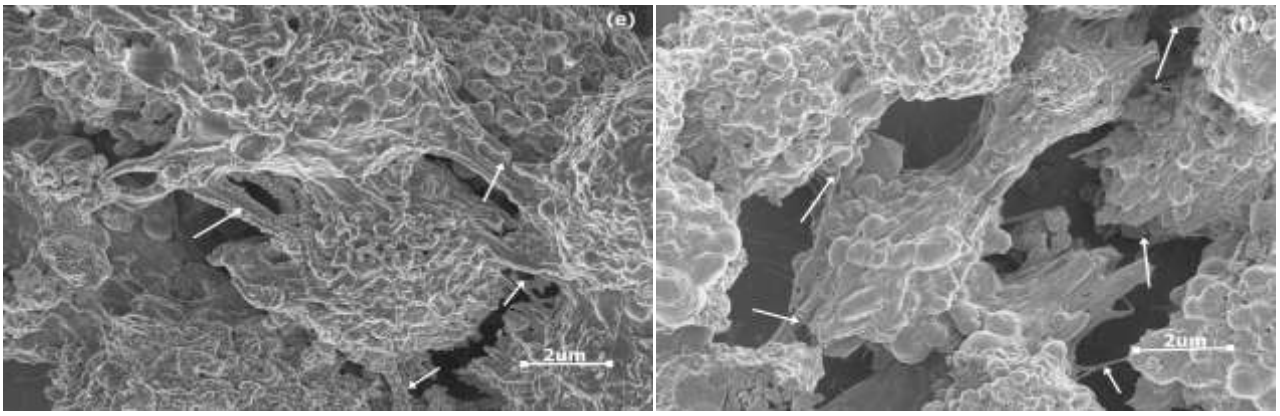

NNRTI;

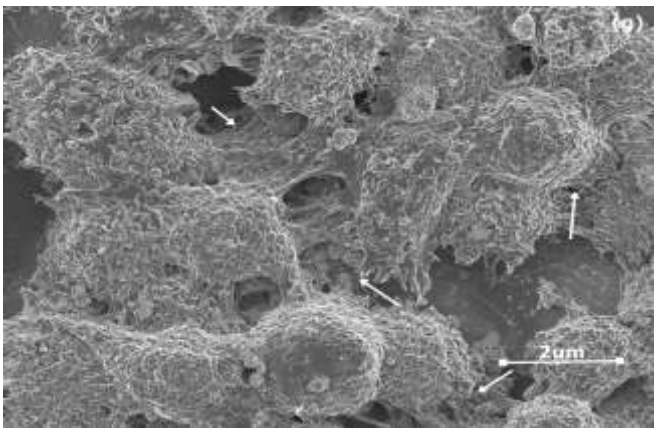

Figure 3.17: The change in cell contacts following drug treatment in HCS-2 cells; **(a)** Negative control, **(b)** Diluent control, **(c)** ATP, **(d)** LPV/r, **(e)** FTC, **(f)** TDF, **(g)** EFV. The arrows show where cell contacts are found represented by long lateral protrusions, filopodia. Extensive cell contacts were characteristic in (a), with drug treatment as observed in (b-g) they were reduced and some were damaged in varying degrees.

Controls;

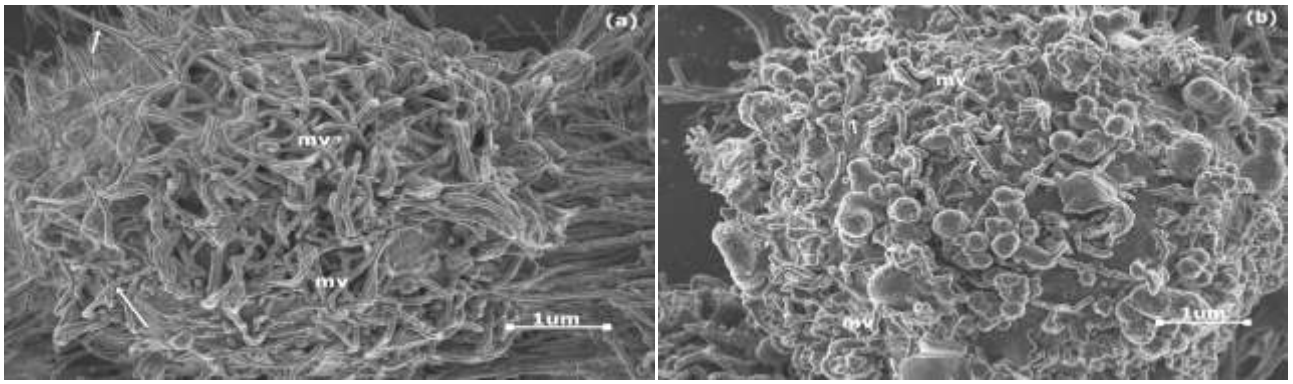

Drug combination;

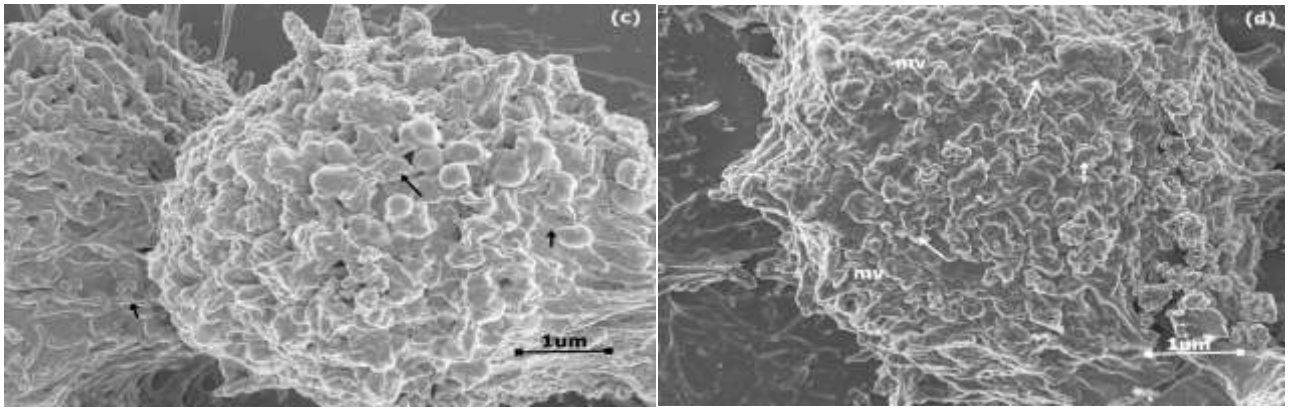

NRTIs;

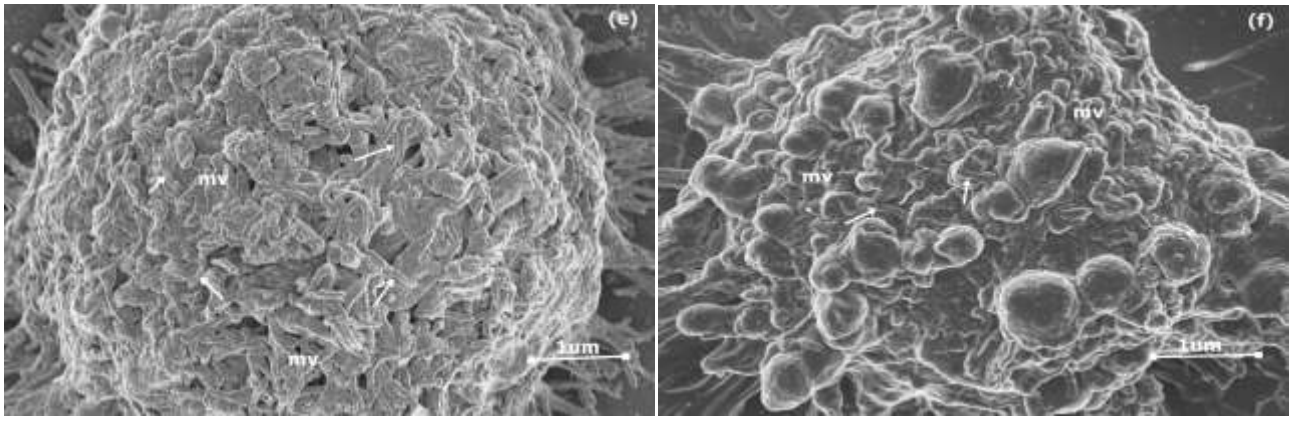

NNRTI;

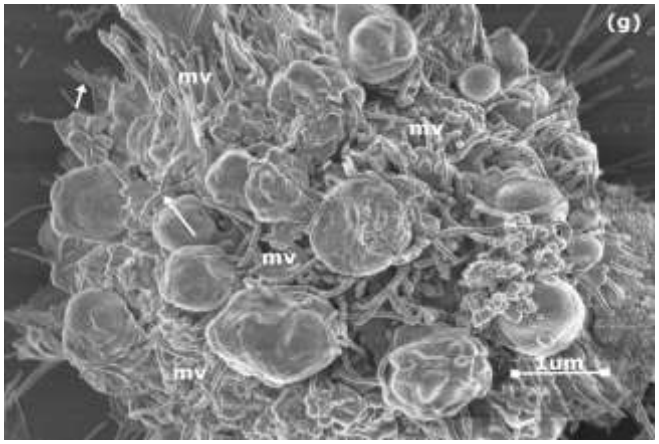

Figure 3.18: The change in density and size of microvilli (mv) following drug treatment (arrows highlight the length of mv) ; **(a)** Negative control, **(b)** Diluent control, **(c)** ATP, **(d)** LPV/r, **(e)** FTC, **(f)** TDF and **(g)** EFV. In all the treated cells (b-g) microvilli density decreased in comparison to (a) and the microvilli observed in (c-f) were shorter in comparison to (a) and those seen in (g) were slightly shorter than those in (a), but longer than those seen in other drug treatments (c-f).

Controls;

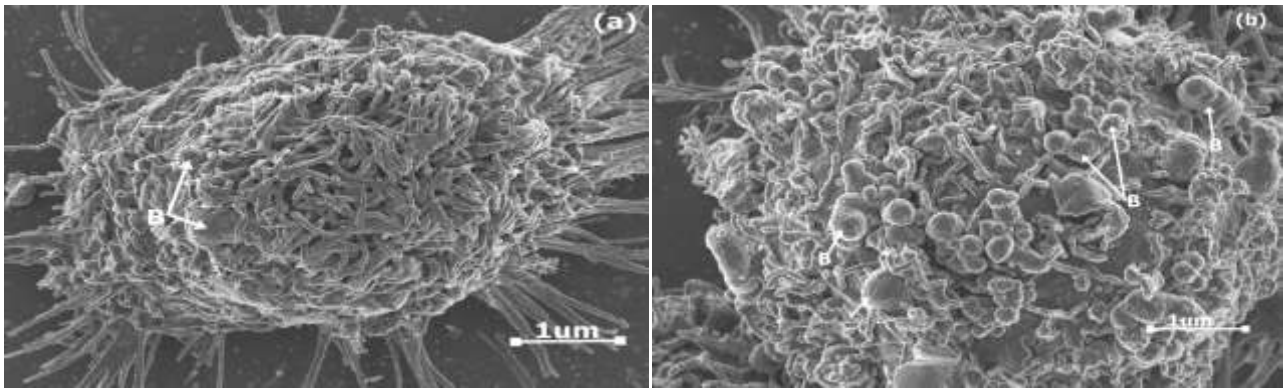

Drug combinations;

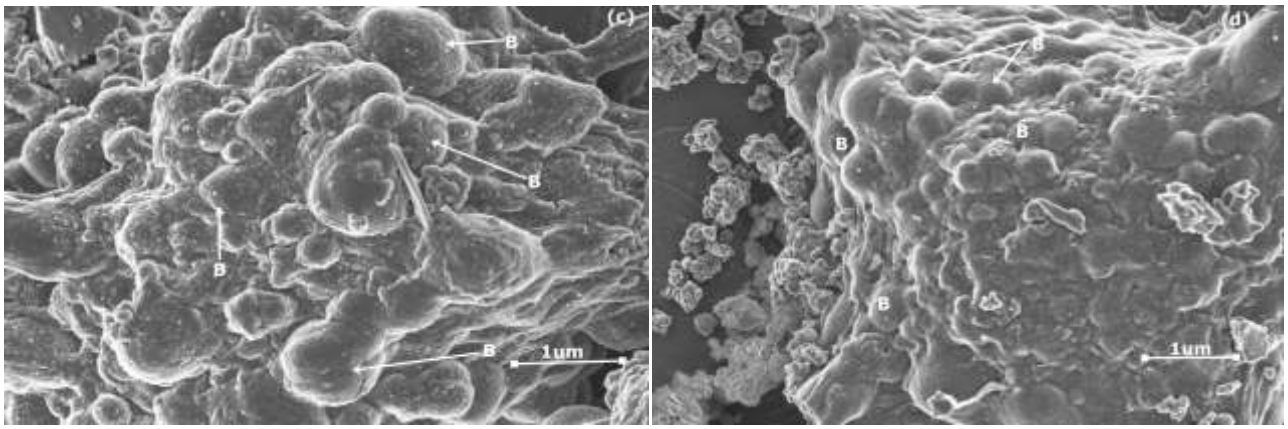

NRTIs;

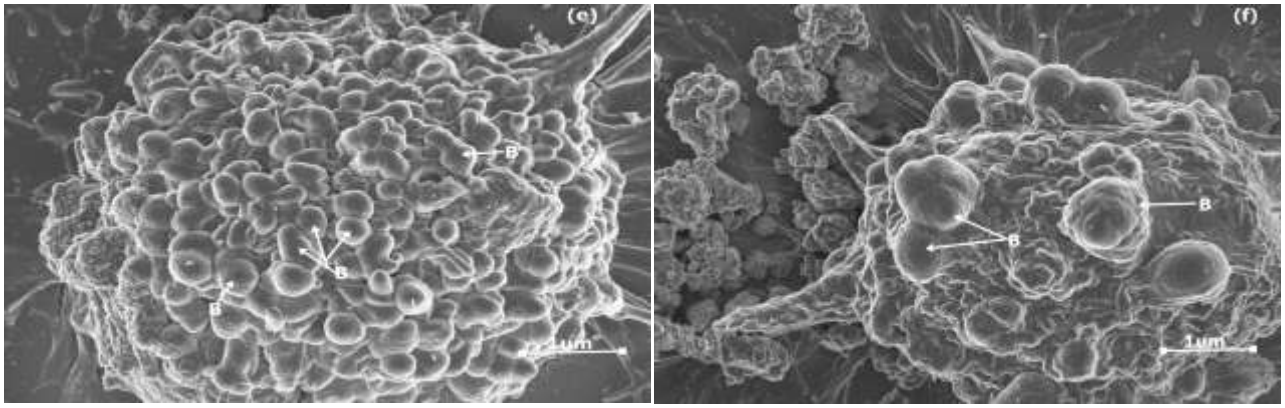

NNRTI;

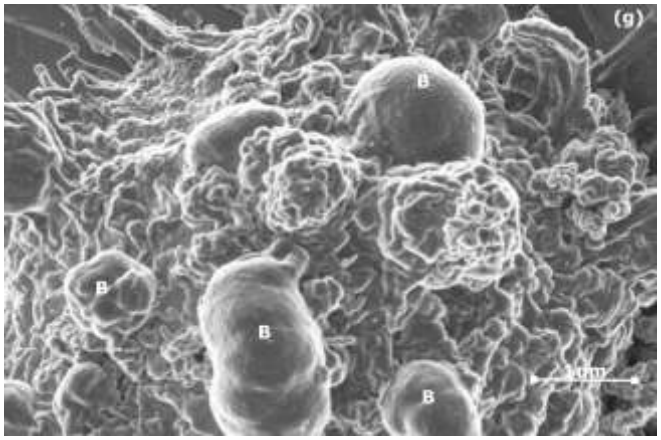

Figure 3.19: The change in bleb density (B) and size following drug treatment; **(a)** Negative control, **(b)** Diluent control, **(c)** ATP, **(d)** LPV/r, **(e)** FTC, **(f)** TDF and **(g)** EFV. A few small blebs were observed in controls (a-b), drug treatment increase the amount and size of blebs, as seen in micrographs (c-g), in comparison to controls.

Controls;

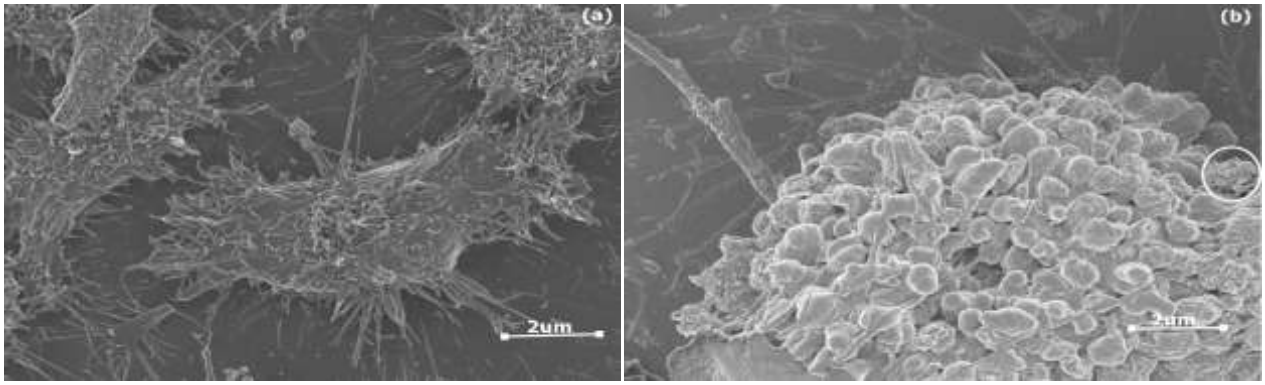

Drug combinations;

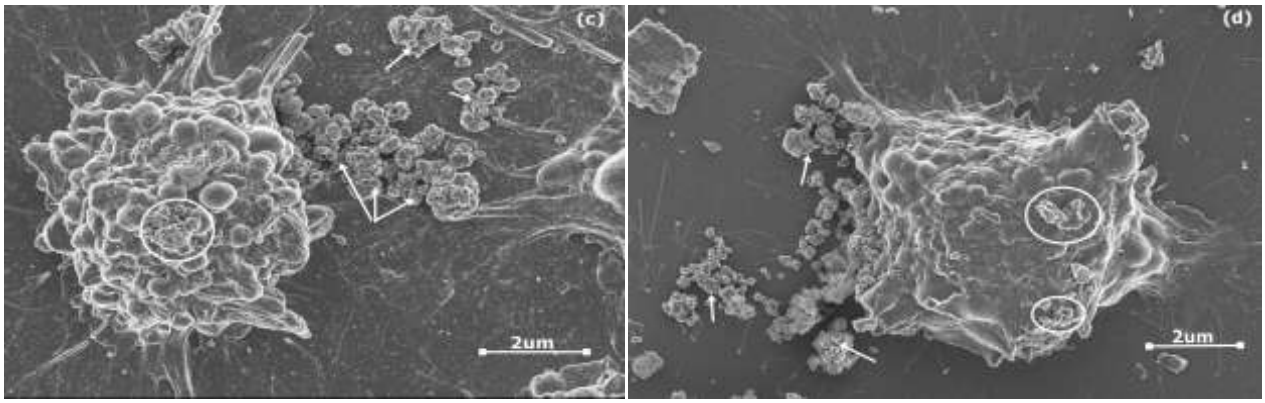

NRTIs;

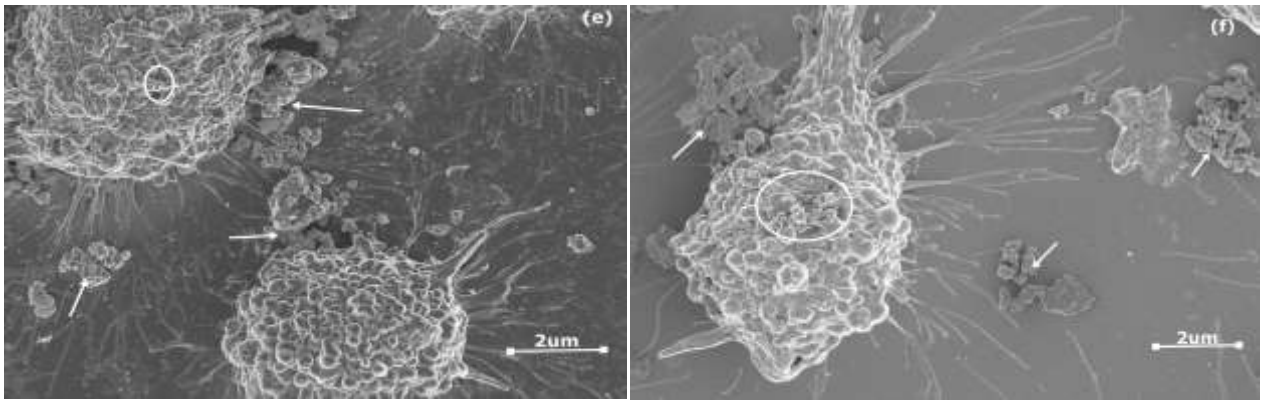

NNRTI;

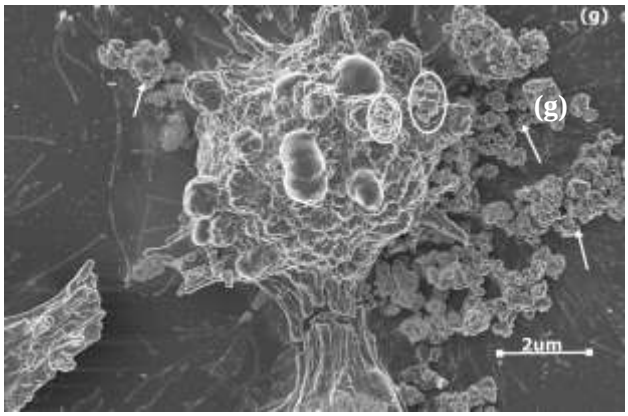

Figure 3.20: cell secretions and change in cell shape following drug treatment; **(a)** Negative control, **(b)** Diluent control, **(c)** ATP, **(d)** LPV/r, **(e)** FTC, **(f)** TDF and **(g)** EFV. Arrows indicate extracellular secretions whereas circles represent membrane-bound secretions. The cell shape changed from flattened polyhedral in (a) to ovoid and/or circular in (b-g).

CHAPTER FOUR: DISCUSSION

In this study the treatment of HCS-2 cells with ARV drugs classified as NRTIs, NNRTI and PIs induced cell death. The gene and protein expression of MUC1 and P65 supports this finding and morphological features observed on the cell surface of the treated cells were characteristic of cell death.

MUC1 is an oncogene and thus makes a suitable therapeutic target against cancer (Klinge *et al.,* 2011). In many cancers the over expression of MUC1 signals reduced survival for patients because it promotes cancer, therefore inhibiting the function of MUC1 is an important target for therapeutic intervention (Klinge *et al.,* 2011). MUC1 expression at appropriate levels is important for the normal function of organs and plays a role in producing protective mucous over epithelial surfaces (Klinge *et al.,* 2011).

MUC1 is over expressed in cancers and its expression has been linked to metastasis in breast cancer (Yuan *et al.,* 2007). The MUC1 protein undergoes post translational proteolytic cleavage which results in the formation of two MUC1 subunits forming a heterodimer on the cell membrane (Yuan *et al.,* 2007). The cytoplasmic domain of MUC1 has been shown to bind to epidermal growth factor receptor (EGFR) family members, c-Src and β-catenin, suggesting that MUC1 plays a role in cell growth related pathways and signal transduction (Yuan *et al.,* 2007).

In this study the gene and protein expression of MUC1 were studied. The expression of MUC1 protein was observed in the cytoplasm and along the cell membrane as previously mentioned in literature. Gene expression studies showed that treatment with *MUC1* expression was reduced following treatment with two drug cocktails; the first cocktail (ATP) consisted of two NRTIs (FTC and TDF) and one NNRTI (EFV) and it slightly reduced *MUC1* expression in comparison to the control and the second cocktail (LPV/r). In contrast

the second cocktail (LPV/r) consisted of two PIs (LPV and RTV) and it resulted in a significant reduction in *MUC1* expression in comparison to the control and the first cocktail (ATP). The drugs also reduced MUC1 protein expression; the drug cocktails both reduced protein expression and the reduction correlated with gene expression because LPV/r reduced MUC1 protein expression more than ATP. When the effects of the individual components of ATP were tested on MUC1 protein expression, only FTC and EFV treatment showed a significant reduction in MUC1 protein expression in comparison to the control.

The reduction of *MUC1* expression suggests that its capacity to regulate cell growth and signalling pathways is compromised and in this state, cells are more susceptible to cell death stimuli. This finding concurs with other studies which have found that most PIs promote cell death *in vitro* and *in vivo* (Gills *et al.,* 2007; Vlahakis *et al.,* 2007; Israr *et al.,* 2011). Although different parameters were investigated in the different studies it is evident that these drugs target a variety of signalling proteins and pathways in order to exhibit their cell death effect.

The NFkβ complex consists of P65 (Rel A) and P50 (NFkβ1), and is a diverse nuclear transcription factor that plays a role in regulating the expression of several genes that play a role in carcinogenesis and inflammation, for example, cyclin D1, c-myc, bcl-2, cyclooxygenase-2 (COX-2) and vascular endothelial growth factor (VEGF) (Jutooru *et al.,* 2010; Xia and Xue, 2012). The NFkβ-IkB complex lies in the cytosol when it is inactive (Jutooru *et al.,* 2010; Xia and Xue, 2012). Its activation relies upon phosphorylation and proteosome dependant degradation of IkB therefore NFkβ accumulates in the nucleus when it is activated (Jutooru *et al.,* 2010; Xia and Xue, 2012). The activation of NFkβ in cancer cells promotes cell proliferation, survival, angiogenesis, metastasis, epithelial to mesenchymal transition and inflammation (Jutooru *et al.,* 2010; Xia and Xue, 2012).

In this study, a reduction in gene and protein expression of *P65* was observed following drug treatment. The protein was inconspicuously expressed in the cytoplasm and mainly in the peri-nuclear region, there was no nuclear expression observed. The cytoplasmic expression of the protein suggests that it was either inactive or its activation was inhibited as described in literature; that cytoplasmic expression of P65 corresponds to an inactive form of the protein (Jutooru *et al.*, 2010; Xia and Xue, 2012). This finding suggests that cell proliferation, angiogenesis, metastasis and other features of cancer regulated by this protein were reduced in the HCS-2 cells, therefore suggesting that the cells were more susceptible to cell death when compared to cell survival.

Cell death is regulated by different signalling molecules and pathways, in addition morphological features are important in describing the type of cell death that cells undergo (Majno and Joris, 1995). In response to death stimuli the morphology of the cell begins to change and these changes are unique depending on the type of cell death the cells are undergoing (Majno and Joris, 1995).

Apoptosis is an energy-dependant, intrinsic and genetically controlled process where the organism removes damaged cells (Bjelaković *et al*., 2005). Apoptosis plays a vital role as one of the factors that regulate the equilibrium between cell death and cell proliferation (Van Engeland *et al*., 1997). In the majority of cancers this equilibrium is often lost due to disruptions to the apoptotic process (Van Engeland *et al*., 1997).

Apoptosis involves a sequence of characteristic morphological features including cell shrinkage, membrane blebbing, nuclear fragmentation and chromatin condensation (Van Engeland *et al*., 1997; Saraste and Pulkki, 2000; Bjelaković *et al*., 2005). Apoptotic cells detach from their substratum in order to acquire a rounded morphology and surface microvilli and cell junctions, for example, desmosomes, are also lost due to the reorganisation of

cytoskeletal structures (Saraste and Pulkki, 2000; Bjelaković *et al*., 2005; Condello *et al*., 2013). The course of cell death is orderly, thereby suggesting the presence of well preserved molecular pathways (Saraste and Pulkki, 2000).

Scanning Electron Microscopy (SEM) has played an important role to date in contributing to the identification of a variety of cell death mechanisms, including necrosis, apoptosis, autophagy, oncosis, mitotic catastrophe, which are induced by disease or noxious stimuli (such as heat, radiation, hypoxia, or cytotoxic drugs) (Condello *et al*., 2013). The findings from this study with regard to apoptosis using SEM are in accordance with those of previous studies.

The morphological analysis of the plasma membrane using the SEM has revealed features which are characteristic of apoptosis; for example rounding-up of cells, retraction of filopodia, blebbing and maintenance of plasma membrane integrity (Bjelaković *et al.,* 2005; Bjelaković *et al.,* 2005; Kroemer *et al.,* 2009). These features are in contrast to those observed in other forms of cell death, specifically necrosis. Necrosis is characterised by morphological features such as increased cell volume (oncosis) and plasma membrane rupture (Kroemer *et al.,* 2009)

Eukaryotic cells respond to intra and extracellular signals by remodelling their sub-membranous cytoskeleton which is reflected by changes in the plasma membrane (Fackler and Grosse, 2008; Norman *et al*., 2010). The cytoskeletal re-arrangements are regulated by small GTPases belonging to the Rho family and downstream signalling caspases and they result in the formation of distinctive types of actin-rich invaginations or protrusions including filopodia, lamellipodia, invadopodia, podosomes, phagocytic cups, and uropods that have specific biological functions (Fackler and Grosse, 2008; Norman *et al*., 2010).

Filopodia are thin cytoplasmic protrusions which play a role in attaching the cells to the growth surface, assisting in cell migration and are important components of cell to cell junctions (Fackler and Grosse, 2008; Norman *et al*., 2010). They were the most common type of protrusion observed in the HCS2 cells in this study.

Untreated cells presented with numerous filopodia which were extending from the cells to form connections with adjacent cells and to adhere to the substratum, a feature which is commonly observed in cancer cells due to their high migratory rate and because the cancer cells are highly active they maintain communication with neighbouring cells and therefore numerous cell contacts are a common feature (Fackler and Grosse, 2008; Norman *et al*., 2010). These features were altered to varying degrees in cells which were treated with the ARV drugs as they acquired characteristic features of cell death.

The treated cells displayed loss of cell contacts as indicated by the reduced amount of prominent cell extensions making contact with adjacent cells and fewer and damaged filopodia were observed in the extracellular space. The PI (LPV/r) drug combination resulted in more damaged cell contacts than the other drugs. These findings suggest an adverse effect of the drug treatments on the cell's capacity for invasion, taking into account that metastasis is dependent on the cell's mobility which is ensured by the actin content (Fackler and Grosse, 2008; Norman *et al*., 2010).

The destruction of actin rich structures such as filopodia weakens the cancer cells capacity to move, therefore the effect of the drugs on the HCS-2 cells suggest that they may potentially prolong onset of metastasis by reducing cancer cell mobility. The change in cell shape from polyhedral and flattened in untreated cells to acquiring a more rounded morphology in treated cells is also an indication of re-organisation of the cytoskeletal components (Hacker, 2000).

Blebs are bulky, round structures which can extend up to 2µm from the plasma membrane (Fackler and Grosse, 2008; Norman *et al*., 2010). The life cycle of blebs lasts for a short period ~1min and is characterised by rapid bleb expansion, a short stationary phase, and low retraction of the bleb to its point of origin in the plasma membrane (Fackler and Grosse, 2008; Norman *et al*., 2010). The formation of blebs is induced by various actions involving local disruption of membrane actin cortex interactions, which lead to rapid protrusion of the plasma membrane due to the internal hydrostatic pressure of the cell (Fackler and Grosse, 2008; Norman *et al*., 2010).

Early studies done on plasma membrane blebs have linked their expression to cell movement, as they were observed during the spreading of human conjunctiva cells and fibroblasts (Fackler and Grosse, 2008; Norman *et al*., 2010). In contrast to these observations plasma membrane blebs were later viewed as a consequence of apoptotic and necrotic processes, in which cells display prominent blebs that do not play a role in locomotion, although blebbing alone is not a pre-requisite for the execution of cell death programmes (Fackler and Grosse, 2008; Norman *et al*., 2010). Non-apoptotic blebs tend to have a reversible nature whereas apoptotic blebs ultimately lead to the formation of apoptotic bodies (Fackler and Grosse, 2008; Norman *et al*., 2010).

In this study there were a few blebs observed on the surface of some untreated cells possibly for locomotion, but following drug treatment the HCS-2 cells had an increase in blebs of various sizes across the cell surface. The amount of blebbing varied in density and size between the treatment groups and these two parameters (density and size) were inversely proportional to one another. NRTIs (FTC and TDF) induced the formation of small to medium blebs however FTC treatment induced lesser bleb density than TDF treatment suggesting that TDF induced changes quicker or was more potent in terms of cell death induction than FTC.

The NNRTI EFV, was amongst the treatments that induced the least amount of bleb occurrence yet the size of the blebs observed following treatment with this drug were the largest. The ATP combination resulted in evenly distributed bleb density and medium sized blebs. These effects were intermediate of those caused by individual drug treatment. The PI combination (LPV/r) showed the least bleb density and smaller blebs.

When the observation of plasma membrane blebbing is reconciled with other morphological features observed in the cells, it is more likely that it resulted from apoptosis induction rather than locomotion. As previously mentioned that blebbing alone cannot be considered to be indicative of apoptosis; this study showed that there were other features present which are known to be characteristic of apoptosis, therefore it is suggested that drug treatment induced some changes in the cytoskeleton that led to the formation of blebs. This feature was not prominent in untreated cells further supporting the hypothesis that it is a result of cell death induction, possibly through apoptosis, and eluding to the fact that drug treatment induced the change.

Changes in cytoskeletal components are not only reflected by bleb formation but can also be shown by changes in surface microvilli (Condello *et al*., 2013). In this study drug treatment with NRTIs (FTC and TDF), NNRTI (EFV), ATP combination (FTC, TDF and EFV) and PIs (LPV/r) reduced microvilli density in contrast to the dense cover and long microvilli observed in untreated cells. FTC and EFV treatment showed less severe reduction in microvilli density and size than TDF and ATP and the PI combination; LPV/r showed the most reduction suggesting that the drugs do not exhibit their effects at the same pace. These changes concur with previous studies which suggest that the cytoskeleton, which forms the core of the microvilli (Lange and Gartzke, 2001), is subject to change in response to cell death stimuli which in this case were the ARV drugs.

Another relationship was observed between blebbing and microvilli density in the plasma membrane. On cell surfaces where there was a high density of blebs the surface microvilli cover was less dense, and where there was low to medium density of blebs the surface microvilli cover was correspondingly denser; in the latter case the blebs would be interspersed among the microvilli. This observation could be an indication of the sequence of events and possibly suggests that loss of microvilli occurs at an early stage of cell death and precedes bleb formation which occurs later.

In addition because both these features (blebs and microvilli) arise from the cytoskeleton, microvilli integrity would be more dependent on an intact cytoskeleton and in cases where a cell is undergoing cell death this is more likely to occur at the initial stages of cell death induction because as time lapses, the cytoskeleton loses integrity and so do the microvilli hence they become shorter. Therefore it is suggested that microvilli gradually decreases in density and size and make way for bleb formation.

In contrast the blebs are more likely to occur at a later stage following loss of microvilli because as previous studies have suggested, the blebs carry degraded products from within the cell and pinch off to become apoptotic bodies (Condello *et al*., 2013); hence an inverse relationship exists between these two morphological features.

At a later stage of apoptosis, the cell condenses and disintegrates into apoptotic bodies which will be detected and removed by macrophages or adjacent cells through phagocytosis (Van Engeland *et al*., 1997; Condello *et al*., 2013). Transmission electron microscopy studies have revealed the structure of apoptotic bodies and they are membrane bound vesicles containing cellular organelles, part of the cytoplasm and nuclear fragments (Condello *et al*., 2013). Failure of the apoptotic cell to be phagocytised, as is the case in isolated conditions like cell

culture, results in degradation which is similar to necrosis and thus cell death is said to be facilitated via secondary necrosis (Saraste and Pulkki, 2000).

In this study the drug treated cells were observed to be releasing some internal cellular secretions into the extra cellular matrix (ECM) as indicated by cell debri in the ECM. These secretions are suggested to represent the end stage of cell death in which the blebs begin to pinch-off forming apoptotic bodies. These apoptotic bodies are released from the cell into the extracellular space so that they can be removed via phagocytosis, as previously mentioned (Condello *et al*., 2013).

Due to the absence of phagocytic cells, the apoptotic bodies were degraded and released their contents, thus the cell secretions represents their remnants. Some of the secretions were membrane bound and these were observed in all the treatment groups although in varying numbers. Extracellular secretions were the least in FTC and EFV and were relatively more abundant in TDF, ATP and LPV/r.

In summary, the ARV drugs used in this study induced morphological features which are known to be characteristic of cell death, especially through apoptosis. Although there were slight differences between the different drugs, TDF seemingly induced morphological changes more rapidly than FTC even though these drugs belong to the same class of ARVs, NRTIs. EFV, like FTC, was a slower acting drug in terms of inducing morphological changes in the cells. The drug combinations were seemingly more effective than individual treatments in inducing cell death because morphological features observed following 24hours treatment were relatively more advanced than in individual treatments, although the PI combination LPV/r was more potent than the ATP combination in inducing cell death.

The results obtained from this study suggest a novel role for reverse transcriptase enzyme inhibitors and protease inhibitors. The anti cancer properties exhibited by these drugs should

be further explored alongside other factors such as drug-drug interactions when administered with other chemotherapeutic drugs in order to investigate whether NRTI, NNRT and PI can provide novel chemotherapeutic agents in the future especially in cervical cancer and HIV because the prevalence of both diseases is high and it would be of great benefit to people affected by both illnesses to be able to take a combined treatment regime for both illnesses.

CHAPTER FIVE: CONCLUSION AND FUTURE STUDIES

5.1 Conclusion

This study revealed that the antiretroviral drugs used reduced the gene and protein expression of MUC1 and P65 in HCS-2 cells. The PI combination (LPV/r) had more distinct effects than the other drugs. This finding suggests that by reducing MUC1 and P65 gene and protein expression the cells were more susceptible to cell death stimuli and cell death pathways were more likely to be activated at this state.

The morphological features observed following drug treatment; loss of cell contacts, reduced microvilli density and length, increased blebbing, formation of apoptotic bodies, are characteristic of cell death, especially through apoptosis, these observations suggests that the cells were undergoing death through apoptosis.

Furthermore the cell secretions are suggested to be contents of apoptotic bodies. *In vivo* apoptotic bodies are removed by macrophages; however, in an isolated system like cell culture where macrophages are not present to engulf the apoptotic bodies they undergo degradation which is similar to necrosis and they ultimately release their contents into the extracellular space and at this stage cell death is known as apoptotic-necrosis or secondary necrosis (Saraste and Pulkki, 2000; Majno and Joris, 1995).

5.2 Future studies

The antiretroviral drugs used in this study induced cell death through apoptosis and had no effect on the gene and protein expression of MUC1 and P65 except for LPV/r which reduced MUC1 expression, although the exact pathway/s they use in order to induce apoptosis has not yet been identified. Drugs that have the potential to induce apoptosis have long been targeted for novel cancer therapy (Plati *et al.,* 2008). Future studies that can be conducted in order to

further investigate the potential of these drugs as novel cancer therapy include *in vitro* and *in vivo* studies where the ARV drugs will be combined with chemotherapeutic agents and their effects on key signalling pathways in cancer such as EGFR and HER2/ErbB-2, Ras, PKC, AKT/PKB and mTOR and angiogenesis (Bianco *et al.*, 2006).

In addition dose-dependent studies should be conducted in order to determine the optimal dosage of the drug to be used in combination with chemotherapy that will result in the best inhibition of cancer cell proliferation. Moreover an identification of key signalling proteins and pathways that are activated by the drugs during cell death will be useful in optimising them for cancer therapy.

This kind of advancement is imperative, especially in light of the high risk and prevalence of HIV/AIDS and cervical cancer, particularly in a majority of developing countries. If cancer and HIV/AIDS treatment can be combined into one regimen, it will possibly reduce production costs of the medication, which will in turn reduce the cost of buying the medication. Consequently it will be more affordable to the public sector, for example public hospitals, thus ensuring that more women have access to and receive the treatment and ultimately it will lead to better manangement of the disease.

6. REFERENCES

- Abbott laboratories, Limited. (2010). KALETRA® product monograph. Pg 1-91.
- Adefolaju, G.A., Theron, K.E., Hosie, M.J. (2013). Effects of HIV protease, nucleoside/non-nucleoside reverse transcriptase inhibitors on Bax, bcl-2 and apoptosis in two cervical cell lines. *Biomedicine and Pharmacotherapy*. http://dx.doi.org/10.1016/j.biopha.2013.08.007.
- Amos, W.B., White, J.G. (2003). How the confocal laser scanning microscope entered biological research. *Biology of the cell* **95:** 335-342.
- Anorlu, R. (2008). Cervical cancer; the sub-Saharan African perspective. *Reproductive Health Matters* **16:** 41-49.
- Arts, E.J., Hazuda, D.J. (2012). HIV-1 antiretroviral drug therapy. *Cold Spring Harbor Perspectives in Medicine* **2:** a007161.
- Arya, M., Shergill, I.S., Williamson, M., Gommersall, L., Arya, N., Patel, H.R.H. (2005). Basic principles of real time quantitative PCR. *Expert Review of Molecular Diagnostics* **5:** 209-219.
- Bafna, S., Kaur, S., Batra, S.K. (2010). Membrane-bound mucins: the mechanistic basis for alterations in the growth and survival of cancer cells. *Oncogene* **29:** 2893-2904.
- Baiocchi, G., Begnami, M.D., Fukazawa, E.M., Oliveira, R.A.R., Faloppa, C.C., Kumagai, L.Y., et al. (2012). Prognostic value of nuclear factor k β expression in patients with advanced cervical cancer undergoing radiation therapy followed by hysterectomy. *Journal of Clinical Pathology* 2011-200599
- Banerjee, S., Mujumdar, N., Dudeja, V., Mackenzie, T., Krosch, T.K., Sangwan, V., et al. (2012). MUC 1-C regulates cell survival in pancreatic cancer by preventing lysosomal permeabilisation. *PLos one* **7:** 1-12.

- Batman, G., Oliver, A.W., Zehbe, I., Richard, C., Hampson, L., Hampson, I.N. (2011). Lopinazir up-regulates expression of the antiviral protein ribonuclease L in human Papillomavirus positive cervical carcinoma cells. *Antiviral Therapy* **16:** 515-525.
- Batra, P., Kuhn, L., Denny, L. (2010). Utilisation and outcomes of cervical cancer prevention services among HIV-infected women in Cape Town. *South African Medical Journal* **100:** 39-44.
- Bean, P. (2005). New drug targets for HIV. *Clinical Infectious Diseases* **41**: 96-100.
- Bharti, A.C., Aggarwal, B.B. (2002). Nuclear factor kappa β and cancer; its role in prevention and therapy. *Biochemical Pharmacology* **64:** 883-888.
- Bianco, R., Melisi, D., Ciardiello, F., Tortora, G. (2006). Key cancer cell signal transduction pathways as therapeutic targets. *European Journal of Cancer* **42:** 290-294.
- Bitler, B.G., MenzI, I., Huerta, C.L., Sands, B., Knowlton, W., Chang, A., Schroeder, J.A. (2009). Intracellular MUC1 peptides inhibit cancer progression. *Clinical Cancer Research* **15:** 100-109.
- Bjelaković, G., Nagorni, A., Bjelaković, M., Stamenković, I., Arsic, R., Katić, V. (2005). Apoptosis: programmed cell death and its clinical implications. *Medicine and Biology* **12:** 6-11.
- Bomela, N., Stevens, M. (2009). Cervical cancer and HIV; the intimate connection. Policy brief.
- Bratcher, L.F., Sahasrabuddhe, V.V. (2010). The impact of antiretroviral therapy on HPV and cervical intraepithelial neoplasia: current evidence and directions for future research. *Infectious Agents and Cancer* **5:** 8.

- Brayman, M., Thathiah, A., Carson, D.D. (2004). MUC1: a multifunctional cell surface component of reproductive tissue epithelia. *Reproductive Biology and Endocrinology* **2:** 4-13.
- Cancer in South Africa 2007 Full Report. National Cancer Registry. www.nhls.ac.za.
- Cascio, S., Zhang, L., Finn, O.J. (2011). MUC1 protein expression in tumour cells regulates transcription of pro-inflammatory cytokines by forming a complex with nuclear factor-kβ P65 and binding to cytokine promoters. *The journal of Biological Chemistry* **286:** 42248-42256.
- Clay, P.G., Taylor, A.H.T., Glaros, A.G., McRae, M., Williams, C., McCandless, D. and Oelklaus, M. (2008). "One pill, once daily": what clinicians need to know about Atripla™. *Therapeutics and Clinical Risk Manangement* **4:** 291-302.
- Condello, M., Caraglia, M., Castellano, M., Arancia, G., Meschini, S. (2013). Structural and functional alterations of cellular components as revealed by electron microscopy. *Microscopy Research and Technique* **76:** 1057-1069.
- Crommentuyn, K.M.L., Mulder, J.W., Mairuhu, A.T.A., Gorp, E.C.M., Meenhorst, P.L., Huitema, A.D.R., Beijnen, J.H. (2004). The plasma and intracellular steady-state pharmacokinetics of Lopinavir/ritonavir in HIV-1-infected patients. *Antiviral Therapy* **9:** 779-785.
- Debatin, K.M. (2004). Apoptosis pathways in cancer and cancer therapy. *Cancer Immunology and Immunotherapy* **53:** 153-159.
- Dekker, J., Rossen, J.W.A., Buller, H.A., Einerhand, A.W.C. (2002). The MUC family: an obituary. *Trends in Biochemical Sciences* **27:** 126-131.
- Fackler, O.T., Grosse, R. (2008). Cell motility through plasma membrane blebbing. *Journal of Cell Biology* **181:** 879-884.

- Ferenczi, A., Gyöngyösi, E., Szalmás, A., Hernádi, Z., Tóth, Z., Kónya, J., Veress, G. (2013). Sequence variation of human Papillomavirus type 31 long control region: phylogenetic and functional implications. *Journal of Medical Virology* **85:** 852-859.
- Firnhaber, C., Westreich, D., Schulze, D., Williams, S., Siminya, M., Michelow, P., et al. (2012). Highly active antiretroviral therapy and cervical dysplasia in HIV-positive women in South Africa. *Journal of the International AIDS Society* **15:** 1-6.
- Gendler, S.J. (2001). MUC1, the renaissance molecule. *Journal of Mammary Gland Biology and Neoplasia* **6:** 339-353.
- Gil, J.F., Augustine, T.N., Hosie, M.J., (2013). Anastrozole and RU486: Effects on estrogen receptor α and mucin 1 expression and correlation in the MCF-7 breast cancer cell line. *Acta Histochemica* **115:** 851-857.
- Gilead Science. (2001). Highlights of prescribing information (VIREAD). *Reactions.* Pg 1-43.
- Gilead Sciences and Bristol-Myers Squibb LLC. (2006). Atripla (Efavirenz/Emtricitabine/Tenofovir Disoproxil fumarate) tables. Pg 1-55.
- Gilead Sciences and Bristol-Myers Squibb. (2006). Highlights of prescribing information (ATRIPLA). *Sciences- New York.* Pg 1-155.
- Gilead Sciences. (2003). Highlights of prescribing information (EMTRIVA). *Pharmacology.* Pg 1-29.
- Gills, J.J., Lopiccolo, J., Tsurutani, J., Schoemaker, R.H., Best, C.J.M., Abu-Asab, M.S., Borojerdi, J., Warfel, N.A., Gardner, E.R., Danish, M., Christine Hollander, M., Kawabata, S., Tsokos, M., Figg, W.D., Steeg, P.S., Dennis, P.A. (2007). Nelfinavir, a lead HIV protease inhibitor, is a broad-spectrum, anticancer agent that induces endoplasmic reticulum stress, autophagy and apoptosis *in vitro* and *in vivo*. *Clinical Cancer Research* **13:** 5183-5195.

- Goldie, S. (2006). A public health approach to cervical cancer control: considerations of screening and vaccination strategies. *International Journal of Gynecology and Obstetrics* **94:** S95-S105.
- Gomez, D.T., Santos, J.L. (2007). Human Papillomavirus infection and cervical cancer: pathogenesis and epidemiology. *Communicating Current Research and Educational Topics and Trends in Applied Microbiology* **(Ed):** 680-688.
- Hertlein, E., Wang, J., Ladner, K.J., Bakkar, N., Guttridge, D.C. (2005). RelA/P65 regulation of IkBβ. *Molecular and Cellular Biology* **25:** 4956-4968.
- Hiscott, J., Kwon, H., Genin, P. (2001). Hostile takeovers; viral appropriation of the NFkβ pathway. *The Journal of Clinical Investigation* **107:** 143-151.
- Horberg, M.A., Klein, D.B. (2010). An update on the use of Atripla® in the treatment of HIV in the United States. *HIV/AIDS-Research and Palliative Care* **2:** 135-140.
- Huxford, T., Ghosh, G. (2009). A structural guide to proteins of the NFkβ signalling module. *Cold Spring Harbour Perspectives on Biology* 1: a000075.
- Invitrogen manual, Real time-PCR from theory to practice. (2008).
- Israr, M., Mitchell, D., Alam, S., Dinello, D., Kishel, J.J., Meyers, C. (2011). The HIV protease inhibitor Lopinavir/ritonavir (Kaletra) alters the growth, differentiation and proliferation of primary gingival epithelium. *HIV Medicine* **12:** 145-156.
- Jemal, A., Bray, F., Center, M.M., Ferlay, J., Ward, E., Forman, D. (2011). Global cancer statistics. *CA Cancer Journal for Clinicians* **61:** 69-90.
- Johnson, M. (2012). Antibody shelf life/ How to store antibodies. *Materials and Methods* **2:** 120.
- Jongebloed, W.L., Stokroos, I., Kalicharan, D., Van der Want, J.J.L. (1999). Is cryopreservation superior over tannic acid/arginine/osmium tetroxide non-coating

preparation in field emission scanning electron microscopy. *Scanning Electron Microscopy* **13:** 93-101.

- Jutooru, I., Chadalapaka, G., Lei, P., Safe, S. (2010). Inhibition of NFkB and pancreatic cancer cell and tumor growth by curcumin is dependent on specificity protein down-regulation. *The Journal of Biological Chemistry* **285:** 25332-25344.
- Keen, O.N. (1995). The log transformation is special. *Statistics in Medicine* **14:** 811-819.
- Klinge, C.M., Radde, B.N., Imbert-Fernandez, Y., Teng, Y., Ivanova, M.M., Abner, S.M., Martin, A.L. (2011). Targeting the intracellular MUC1 c-terminal domain inhibits proliferation and estrogen receptor transcriptional activity in lung adenocarcinoma cells. *Molecular Cancer Therapeutics* **10:** 2062-2071.
- Kroemer, G., Galluzzi, L., Vandenabeele, P., Abrams, J., Alnemri, E.S., Baehrecke, E.H., Blagosklonny, M.V., El-Deiry, W.S., Golstein, P., Green, D.R., Hengartner, M., Knight, R.A., Kumar, S., Lipton, S.A., Malorni, W., Nunez, G., Peter, M.E., Tschopp, J., Yuan, J., Piacentini, M., Zhivotovsky, B. and Melino, G. (2009). Classification of cell death. *Cell Death and Differentiation* **1:** 3-11.
- Kufe, D.W. (2009). Mucins in cancer: function, prognosis and therapy. *Nature Reviews Cancer* **9:** 874-885.
- Kumar, P., Lindberg, L., Thirkill, T.L., Li, J.W., Martsching, L., et al. (2012). The MUC1 extracellular domain subunit is found in nuclear speckles and associates with spliceosomes. *PLos one* **7:** 1-18.
- Lange, K., Gartzke, J. (2001). Microvillar cell surface as a natural defense system against xenobiotics: a new interpretation of multidrug resistance. *American Journal of Physiology* **281:** C369-C385.

- Li, F., Lu, J., Ma, X. (2011). CPY3A4- mediated Lopinavir bio-activation and its inhibition by Ritonavir. *Drug Metabolism and Disposition* **40:** 18-24.
- Livak, K.J., Schmittgen, T.D. (2001). Analysis of relative gene expression data using real-time quantitative PCR and the $2^{-\Delta\Delta Ct}$ method. *Methods* **25:** 402-408.
- Majno, G. and Joris, I. (1995). Apoptosis, oncosis and necrosis. An overview of cell death. *American Journal of Pathology* **146:** 3-15.
- Masters, J.R., Stacey, G.N. (2007). Changing medium and passaging cell lines. *Nature Protocols* **2:** 2276-2284.
- Mbulaiteye, S. M., Biggar, R.J., Goedert, J.J. and Engels, A.E. (2003). Immune Deficiency and Risk for Malignancy among Persons with AIDS. *Journal of acquired immune deficiency syndromes* **32:** 527-533.
- Meseguer, M., Pellicer, A., Simón, C. (1998). MUC1 and endometrial receptivity. *Molecular Human Reproduction* **4:** 1089-1098.
- Mistro, A.D., Bertorelle, R., Franzetti, M., Cattenlan, A., Torrisi, A., Giordani, M.T., Sposetti, R., Bonoldi, E., Sasset, L., Bonaldi, L., Minucci, D., Chieco-Bianchi, L. (2004). Antiretroviral therapy and the clinical evolution of Human Papillomavirus associated genital lesions in HIV positive women. *Clinical Infectious Diseases* **38:** 737-742.
- Mojakgomo, R.M. (2012). Molecular analysis of longevity assurance genes (LASS)/ ceramide synthases (CerS) 4 and 5 in endometrial and colon cancer. [Dissertation]. University of the Witwatersrand, Johannesburg, South Africa.
- Murakami, T., Song, Z., Hinenoya, H., Ohtsuka, A., Taguchi, T., Liu, J., Sano, T. (1987). Lysine-mediated tissue osmication in combination with a tannin-osmium conductive staining method for non-coated scanning electron microscopy of biological specimens. *Archives of Histology and Cytology* **50:** 485-493.

- Norman, L.L, Brugés, J., Sengupta, K., Sens, P., Aranda-Espinoza, H. (2010). Cell blebbing and membrane area homeostasis in spreading and retracting cells. *Biophysical Journal* **99:** 1726-1733.
- Paddock, S.W. (2000). Principles and practices of laser scanning confocal microscopy. *Molecular Biotechnology* **16:** 127-149.
- Plati, J., Bucur, O., Khosravi-Far, R. (2008). Dysregulation of apoptotic signalling in cancer: molecular mechanisms and therapeutic opportunities. *Journal of Cellular Biochemistry* **104:** 1124-1149.
- Rabkin, C.S. (2001). AIDS and cancer in the era of highly active antiretroviral therapy (HAART). *European Journal of Cancer* **37:** 1316-1319.
- Saraste, A., Pulkki, K. (2000). Morphologic and biochemical hallmarks of apoptosis. *Cardiovascular Research* **45:** 528-537.
- Shukla, S., MacLennan, G.T., Fu, P., Patel, J., Marengo, S.R., Resnick, M.I., Gupta, S. (2004). Nuclear factor-kβ /P65 (RelA) is constitutively activated in human prostate adenocarcinoma and correlates with disease progression. *Neoplasia* **6:** 390-400.
- Sibiya, N. (2012). Challenges to cervical cancer in the developing countries; South African context. *Topics on Cervical Cancer with Advocacy for Prevention.* ISBN 978-953-51-0183-3.
- Sirera, G., Videla, S., Lopez-Blazquez, R., Llatjos, M., Tarrats, A., Castella, E., et al. (2008). Highly active antiretroviral therapy and incidence of cervical squamous intraepithelial lesions among HIV-infected women with normal cytology and CD4 counts above 350 cells/ mm^3. *Journal of Anti-microbial Chemotherapy* **61:** 191-194.
- Stanley, M. (2010). Pathology and epidemiology of HPV infection in females. *Gynecologic Oncology* **117:** S5-S10.

- Thabethe, K., Adefolaju, G., Hosie, M. (2013). An in vitro study of the effects of Emtricitabine, Tenofovir disoproxil fumarate and efavirenz on a breast cancer cell line, MCF-7. *Journal of Basic and Applied Scientific Research* **3:** 444-452.
- Thomas, M., Narayan, N., Pim, D., Tomaić, V., Massimi, P., Nagasaka, K., Kranjec, C., Gammoh, N., Banks, L. (2008). Human Papillomaviruses, cervical cancer and cell polarity. *Oncogene* **27:** 7018-7030.
- Thompson, E.J., Shanmugam, K., Hattrup, C.L. (2006). Tyrosines in the MUC1 cytoplasmic tail modulate transcription via the extracellular signal-regulated kinase ½ and nuclear factor kβ pathways. *Molecular Cancer Research* **4:** 489-497.
- Uleberg, K., Munk, A.C., Skaland, I., Furlan, C., Van Diermen, B., Gudlaugsson, E., et al. (2011). A protein profile study to discriminate CIN lesions from normal cervical epithelium. *Cell Oncology* **34:** 443-450.
- Van England, M., Kuijpers, H.J.H., Ramaekers, F.C.S., Reutelingsperger, C.P.M., Schuttle, B. (1997). Plasma membrane alterations and cytoskeletal changes in apoptosis. *Experimental Cell Research* **235:** 421-430.
- Villa, L.L. (2006). Biology of genital human Papillomaviruses. *International Journal of Gynecology and Obstetrics* **94:** S3-S7.
- Vlahakis, S.R., Bennett, S.A.L., Whitehead, S.N., Bradley, A.D. (2007). HIV protease inhibitors modulate apoptosis signalling *in vitro* and *in vivo*. *Apoptosis* **12:** 969-977.
- Xi, L.F., Kiviat, N.B. (2004). Cervical neoplasia and highly active antiretroviral therapy. *Journal of the National Cancer Institute* **96:** 1051-1053.
- Xia, L., Xue, X. (2012). Immunohistochemical study of NF-kB P65, c-IAP2 and caspase-3 expression in cervical cancer. *Oncology Letters* **3:** 839-844.
- Xu, M., Deng, P., Qi, C., Deng, B., Zhao, Z., Wong, V., Ngan, T., Kan, V., Tian, X., Xu, D., Au, D. (2009). Adjuvant phytotherapy in the treatment of cervical cancer: a

systematic review and meta-analysis. *The Journal of Alternative and Complementary Medicine* **15:** 1347-1353.

- Yang, B.H., Bray, F.I., Maxwell Parkin, D., Sellors, J.W., Zhang, Z. (2004). Cervical cancer as a priority for prevention in different world regions; an evaluation using years of life lost. *International Journal of Cancer* **109:** 418-424.
- Yuan, Z., Wong, S., Borrelli, A., Chung, M.A. (2007). Down-regulation of MUC1 in cancer cells inhibits cell migration by promoting E-cadherin/catenin complex formation. *Biochemical and Biophysical Research Communications* **362:** 740-746.
- Zaretsky, J.Z., Barnea, I., Aylon, Y., Gorivodsky, M., Wreschner, D.H., Keydar, I. (2006). MUC1 gene over-expressed in breast cancer: structure and transcriptional activity of the MUC1 promoter and role of estrogen receptor alpha (ERα) in regulation of the MUC1 gene expression. *Molecular Cancer* **5:** 57.
- Zhang, Y., Hu, B., Dai, Y., Yang, H., Huang, W., Xue, X., Li, F., Zhang, X., Jiang, C., Gao, F., Chang, J. (2013). A new multichannel spectral imaging laser scanning confocal microscope. *Computational and Mathematical Methods in Medicine* **2013:** 1-8.
- Zheng, C., Yin, Q., Wu, H. (2011). Structural studies of NFkB signalling. *Cell Research* **21:** 183-195.

7. APPENDICES

7.1 APPENDIX I:Cell culture solutions

7.1.1 0.1M Phosphate buffered solution (PBS), ph 7.4 (1*l*)

- 8g NaCl
- 1.15g Na_2HPO_4
- 0.2g KCL
- 0.2g KH_2PO_4

Dissolve the salts in 800ml of distilled water (dH_2O), measure the pH using a pH meter and adjust using appropriate solution (either KCl or NAOH) to get a final ph of 7.4. Then add the remaining 200ml of dH_2O to make up a final volume of 1*l*.

7.1.2 Trypan blue exclusion method for viable cells

- 0.4% Trypan blue in PBS
- Haemocytometer and coverslip
- Pipette and tips
- Inverted microscope

Suspend cells in 1ml of medium (following harvesting with Trypsin-EDTA) and collect 10µl of the cell suspension into an Eppendorff tube. Dilute the cell suspension with 40µl of 0.4% Trypan blue to make up 50µl of cell suspension. Pipette 15µl of the cell suspension in Trypan blue onto a haemocytometer and observe the grid under the inverted microscope at 5X and 20X magnification (Refer to figure 7.1 for the layout of the grid). Viable cells will appear unstained, whereas dead cells will engulf the Trypan blue dye and as a result will be stained

blue and are therefore excluded from cell counting. The live cells that lie within the large squares of the grid located at the corners are counted and cell counts are recorded.

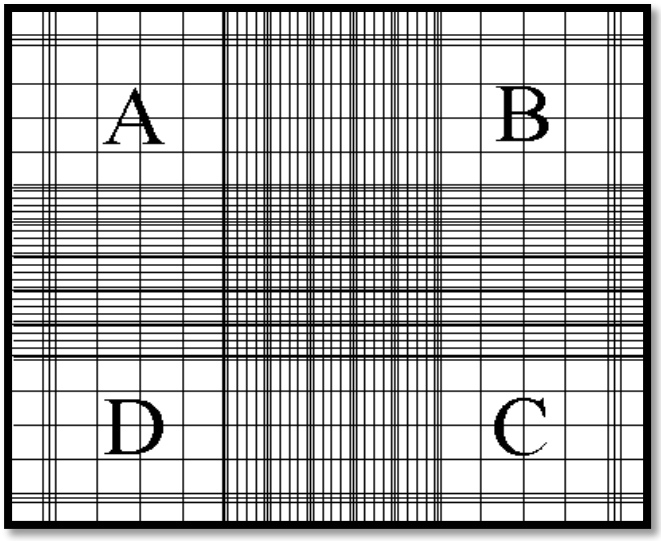

Figure 7.1: A diagram showing the haemocytometer with the blocks in which the cells were counted labelled alphabetically (A,B,C and D). Image obtained from: home.cc.umanitabo.ca

7.1.3 Cell counting

To calculate cell concentration per ml;

- Get an average number of cells (n) in the four large squares
- Using the following formula calculate the cell concentration in 1ml:

  Cell concentration in 1ml= average number of cells counted per square (*n*) *dilution factor (dilution factor was 5 in this case)* 10^4(conversion factor to convert 10-4ml to 1ml)

- To get the amount needed for seeding:

X amount= no. of cells required/ concentration of cells in 1ml

$= Y\ ml * 1000$

$= z\ \mu l$

- Therefore *z* μl is seeded in order to get the required number of cells.

7.2 APPENDIX II: Additional methods for qPCR

7.2.1 Principle of quantitative real time Polymerase Chain Reaction (qPCR) and rationale for its use

Polymerase chain reaction (PCR) amplifies and detects as little as one copy of a specific sequence of DNA by generating copies of a DNA template exponentially (Arya *et al*., 2005). Therefore it enables the quantification of the amount of starting target sequence and PCR product accumulated during the course of the amplification cycle (Arya *et al*., 2005). The end point of the PCR cycle is the plateaux phase and it is reached when polymerase reaction inhibitors are dominant within the template and the reagents are used up (Arya *et al*., 2005). At this phase the PCR reaction no longer produces the template at an exponential rate therefore quantifying PCR products during this phase is deemed unreliable (Arya *et al*., 2005). The exponential phase is considered the most accurate phase of the PCR reaction where the amount of starting material of the template sequence can be determined (Arya *et al*., 2005). Real time PCR measures the amount of amplified product present during each stage of the PCR cycle, especially the exponential phase, and quantifies it; therefore it is considered to be superior to conventional PCR which measures the PCR products at the end of the plateaux phase (Invitrogen, 2008; Arya *et al*., 2005). If the starting material of the particular sequence was abundant, amplification is observed rapidly whereas if the starting material of the sequence was less abundant amplification will be observed at a later stage (Invitrogen, 2008). The amplified product is quantified by use of fluorescent probes (Taqman polymerase) or fluorescent DNA-binding dyes (SYB Green) (Invitrogen, 2008). In addition to performing the necessary temperature changes needed for the PCR cycles real time PCR thermocyclers are equipped to measure the increase in fluorescence emission during a PCR reaction and computer software plots an amplification plot using that data (Invitrogen, 2008).

Real time PCR has been widely used in various experiment such as mRNA expression studies, measure of DNA copy numbers in genomic or viral DNAs, gene expression studies in tissues and cells etc because it monitors the PCR reaction as it progresses in real time and it accurately measures the amount of PCR product at each cycle (Arya *et al*., 2005). Overall it is a rapid but precise method of measuring gene expression (Arya *et al*., 2005).

7.2.2. RNA extraction method

The cell suspension was centrifuged for 5 mins at 250Xg. The cell pellet collected at bottom of the tube and the supernatant was discarded. The cell pellet was resuspended in 600µl of lysis buffer (supplemented with 2% β-mercaptoethanol purchased from uniLAB) and mixed by pipetting. The sample was then pipetted into a QIAshredder spin column placed in a 2ml collecting tube (QIAGEN). Thereafter the sample was centrifuged at maximum speed for 2 minutes. 360µl of ethanol was added onto the sample and mixed by pipetting; ethanol helps the RNA in binding to the silica membrane of the spin column. A maximum of 700µl of lysate was transferred into a Gene-JET RNA purification column inserted in a collecting tube. The column was centrifuged for 1 minute at 12000Xg, thereafter the collecting tube containing the flow through was removed from the column, the flow through was discarded and the collecting tube was placed back below the column. This step was repeated until all the lysate was transferred into the column.

700µl of wash buffer1 (supplemented with 20% ethanol) was added into the Gene-JET RNA Purification column and the column was centrifuged for 1 minute at 12000X g. The flow through in the collecting tube was discarded and the column was placed back into the collecting tube. 600µl of wash buffer 2 (supplemented with 63% ethanol) was added to the Gene-JET RNA Purification column and centrifuged for 1 minute at 12000X g. The flow through in the collecting tube was discarded and the column was placed back into the

collecting tube. 250 µl of wash buffer 2 (supplemented with 63% ethanol) was added to the Gene-JET RNA purification column and centrifuged for 2 minutes at 12000X g. The collecting tube was emptied and placed back into the column and centrifuged for 2 minutes at 12000X g. The collecting tube containing the flow through was discarded and the Gene-JET RNA purification column was transferred into a sterile 1.5ml microcentrifuge tube. 100µl of nuclease-free water was added into the Gene-JET RNA purification column membrane and centrifuged for 1 minute at 12000X g in order to elute RNA

7.2.3 Nanodrop method

Switch on the Nanodrop and wipe with RNase-free water and lab paper. Pipette 2µl of RNase-free water to initiate it and press ok. Click on nucleic acid and select RNA (constant=40) wipe Nanodrop with lab paper. Pipette 1.5µl of RNA sample onto the Nanodrop and click measure. The Nanodrop measures the concentration of RNA per µl and gives a value for the 260/280 ratio and 260/230 ratio.

- 260/280 ratio: measures nucleic acid purity, the ideal ratio ranges between 1.8- 2.1.
- 260/230 ratio: measures the level of contaminants in the sample from the preparation (ideal ratio greater than 1.5, ideally 2)

Table 7.1: Summary of the RNA concentrations and purification ratios per group

Sample ID	~Cells/ml	[RNA] ng/µl	260/280	260/230
Untreated 1	1 378 500	59	2.0	1.92
Untreated 2	7 100 000	265.4	1.96	2.26
Untreated 3	6 737 500	306.6	2.02	1.95
Methanol 1	8 250 000	595.8	2.01	2.17
Methanol 2	6 237 500	701.7	2.04	2.10
Methanol 3	6 637 500	168.3	1.97	2.17
ATP 1	7 387 500	392.0	1.94	2.20
ATP 2	4 012 500	452.3	1.97	1.93
ATP 3	4 375 000	415.2	1.96	2.18
LPV/r 1	3 787 500	423.3	1.95	2.25
LPV/r 2	4 925 000	458.7	1.94	2.09
LPV/r 3	4 537 500	386.0	1.98	2.19

7.2.4 Genomic DNA removal from RNA preparations

Add the following to an RNase free tube;

- 1µg RNA
- 1µl 10X reaction buffer with $MgCl_2$
- 1µl DNaseI, RNase free
- RNase free water to make up 10µl

Incubate the mixture for 30minutes at 37°C. Add 1µl 50mM EDTA and incubate for 10minutes at 65°C in order to inactivate DNaseI activity. The final concentration of RNA in the mixture will be 0.1µg/µl.

Table 7.2: The amount of RNA used in the cDNA reaction

RNA sample	Amount needed to make 1µg of RNA in cDNA reaction (µl)	Nuclease-free water used (µl)	Combined volume of 10X reaction buffer and DNaseI (µl)	Total (µl)
Untreated R1	7	1	2	10
Untreated R2	4	4	2	10
Untreated R3	3.5	4.5	2	10
0.02% Methanol R1	1.7	6.3	2	10
0.02% Methanol R2	1.5	6.5	2	10
0.02% Methanol R3	6	2	2	10
ATP R1	2.8	5.2	2	10
ATP R2	2.3	5.7	2	10
ATP R3	2.5	5.5	2	10
LPV/r R1	2.4	5.6	2	10
LPV/r R2	2.2	5.8	2	10
LPV/r R3	2.6	5.4	2	10

7.2.5 cDNA synthesis (RNA and H_2O combinations used)

Table 7.3: The table show the various components of the master mix used for cDNA synthesis.

Component	**Volume per reaction (µl)**
10X RT buffer	2.0
25X dNTP mix (100mM)	0.8
10X RT random primers	2.0
Multiscribe Reverse transcriptase	1.0
RNase inhibitor	1.0
Nuclease-free H_2O	3.2
Total	**10**

10µl of the master mix was pipetted using filter pipettes into RNase-free 1.5 ml eppendorfs tubes and the corresponding amount of RNA and RNA-free H_2O which together made up 10µl was added to each reaction tube to make up a final reaction volume of 20µl with an RNA concentration of ~100ng/20µl reaction (Table 7.5). All the work was carried out on ice. Following master mix preparation the cDNA reaction was run in the Applied Biosystems GeneAmp PCR System 2400 machine under the conditions indicated in the table below.

Table 7.4: Table depicting thermocycler conditions for cDNA synthesis

	Step1	**Step2**	**Step3**	**Step4**
Temperature (°C)	25	37	85	4
Time (minutes)	10	120	5	∞

Table 7.5: The RNA and water combination that were used in order to synthesize cDNA from each sample.

	RNA (µl)	**H_2O (µl)**	**Total (µl)**
Untreated R1	5	5	10
Untreated R2	2	8	10
Untreated R3	1.9	8.1	10
0.02% Methanol R1	2	8	10
0.02% Methanol R2	2	8	10
0.02% Methanol R3	2	8	10
ATP R1	1.9	8.1	10
ATP R2	2	8	10
ATP R3	2	8	10
LPV/r R1	2	8	10
LPV/r R2	2	8	10
LPV/r R3	2	8	10

The final volume of 10µl from table X together with the 10µl from the cDNA master mix made up a volume of 20µl which was then put into the Applied Biosystems GeneAmp PCR System 2400 machine for cDNA synthesis.

7.2.6 Tukey Kramer *Post Hoc* test results

Table 7.6: Analysis of means using Tukey-Kramer *Post Hoc* test for *MUC1* expression, levels not connected by the same letter are significantly different.

Level	
Untreated	A
ATP	A
0.02% methanol	A
LPV/r	B

Table 7.7: Analysis of means using Tukey-Kramer *Post Hoc* test for *P65* expression, levels not connected by the same letter are significantly different.

Level	
Untreated	A
LPV/r	A
0.02% methanol	A
ATP	A

7.3 APPENDIX III: Immunocytochemistry solutions and additional information

7.3.1 4% Paraformaldehyde

- 4g Paraformaldehyde (PFA)
- 100ml PBS (pH 7.4)
- Hot plate
- NaOH

Weigh out 4g of PFA and dissolve in 100ml of PBS (pH 7.4). Place the solution onto a hot plate heated to 60°C and stir with magnetic stirrer until all the PFA is dissolved. Then add a few drops of NaOH until the solution is clear. Filter the solution and adjust the pH to 7.4, autoclave then store the solution in the freezer until use.

7.3.2 0.1M Citrate buffer, pH 6

- Solution A; dissolve 10.5g of citric acid in 500ml distilled water
- Solution B; dissolve 29.4g of sodium citrate in 1000ml distilled water

To make up 500ml of citrate buffer mix 9ml of solution A and 41ml of solution B.

7.3.3 Permeabilisation solution (0.25% Triton X-100 in PBS)

- Triton X-100
- PBS (pH 7.4)

To make up 25ml of solution; add 62.5µl of Triton X-100 in 25ml of PBS (pH 7.4)

7.3.4 Blocking solution (10% normal serum in PBS)

- Normal goat serum
- PBS (pH 7.4)

To make up 10ml of the solution add 1ml of normal goat serum to 9ml of PBS (pH 7.4).

7.3.5 Antibody dilution solution (1% BSA/PBS)

- 5g Bovine serum albumin (BSA)
- 500ml PBS (pH 7.4)

Dissolve 5g of BSA in 500ml of PBS (pH 7.4) to make up 500ml solution of 1%BSA in PBS.

7.3.6 Principle of Laser Scanning Confocal Microscopy and rationale for its use

The concept for the confocal microscope was proposed by Minsky in 1950s but it first became commercially available in 1987 (Zhang *et al*., 2013). The design for a Laser Scanning Confocal Microscope (LSCM) is derived from a conventional Light Microscope (LM), however the source of light is a laser instead of a mercury or xenon lamp as in the LM (Amos and White, 2003; Paddock, 2000). Unlike LM whereby the whole specimen is immersed in light and the image is visible by the naked eye, In the LSCM light and detection are restricted to a single, diffraction-limited point which is focused on the specimen by an objective lens and scanned across the specimen, thereby producing optical sections; images produced by means of scanning the specimen with a beam of light (Amos and White, 2003; Paddock, 2000). The confocal microscope eliminates out-of-focal-plane light by means of spatial filters therefore allows the detection of light from the focal plane (Zhang *et al*., 2013). Consequently it has high spatial resolution and signal-to-noise ratio; in addition it is capable of optically sectioning samples in the z axis in order to create 3D images of thick samples (Zhang *et al*., 2013). This technique is a non invasive process of sectioning specimen,

therefore it preserves cell and tissue integrity (Amos and White, 2003; Paddock, 2000). LSCM is equipped with sensitive photomultiplier detectors (PMTs) which are positioned behind a pin hole and are connected to a computer which controls the scanning mirrors and facilitates compilation and display of images (Amos and White, 2003; Paddock, 2000). The PMT detects light from the specimen and its output develops an image on the computer (Amos and White, 2003; Paddock, 2000).The obtained images are stored in the computer and can be analysed using a variety of computer software installed on the confocal computer or another computer (Amos and White, 2003; Paddock, 2000). LSCM is a valuable and essential instrument for the observation of fixed and live tissues/cells, which are often labelled with fluorescent probes through immunocytochemistry (Zhang *et al*., 2013). It has gradually become a vastly used tool in various disciplines for example tissue biology, cell biology, molecular biology, genomics, embryology, neurology, pathology, immunology etc. (Zhang *et al*., 2013; Amos and White, 2003; Paddock, 200).

7.3.7 Antibody dilution for MUC1 and P65 primary antibodies

Dilution	**1:100**	**1:150**	**1:250**
Anti-MUC1 antibody [EPR1023] (ab109185)	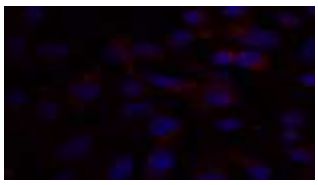	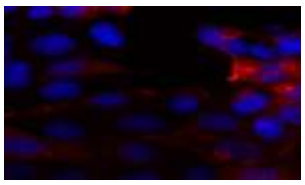	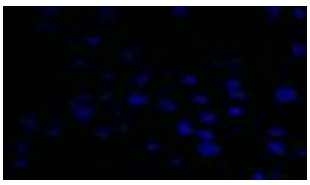
Dilution	**1: 250**	**1: 500**	**1: 1000**
Anti-NFkB p65 antibody [NF-12] (ab10437)	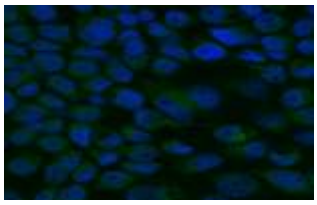	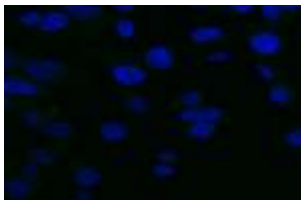	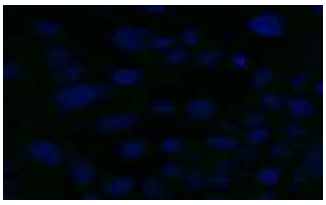

7.4 APPENDIX IV: SEM SOLUTIONS AND TUKEY KRAMER POST HOC TEST TABLES

7.4.1. Principle of Scanning Electron Microscopy and rationale for its use

Ernst Ruska and Max Knoll constructed the first prototype electron microscope in 1931 and since its commercialisation in 1939, they have enabled biologists to explore the interesting intracellular world and study surface morphology in more detail (Condello *et al*., 2013). The electron microscope has been shown to be superior to light microscope (LM) because it has better resolving power than a LM (Condello *et al*., 2013). Electron microscopes make use of an electron beam to form images with higher magnification and greater resolving power than a light microscope (Condello *et al*., 2013). The SEM is designed to provide information about the general morphology and surface structure of biological samples (Condello *et al*., 2013). In the SEM, an electron beam is focused and scanned within a narrow area on the specimen (Condello *et al*., 2013). Upon interaction of the primary incident beam electrons with the surface layer of the specimen, emissions of various signals which carry information about surface topography and composition are produced (Condello *et al*., 2013). The SEM is able to image bulk samples with a great depth of field therefore it produces images which are a good representation of the accurate 3 dimensional structure of the specimen (Condello *et al*., 2013). Surface morphology of the cells was of great interest in this study because the information gathered provides important information about the physiology of the cell and the sample preparation is simple and less damaging to the cells.

7.4.2 0.1M Phosphate ($NaPO_4$) buffer (pH 7.4)

- Solution A; dissolve 78g $NaH_2PO_4\,2H_2O$ in 500ml distilled water
- Solution B; dissolve 8.9g $Na_2HPO_4\,2H_2O$ in 500ml distilled water

To make up 500ml of phosphate buffer mix 140ml of solution A and 360ml of solution B.

7.4.3 2.5% Formaldehyde/Glutaraldehyde

- 2ml of 25% Formaldehyde
- 2ml of 25% glutaraldehyde
- 6ml of distilled water
- 10ml of 0.1M phosphate buffer

Mix the above solutions in order to make a final volume of 20ml of the fixative.

7.4.4 1% Osmium Tetroxide

- Ampoule of 2ml containing 4% Osmium tetroxide
- Phosphate buffer

Add 4ml of phosphate buffer to 2ml of 4% osmium tetroxide solution in order to dilute the percentage of osmium tetroxide to 1% and the final volume of the solution will be 6ml.

7.4.5 Graded ethanol solutions

- 100% (pure) ethanol
- Distilled water (dH_2O)

To make 100ml solution of 50% ethanol; mix 50ml of pure ethanol with 50ml dH_2O.

To make 100ml solution of 70% ethanol; mix 70ml of pure ethanol with 30ml dH_2O.

To make 100ml solution of 80% ethanol; mix 80ml of pure ethanol with 20ml dH_2O.

To make 100ml solution of 95% ethanol; mix 95ml of pure ethanol with 5ml dH_2O.

7.4.6 Tukey Kramer *Post Hoc* test results

Table 7.8: The analysis of means using a Tukey Kramer *Post Hoc* test in order to assess changes in cell connections between the various groups, levels not connected by the same letter are significantly different.

Level				
Untreated	A			
0.02% Methanol	A	B		
ATP	A	B	C	
TDF		B	C	
FTC		B	C	
EFV			C	D
LPV/r				D

Table 7.9: The analysis of means using a Tukey Kramer *Post Hoc* test in order to assess changes in microvilli density between the various groups, levels not connected by the same letter are significantly different.

Level			
Untreated	A		
0.02% Methanol	A	B	
EFV	A	B	
FTC	A	B	C
LPV/r		B	C
ATP			C
TDF			C

Table 7.10: The analysis of means using a Tukey Kramer *Post Hoc* test in order to assess changes in microvilli size between the various groups, levels not connected by the same letter are significantly different.

Level				
Untreated	A			
0.02% Methanol	A			
FTC		B		
EFV		B	C	
TDF			C	D
ATP				D
LPV/r				D

Table 7.11: The analysis of means using a Tukey Kramer *Post Hoc* test in order to assess blebbing density between the various groups, levels not connected by the same letter are significantly different.

Level		
ATP	A	
TDF	A	
EFV	A	B
FTC	A	B
LPV/r	A	B
Untreated		B
0.02% Methanol		B

Table 7.12: The analysis of means using a Tukey Kramer *Post Hoc* test in order to assess changes in bleb size between the various groups, levels not connected by the same letter are significantly different.

Level		
EFV	A	
ATP	A	B
TDF	A	B
LPV/r	A	B
FTC	A	B
0.02% Methanol		B
Untreated		B

Table 7.13: The analysis of means using a Tukey Kramer *Post Hoc* test in order to assess differences in cell shape between the various groups, levels not connected by the same letter are significantly different.

Level			
Untreated	A		
0.02% Methanol	A	B	
TDF		B	C
EFV		B	C
FTC		B	C
ATP			C
LPV/r			C

Table 7.14: The analysis of means using a Tukey Kramer *Post Hoc* test on transformed data in order to assess the presence of membrane bound secretions between the various groups, levels not connected by the same letter are significantly different.

Level				
LPV/r	A			
ATP	A	B		
EFV	A	B	C	
TDF		B	C	
FTC		B	C	
0.02% Methanol			C	D
Untreated				D

Table 7.15: The analysis of means using a Tukey Kramer *Post Hoc* test in order to assess the presence of secretions in the extracellular matrix between the various groups, levels not connected by the same letter are significantly different.

Level		
TDF	A	
ATP	A	
LPV/r	A	
EFV	A	B
0.02% Methanol		B
FTC		B
Untreated		B